Chair of Astronautics

Architectural Options and Optimization of Suborbital Space Tourism Vehicles

Author:

Markus Guerster

Master Thesis, RT-MA 2017/2

Supervisors

Prof. Edward F. Crawley
Department of Aeronautics and Astronautics
Massachusetts Institute of Technology

Prof. Ulrich Walter
Institute of Astronautics
Technical University of Munich

Dr. Christian Hock
CEO
in-tech industry GmbH

Christian Bühler
Institute of Astronautics
Technical University of Munich

“I wanted to be involved in something that has an outside chance of doing some good. If there is not something meaningful in what you are doing above and beyond any commercial returns, then I think life is a bit hollow.”

Elon Musk, 2013

Erklärung

Ich erkläre, dass ich alle Einrichtungen, Anlagen, Geräte und Programme, die mir im Rahmen meiner Masterarbeit von der TU München bzw. vom Lehrstuhl für Raumfahrttechnik zur Verfügung gestellt werden, entsprechend dem vorgesehenen Zweck, den gültigen Richtlinien, Benutzerordnungen oder Gebrauchsanleitungen und soweit nötig erst nach erfolgter Einweisung und mit aller Sorgfalt benutze. Insbesondere werde ich Programme ohne besondere Anweisung durch den Betreuer weder kopieren noch für andere als für meine Tätigkeit am Lehrstuhl vorgesehene Zwecke verwenden.

Mir als vertraulich genannte Informationen, Unterlagen und Erkenntnisse werde ich weder während noch nach meiner Tätigkeit am Lehrstuhl an Dritte weitergeben.

Ich erkläre mich außerdem damit einverstanden, dass meine Masterarbeit vom Lehrstuhl auf Anfrage fachlich interessierten Personen, auch über eine Bibliothek, zugänglich gemacht wird.

Ich erkläre außerdem, dass ich diese Arbeit ohne fremde Hilfe angefertigt und nur die in dem Literaturverzeichnis angeführten Quellen und Hilfsmittel benutzt habe.

Garching, den 28. April 2017

Name: Markus Guerster

Matrikelnummer: 03628540

Zusammenfassung

Der Ansari X-Prize legte den Grundstein für den suborbitalen Weltraumtourismus. Seitdem ist sowohl das technische wie auch wirtschaftliche Interesse deutlich angestiegen. Es stellt sich daher die augenscheinliche Frage: Welche System-Architektur verfügt über die beste Kombination aus Sicherheit und wirtschaftlicher Rentabilität? Das Ziel dieser Arbeit ist es, diese Frage zu adressieren. Dazu wird der architektonische Design Space gründlich durchsucht und jede optimierte Architektur nach Kosten- und Sicherheitskriterien ausgewertet.

Im Allgemeinen haben Systeme, die für eine spezifische Funktion gebaut werden, gerade in frühen Phasen einen großen architektonischen Design Space. Es werden zahlreiche Konzepte entwickelt, gebaut und getestet. Sobald sich das Produkt weiterentwickelt, stellen sich bestimmte Konzepte als überlegen heraus und die im Einsatz befindliche Vielfalt reduziert sich [1]. Als Beispiel beachte man die Mannigfaltigkeit von „Flugmaschinen“ in den Jahrzehnten vor und nach den Wrights Brüdern. Ursprüngliche architektonische Entscheidungen wie Doppeldecker, Druckpropeller oder Entenflügel überdauern nicht zwingend als das dominierende Konzept [2]. Dieses Phänomen einer großen Vielfalt an verschiedenen Konzepten kann derzeit in der suborbitalen Raumfahrttouristenbranche beobachtet werden.

Das spezifische Ziel dieser Arbeit ist es, den Design Space so komplett wie möglich zu untersuchen und die Architekturen zu identifizieren, die realisierbar und voraussichtlich erfolgreich sind. Hierbei werden die Grenzen des plausiblen Design Space bestimmt und die Entscheidungen identifiziert, die diesen Entwurfsraum definieren. Anschließend wird ein parametrisches Modell für alle möglichen Optionen erstellt und die Architekturen hinsichtlich der Zielfunktionen optimiert. Die nicht-dominierten Architekturen werden in der Sicherheits- und Kostendimension bewertet. Aus diesen wird eine geringe Anzahl an Entwürfen ausgewählt, die eine detaillierte Analyse rechtfertigen. Zuletzt wird eine Handlungsempfehlung ausgesprochen, wie der Entscheidungsprozess für eine Architektur strukturiert werden könnte.

Abstract

Since the creation of the Ansari X-Prize, a significant technical and commercial interest has developed in sub-orbital space tourism. An obvious question arises: what system architecture will provide the best combination of safety and economic return? The objective of this thesis is to address this question, by searching comprehensively through the architectural design space, and evaluating optimized architectures for cost and safety.

Generally, in the early stages of development, systems built for a specific function lie in a broad architectural space with numerous concepts being developed, built and tested. As the product matures, certain concepts become more dominant and the variety of concepts in use decreases [1]. Consider the wide range of “flying machines” in the decades before and after the Wrights. History teaches us that the original architectural decisions (e.g. biplane, pusher propeller and canard) do not always survive as the dominant design [2]. This phenomenon of a wide variety of concepts can currently be observed in the suborbital tourism industry.

The specific objective of this work is to explore the design space as thoroughly as possible to identify architectures that are more likely to succeed. In doing so we will identify the limits of the plausible design space and identify decisions that define the space. Then, we will build a parametric model for each of the viable options, and optimize that architecture with respect to the objective functions. Finally, we will assess the un-dominated architectures in the risk and cost dimensions, identify the small handful of designs that merit more refined design analysis and we give guidance to structure the decision-making process to choose one architecture.

Acknowledgment

First, I would like to thank my advisor, Edward F. Crawley, Ford Professor of Engineering at MIT and Founding President of Skoltech. Ed has introduced me to the field of system architecture and taught me how to think of things as systems. He has been a constant source of guidance and advice, both professional and personal. As an advisor, he was hands-off for weeks at a time allowing me to work on new ideas. At the right time, we worked intensively to refine the thoughts. I appreciate the confidence he placed in me from the very beginning on and look forward to starting my PhD under his advice.

Without the support of my home university Professor Ulrich Walter, this thesis would not have been possible. He connected me with Ed and was the key to make this program reality. I would also like to thank Christian Bühler who took care of the organizational aspects related to this thesis. I very deeply thank Christopher Frank for sharing his design framework code with me. I am grateful to Dr. Christian Hock from in-tech industry for being my Mentor and supporting my plan. Without him the financing of this program would still be uncertain. In addition, this program was partly financed by a scholarship from the Heinrich und Lotte Mühlfenzl Stiftung.

I would also like to thank all lab-mates from 33-409. They made the office a warm and inspirational place for sometimes 7 days a week. Particularly, I want to thank Yaroslav Menshenin, Axel Garcia Burgos, Narek Shougarian, Íñigo Portillo Barrios, Marc Sanchez, Johannes Norheim, Juan José Garau Luis, Anne Collin, George Lordos, Bastien Gorret and Veronica Foreman. I wish all of them the best of luck for their future and hope to cross path with all of them again. There are many other individuals around the campus that helped to make my time at MIT unique. It would be too lengthy to list them all. We spent some great weekends of Skiing, Climbing and Hiking in the Whites. My roommate, Carson Darling, made my arrival and stay as easy as it can get.

Finally, and very importantly, I want to thank my family: my parents, Petra and Alfred, and my brother Tobias. My mum gave me everything as a child without ever asking for return. My dad passed on the engineering spirit and set an example to aspire to. I have learned and I am still learning so many things from my him. And foremost, I would like to thank my girlfriend and best friend Jana. Without her selfless encouragement and optimism, I would not be the person I am today.

Table of Content

List of Figures

List of Tables

Symbols and Formulas

a	Acceleration
a_0	Acceleration at engine ignition
a_F	Acceleration at engine shut-off
$c_{D,AF}$	Airframe development cost
h	Altitude of vehicle
$h_{Ignition}$	Altitude of vehicle at landing engine ignition
t_{burn}	Burn time of engine
R^2	Coefficient of determination
$f_{C_{AP}}$	Commercial factor for airplane
$f_{C_{Caps}}$	Commercial factor for capsule
f_{C_R}	Commercial factor for rocket
$f_{C_{RP}}$	Commercial factor for rocketplane
d	Cost conversion value
f_{CR}	Cost Reduction Factor
$\Delta v_{landing}$	Delta-v needed for powered landing
$\Delta v_{D-losses}$	Delta-v of drag losses
$\Delta v_{G-losses}$	Delta-v of gravity losses
ρ	Density of the air
D	Drag
C_D	Drag coefficient
t_F	End time of trajectory
k	Exponential factor for hazard severity
$E_{s,F}$	Final specific energy at the end of the burn time
b	Fiscal year
γ	Flight path angle
g	Gravitational acceleration
$x_{HMI_{h,c}}$	Hazard Mitigation Indices for each hazard *h* and each category *c*
Δt	Incremental change in time
Δv	Incremental change in velocity
$c_{D,J}$	Jet engine development cost
$c_{Likelihood}$	Likelihood value
m	mass
m_0	Mass at engine ignition
m_F	Mass at engine shut-off
m_F	Mass at engine shut-off
m_{dry}	Mass dry of airframe without engines
m_{Empty}	Mass empty of vehicle
m_{Caps}	Mass of capsule
m_{fuel}	Mass of fuel
m	Mass of vehicle
m_p	Mass propellant
$t_{mission}$	Max mission design time
ROC_{max}	Maximum climb rate
$x_{MMF_{h,c}}$	Maximum Mitigation Factor for each category *c* and hazard *h*
$x_{MF_{h,c,d}}$	Mitigation Factor for each category *c*, hazard *h* and each decision option *d*
$x_{MF_{a,c,d}}$	Mitigation Factor for each category *c*, hazard *h* for the selected architecture *a*
n_{PAX_i}	Number of annual participants in period i
n_{crew}	Number of crew consist of participant and pilots
$n_{flights}$	Number of flights

n_{jet}	Number of jet engines
n_{Units}	Number of produced units
$n_{vehicles}$	Number of vehicles
C_{Oper_i}	Operation cost
c_{oper}	Operational cost per vehicle per flight
m_{OWE}	Operational Weight Empty (Vehicle dry mass with engines)
C_{Prod_i}	Production cost
$c_{Prod_{Caps}}$	Production cost for a crew capsule
$c_{Prod_{AP}}$	Production cost for airplane airframes
$c_{Prod_{R-C}}$	Production cost for cryogenic rocket airframes
$c_{Prod_{RP}}$	Production cost for rocketplane airframes
$c_{Prod_{R-S}}$	Production cost for storable rocket airframes
$c_{RDT\&E_{RP}}$	RDT&E cost for a rocketplane airframe
$c_{RDT\&E_{AP}}$	RDT&E cost for an airplane
$c_{RDT\&E_{Cap}}$	RDT&E cost for crewed airframe
$c_{RDT\&E_R}$	RDT&E cost for rocket airframe
$x_{RRR_{h,c}}$	Relative Residual Risk for each hazard *h* and each category *c*
x_{RRM_c}	Relative Risk Metric for each category *c*
$x_{RSI_{h,c}}$	Relative Severity Index for each hazard *h* and each category *c*
$c_{RDT\&E_m}$	Research Development Test & Evaluation cost for each module *m*
$C_{RDT\&E_i}$	Research, Development, Testing and Evaluation costs
c_{Risk}	Risk value
$c_{D,R}$	Rocket engine development cost
s_h	Severity factor
$c_{Severity}$	Severity value
$E_{s,0}$	Specific energy at the start of the burn time
Isp	Specific impulse of the rocket engine
g_0	Standard gravitational acceleration
w_c	Subjective weighting factors
f_{TQ}	Technical quality factor
f_{TQ}	Technical quality factor
F_*	Thrust
T	Thrust
c_{TSFC}	Thrust specific fuel consumption
α	Thrust/steering angle
x_i	Ticket price in $ for period i
t	time
t_0	Time at engine ignition
t_F	Time at engine shut-off
Δv_{tot}	Total Δv needed to reach the destination
$\Delta v_{tot,losses}$	Total delta-v losses
C_{tot_i}	Total life-cycle cost for each period *i*
v	velocity
v_0	Velocity at engine ignition
v_F	Velocity at engine shut-off
$v_{Ignition}$	Velocity at landing engine ignition
A	Wetted area

Abbreviations

ABS	Antilock Braking System	NMF	Net Mass Fraction
ALCCA	Aircraft Life-Cycle Costs Analysis	nModules	number of Modules
CCDev	Commercial Crew Development	OCPP	Overall Cost Per Participant
CER	Cost Estimating Relationships	OPM	Object-Process Methodology
conops	concept of operations	ORSRM	Overall Residual Safety-Risk Metric
COTS	Commercial Orbital Transportation Services	OWE	Operational Weight Empty
DoE	Design of Experiment	PHA	Preliminary Hazard Analysis
DSM	Design Structure Matrix	RDT&E	Research Development Test & Evaluation
ECLSS	Environmental Control and Life Support System	REL	Reaction Engines Limited
FAA	Federal Aviation Administration	ROC	Rate Of Climb
FMEA	Failure Mode and Effect Analysis	RRM	Relative Risk Metric
FTA	Fault Tree Analysis	RRR	Relative Residual Risk
GA	Genetic Algorithm	RSE	Response Surface Equation
GTO	Geostationary Transfer Orbit	RSI	Relative Severity Index
HMI	Hazard Mitigation Indices	RSM	Response Surface Methodology
HPowered	Horizontal Powered landing	SABRE	Synergistic Air-Breathing Rocket Engine
ISS	International Space Station	SLS	Space Launch System
LAmode	Landing mode	SSTO	Single Stage To Orbit
LC	Learning Curve	TIT	Turbine Inlet Temperature
LEO	Low Earth Orbit	TOmode	Take-off mode
MF	Mitigation Factors	TSFC	Thrust Specific Fuel Consumption
MMF	Maximum Mitigation Factor	WYr	Work-Years
MSV	Manned Suborbital Vehicle		

1 Introduction

1.1 Motivation

Recently, in February 2017, SpaceX announced to fly two citizens around the moon in late 2018. The name of the participants is disclosed but according to SpaceX they have already deposit a significant amount of money [3]. Elon Musk expects that there are more tourists to come in the near-term. No ticket price was officially announced for the trip, but we know that the Dragon V2 capsule will be launched by a Falcon Heavy listed with $90 million per launch (8 t of payload to the Geostationary Transfer Orbit (GTO)) [4]. NASA will pay $58 million per seat to SpaceX for bringing their astronauts to the International Space Station (ISS) [5]. According to Space Adventures, their eighth client would have paid $52 million for a 10-day trip to the ISS [6]. In 2007 they offered an advance booking for future lunar mission for $100 million per seat [7]. With these data, we can certainly argue that the ticket price for SpaceX's trip around the moon may be in the order of $50 - $100 million. The company sees these tourists missions as a milestone to extend their Dragon capabilities to deep space and finally to transport humans to Mars [3].

In parallel to these space tourist activities, Blue Origin and Virgin Galactic are entering the suborbital market. This market differs from the orbital one by not entering an orbit around the earth. The focus relies on providing the participants an adventures experience with a few minutes of weightlessness time, a view of the earth's curvature and entering the space, which is defined by the Kármán line (an altitude of 100 km). As the vehicle does not need to enter an orbit around the earth, the required energy is considerable less compared to orbital launches. For re-entry, the energy can be absorbed without the need for a specific thermal protection systems. This all results in a more affordable launch vehicle and finally in a one-to-two order of magnitude lower ticket price. For example, Virgin Galactic already sold several hundreds of tickets for around $250,000 [8]. To compete, it is likely that Blue Origin will price their flights in the same range. For Blue Origin, the suborbital tourist market is an intermediate step to enter the commercial orbital launch market. It is a testbed for developing and testing the technology and systems needed for a reusable orbital launch system [9]. Virgin Galactic tries to enter the orbital launch business for small satellites around 200 kg for under $10 million per mission [10]. They are developing the so called LauncherOne, which will be launched like the Pegasus from a carrier aircraft.

We can observe a common pattern in the suborbital and space tourism industry. The companies see the tourism industry as intermediate step and their larger mission is to make space more accessible. This includes making launches more affordable as well as more frequently. A key technology to achieve both goals will be increased reusability. From the economic view, more frequent launches drive down the costs due to economic scaling and efficiency factors. Dropping cost in return, increase the demand which again reduces cost. These dependencies would result in a virtuous circle of economic growth. As mentioned by Goehlich [11], this stage of well operating is not reached yet. The space tourism is presently in a pioneer stage with as less as two tourists per year [11]. The suborbital space tourism is even in an earlier stage. As of April 2017, no tourist participated in suborbital space flights.

The birth of the suborbital space tourism dates to May 1996, where the Ansari XPrize was launched by the Ansari family. This competition challenged teams all around the world to build a reusable, private-funded and manned spaceship. The first team carrying three people to 100 km above the Earth's surface twice within two weeks received the $10 million price. 26 teams from 7 nations proposed their concept. Finally, the Mojave Aerospace Ventures team, which was led by Burt Rutan and his company Scaled Composites and financed from Paul Allen, won the competition on October 4, 2004. Richard Branson licensed Burt Rutan's technology and created Virgin Galactic. The competition launched a billion dollar market for suborbital space travel. [12]

The competition stimulated the creation of reusable (twice within two weeks), suborbital (100 km) and manned (three people) vehicles. Different names can be found for this kind of system, like *suborbital human vehicle*, *space tourism vehicles*, *suborbital reusable vehicles*, *suborbital reusable launch vehicles*. In this text we use the naming of The Student Aerospace Challenge [13] and define:

> **Manned Suborbital Vehicle**
> A Manned Suborbital Vehicle (MSV) carries participants above the Kármán line (100 km) without reaching an orbit around earth.

Intentionally, this definition does not imply any information about the reusability or turnaround time since the main function of carrying people above the Kármán line can be achieved independently from the level of reusability. Participants are the people who pay for the adventure. This does not include the pilots.

1.2 General thesis objectives

Generally, in the early stages of development, systems built for a specific function lie in a broad architectural space with numerous concepts being developed, built and tested. As the product matures, certain concepts become more dominant and the variety of concepts in use decreases [1]. Consider the wide range of “flying machines” in the decades before and after the Wrights. History teaches us that the original architectural decisions (e.g. biplane, pusher propeller and canard) do not always survive as the dominant design [2]. This phenomenon of a wide variety of concepts can currently be observed in the suborbital tourism industry. An obvious question arises:

What system architecture of MSV will provide the best combination of safety and economic return?

1.3 Literature review

To approach the previous research question, we review the suitable literature and find that System Architecture provides us with the methodology to approach this challenge. It is described hereafter and followed by a summary of the existing design framework needed to evaluate MSV architecture with respect to their benefit and cost.

1.3.1 System Architecture

Originated as a discipline in civil engineering, System Architecture was spun off in the late 1980s and was used since then by several other industries. The methodology has proven its success in early phases of complex aerospace engineering system designs [14]. Like System Engineering, it is a system thinking approach that considers a system as *a set of interrelated entities which perform a function, whose functionality is greater than the sum of the parts* [15]. System Architecture is a process in the very early system development, where the focus lies on carefully identifying and making the decisions that define the highest-level design. These architectural decision aim to determine much of the systems performance, cost and safety.

The term *architecture* is used in very different scopes, e.g. to differentiate between existing systems, for circuit-switch architectures or for software as a service architecture. As proposed by Crawley et al. we use *architecture* as an abstract description of the entities of a system as well as the relationship between those. For man-made systems, decisions can

represent the architecture. This idea of *architecture as decisions* is used later to describe MSVs. [15]

A detailed definition of the term *System Architecture* is given by Crawley et al.:

> **System Architecture**
>
> "System architecture is the embodiment of *concept*, the allocation of physical/informational *function* to the elements of *form*, and the definition of *relationships* among the elements and with the surrounding *context*." [15]

This definition includes the five key elements *form, function, structure*, *context* and *concept*. Hereafter we describe them shortly. For more detailed definition of form, object, structure, function, operand, process, context and concept refer to annex A.2 and reference [15].

Form consist of objects and **structure**, which is the formal relationship between the objects. It describes what the system is and is the main source of cost.

Function consists of processes and operands. The operands are created, modified or consumed by the process. It describes what the system does and is the main source of external benefit.

To provide an example of these terms, we show in Figure 1-1 an Object-Process Methodology (OPM) representation of form and function as well as the interconnection between them. For further information on the OPM notation refer to the books of Dov Dori [16, 17]. We have attached in annex A.3 an overview of the most important notation elements. The form enables function or the function requires an instrument of form. Between the objects of forms exist a formal relationship (e.g. for mechanical systems: "is close to", "touches", "within", "is aligned with"). The combination of objects and structure is form. The operand is an object that is created, modified or destroyed by the process.

An example is a pump that pressures water. Figure 1-2 shows this example with two objects of form (in a real pump there are much more objects and formal relationships).

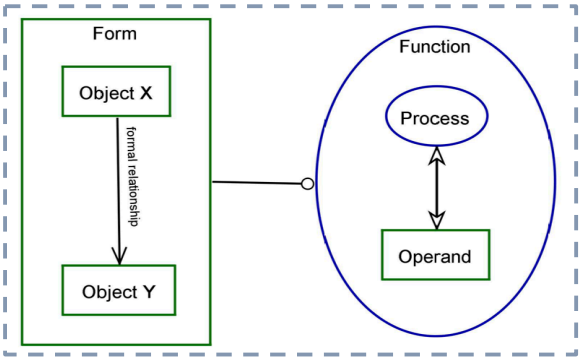

Figure 1-1: Form and Function OPM representation

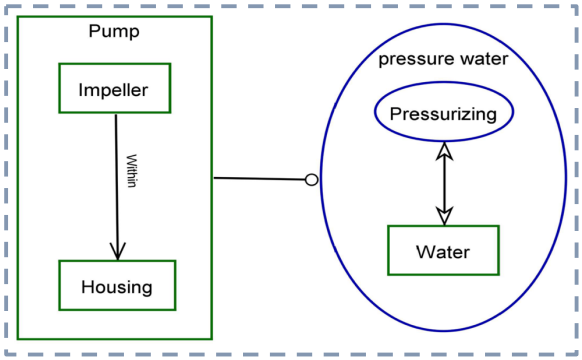

Figure 1-2: OPM representation of a pump

The *form* is “pump” which consists of different *objects* like “housing”, “motor”, “impeller”, “cover”. “Within” is a *formal relationship/structure* between the objects “impeller” and “housing”. The *process* of pressure water is “pressurizing” whereas the *operand* that is changed by the process (from lower to higher pressure) is “water”. The *form* “pump” enables the *function* “pressure water”.

Context is the entities that surround the system. They are outside of the system boundary but are relevant to it. If the context has a relationship to the system, it is defined as an *external interface*. The dashed rectangle of Figure 1-1 is the system boundary. The context with its entities is just on the outside of it [15]. An operator who controls the pump or the pipes who feed the water to and from the pump are the context of the example pump.

Concept is a mapping between form and function. It simplifies the system architecture and allows for high-level reasoning. It embodies a sense for how the product or system works. The pump shown in Figure 1-2 is a high-level representation of the concept for a centrifugal pump (the impeller indicates the type of pump). The so-called *solution-neutral function* is in case of the pump “moving of a fluid”. One concept to do this, is a centrifugal pump. Other concepts can be “Axial flow pump”, “Rotatory pump” or for the fluid “air” a “fan”. All possible concepts are part of the system architecture. Concepts are defined by mapping form to function, e.g. to move the fluid by pressurizing instead of displacing. [15]

Using these definitions, the architecture becomes *the materialization of the mental model into a system that is implementable in the real world* [18]. To rank architectures and call one architecture “better” than the other, the sources of associated benefit and cost must be determined. As stated in the definition of the terms form and function, the form is associated

with cost and the function delivers benefit to customers. A good architecture is then defined by providing the most benefit with the least cost. The quantitative measurement of benefit and cost is called metric. These are solution-specific and must be define for each problem statement specifically.

Each architecture can be represented by a set of decisions [19]. We can encode these decision into mathematical design variables. If the benefit and cost of the system becomes the objective functions, we can view the system architecting process as an optimization problem. Reduction in computational cost during the last years allows us to explore larger architectural design spaces in more detail, which makes it more likely to find a better architecture with respect to the defined metrics for benefit and cost.

1.3.2 Design frameworks for MSV

A design framework generates output parameters for given input design variables. The kind of input variables are defined by the architecture. The output parameters are used to calculate the metrics for which the architecture is then optimized. Our literature research on existing design frameworks matches with the one executed by Frank [20-22] and Burgaud [23]. Including the one from Frank, we found twelve sizing and synthesis codes. They are displayed in Table 1-1 and compared in the categories, computational speed, availability, easiness of use, design space exploration and their level of abstraction suitable for conceptual studies. The scale we use consists of a **+** for good and *0* for average fulfillment of the category. The rating was based on the ones from Frank and Burgaud. For a detailed description of each code the reader is referred to Frank's PhD thesis [20].

The comparison of the design framework evaluation codes show that Frank's code has the best overall performance in the categories of interests and would suit our research interest the most. Fortunately, he provided us his design framework. We deeply thank him for sharing his code with us and gratefully acknowledge his contribution.

Table 1-1: Comparison of the twelve sizing and synthesis codes [20, 23]

	Computa-tional speed	Availability	Easiness of use	Design space exploration	Suitable for conceptual studies
Sarigul [24]		+	+	+	
Design Sheet [25]	+			+	0
TSSP [26]	+		0		0
Mattingly [27]	+	+	+		0
FLOPS [28]	+	+	0		0
ASTOS [29]	0	0		+	
RASAC [30]	+	+	0		+
Stanley [31]	+		0		+
Olds [32]		0	0		0
Havoc [33]	+		0		0
Braun [34]				0	0
Frank [20-22, 35]	0	+	+	+	+

1.4 Specific thesis objectives

After we reviewed the literature and the available methodology, we can formulate the solution specific research objectives of this thesis. The text should address the solution neutral research question from section 1.2 by searching comprehensively through the architectural design space, and evaluating optimized architectures for benefit and cost. In doing so we will identify the limits of the plausible design space and identify decisions that define the space. Then we will build a parametric model for each of the viable options, and optimize that architecture. Finally, we will assess the un-dominated architectures, and identify the small handful of designs that merit more refined design analysis.

We can phrase this specific research objective with the **To-By-Using** goal statement formalism in a more structured way:

To identify a set of good MSV architectures that provide the most benefit for the least cost **by:**

1. Defining the plausible design space
2. Building a parametric model for each viable architecture
3. Optimizing the viable architecture
4. Visualizing and making sense of the result to support the decision-making process

Using the System Architecture paradigm and a tradespace exploration tool build upon Frank's design framework.

1.5 Thesis Overview

The following chapter 2 defines the plausible design space by building a database of existing projects, defining the decision matrix and the constraints and finally enumerating the feasible architectures and visualize them.

Chapter 3 describes our design exploration tool to evaluate the previous defined design space. Adaptions and supplements to Frank's design framework are described in chapter 4. The subsequent two chapters 5 and 6 aim to describe the metrics used for safety and cost, respectively.

Chapter 7 describes the results of the optimization process followed by the conclusions in chapter 8 with a summary of the thesis, the main findings, the contribution of the thesis and lastly, an outlook for future work.

2 Defining the plausible design space

Before we can optimize each architecture and evaluate the design space, we must define our design space. A common axiom is that if a larger design space can be explored, it is more likely to find better architectures or designs. Based on this, the objective of this chapter is to define the design space as broad as a feasible evaluation of it allows. The latter is limited by computational resources as well as limitations of the design framework used to calculate the metrics. We identify four main steps to define the design space:

1. Building a database of existing concepts in the design space of interest
2. Defining a morphological decision matrix based on the database
3. Defining of logical, reasonable and model-limitation constraints
4. Enumeration of the feasible architectures which represent the plausible design space

These four steps are described for our problem-specific case of MSV in the following four sections 2.1 - 2.4. The definition of the morphological decision matrix, the reasoning about the constraints and the enumeration of the feasible architectures are coupled and consequently iterative processes. We therefore used numerical methods to reduce the effort per iteration. The decision and constraints are defined in Excel and then imported into Matlab to enumerate the feasible architectures. With this approach, we can quantify the influence of changing constraints on the resulting design space.

2.1 Building a database of existing concepts

The first step in defining the design space is to look at existing concepts that have similar requirements. These can be concepts from competitions, current competitors who have already decided for an architecture or existing studies on the market. This sort of market and competitor analysis should anyway be done during the decision process of forming a Suborbital Space Tourism company or creating a project inside an existing company.

We first define our notation of stage and module. To distinguish an unpowered stage and a powered stage, we introduce the term *module*, which we define as:

Module
A module is launched as a part of the MSV, undergoes a separation during flight and lands separately from other modules. The higher the number, the higher the energy state of the module.

It is important to note that the term module is not equal to a stage of a rocket. Stage describes a propulsive system of a rocket with typically the last one containing the payload [36]. For example, Blue Origin's New Shepard is a one stage rocket with a capsule carrying the payload/people (see Figure 2-1 for the concept of operations (conops)). In our notation, this concept is a two-module system since the capsule is separated during the flight and lands separately. The first module is the rocket stage and the second one is the capsule due to its higher energy state.

The literature research on existing concepts revealed team summaries of almost all the companies competed in the Ansari X-Prize, previous studies of the market, books about space tourism as well as extracted data from companies' websites. The used sources are:

- **1998:** Report from the Associate Administrator for Commercial Space Transportation [37]
- **2002:** Report "Suborbital reusable launch vehicles and applicable markets" from Martin J.C. [38]
- **2003:** Ansari XPrize Team Summaries [12]
- **2011:** The U.S. Commercial Suborbital Industry: A Space Renaissance in the Making from the Tauri Group [39]
- **2012:** A report from the Tauri Group: Suborbital Reusable Vehicles: A 10-Year Forecast for Market Demand [40]
- **2014:** The book "Suborbital industry at the edge of space" from Seedhouse Erik [41]
- **2016:** Current webpages from ARCA [42], Blue Origin [43], Virgin Galactic [44], XCOR [45], Copenhagen Suborbital [46], Dassault-Aviation [47], EADS [48], Cosmocourse [49] and Scaled Composites [50]

We found 37 companies, extracted the main parameters and consolidated them into one table, which can be seen in annex A.4. Some information is not available due to the early stage of development of these projects (indicated with a question mark). In addition, some companies do not longer exist, e.g. due to the lack of financial funding. We limit the number of information for each company to top-level systems attributes and conops differences.

Unintentionally, by deciding for a set of attributes, we already have chosen a first draft set of decisions. For example, the type of engine (rocket or jet) or the propellant type are obviously important enough that the sources provide information about it. Furthermore, we could find for all companies, information about the top-level design of the vehicle, either in form of pictures and drawings or in form of text, which somehow is a description of the architecture. The next section describes how we use this database to identify the main architectural decisions.

2.2 Defining the morphological decision matrix

The concept of using a morphological matrix to study the design space of different configurations dates back to Zwicky in 1969 [15, 51]. It has shown great usage as a decision support tool since then [52]. The morphological matrix we use has the main architectural decision as rows and the possible options as columns (see Table 2-1). The options for a certain decision must be mutually exclusive. An architecture is then defined by choosing one option for each decision. They do not have to be from the same column.

Our final decision matrix is shown Table 2-1 below. It will define together with the constraints from section 2.3 our design space. The matrix consists of one vehicle level decision about the number of module, followed by five and three decision for the first and second module, respectively. The module level decision cover all three operational aspects launching, flying and landing. The take-off mode (TOmode) can be horizontal or vertical. This decision does not exist for the second module because the second module has the same initial take-off mode as the first module and then separates during the ascent phase. The flying decision covers the configuration of the vehicle, if it has wings or not, if it has jet engines or not and if it has a rocket engine or not. With excluding the decision about the jet engine for the second module we implicitly integrate the constraints that the final ascent must be made by a rocket engine and it is not reasonable to add an additional jet engine to the second module. If a jet engine is used by the architecture, then it must be part of the first module. Finally, the last decision for each module is about the landing mode (LAmode).

The options cover powered and unpowered landing methods. Unpowered methods are gliding and parachute, where the orientation of the first one is horizontal and the latter vertical. Powered methods are horizontal powered landing (HPowered) and vertical powered landing with a rocket engine (Rocket). We assume a horizontal powered landing with a rocket engine is not feasible (justified in section 2.3). As the second module cannot have a jet engine, there is no HPowered option for the second module. However, we include the option None as an option which must be chosen if the vehicle just has one module. A full combinatorial enumeration leads to 2,048 unconstraint architectures.

Table 2-1: Morphological architecture decision matrix

shortID			Option 1	Option 2	Option 3	Option 4	number of options
nModules			1	2			**2**
Module 1	**Launching**	TOmode1	Horizontal	Vertical			**2**
	Flying	wing1	No	Yes			**2**
		JetEngine1	No	Yes			**2**
		RocketEngine1	No	Yes			**2**
	Landing	LAmode1	Gliding	HPowered	Parachute	Rocket	**4**
Module 2	**Flying**	wing2	No	Yes			**2**
		RocketEngine2	No	Yes			**2**
	Landing	LAmode2	Gliding	Parachute	Rocket	None	**4**
Number of total possible combinations						**2,048**	**O(4)**

We apply this matrix to Blue Origin's New Shepard to provide an example of how this matrix can be used to represent an architecture. The conops of this vehicle are shown in Figure 2-1. By our definition, this vehicle is a two-module vehicle. The first module is a vertical launching rocket with a rocket engine. It has no wings and no jet engine. The landing mode is vertically powered. The capsule separates during flight, has no propulsion and wings, and lands with a parachute. If we encode this information in form of our decision, we obtain Table 2-2 where the blue marked options are the one which are chosen to represent the architecture. Note, that our matrix does not include scaling attributes like the number of

participants, passengers or crew. We treat the number of participant as a requirement variable and the number of pilots as a design variable, which is optimized. Chapter 3 describes these variables in more detail. Two additional examples of the Virgin Galactic as well as Rocketplane XP architecture are provided in annex A.6.

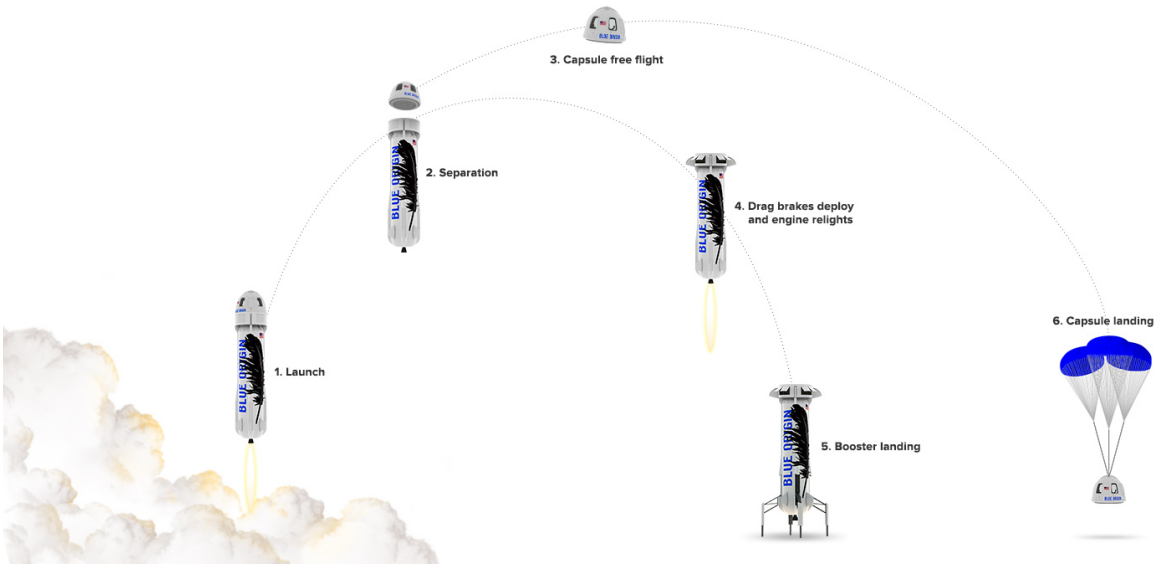

Figure 2-1: Conops of Blue Origin's New Shepard [43]

Table 2-2: Decision matrix representing the architecture of New Shepard

shortID			Option 1	Option 2	Option 3	Option 4	number of options
nModules			1	2			**2**
Module 1	**Launching**	TOmode1	Horizontal	Vertical			**2**
	Flying	wing1	No	Yes			**2**
		JetEngine1	No	Yes			**2**
		RocketEngine1	No	Yes			**2**
	Landing	LAmode1	Gliding	HPowered	Parachute	Rocket	**4**
Module 2	**Flying**	wing2	No	Yes			**2**
		RocketEngine2	No	Yes			**2**
	Landing	LAmode2	Gliding	Parachute	Rocket	None	**4**

2.3 Defining of logical, reasonable and model-limitation constraints

With the morphological matrix presented in Table 2-1 we can define almost all concepts from our database. The ones which cannot be characterized are these who are very likely to be dominated by others, including architectures that launch from underneath the water or architectures with more than two modules. Our first draft version of the morphological decision matrix can represent all these concepts. It is shown in A.6. A full enumeration would lead to 6 billion unconstraint architectures. We argue with common-sense that some of these concepts are very likely to be dominated. The three constraints applied to narrow down the design space are:

1. **The maximum number of modules is 2**
   36 out of 37 companies proposed a concept with two modules, only one uses a three-module rocket. Most of the current orbital launch vehicles use two stage rockets. The energy needed to reach the Kármán line is well below the one for orbital trajectories. We reason that a MSV with three modules is not competitive due to the increasing complexity, development and maintenance cost accompanied with the third module.

2. **No launching from the water**
   Only one company proposes a launch from out of the water. One can grasp that this type of launch adds complexity, operational challenges and cost without an obvious benefit.

3. **No balloon as ascent method**
   We excluded the balloon option as ascent method as our design framework does not have the model to optimize and evaluate the metrics for a vehicle with this feature. Moreover, we can argue that it is not feasible to reach 100 km with only a balloon. This means that the second module need to have a rocket engine. This whole module must be carried by the balloon. Given the weight of the second module, it is questionable if this approach is feasible.

Our final morphological matrix from Table 2-1 defines the design space for all unconstraint architectures. Some of them are logically not possible, like the combination of jet engine *yes*, rocket engine *yes* and the landing mode *none* for the second module. The option *none* as landing mode indicates that the vehicle has one module and therefore by default the decisions about the engines are *no*. This is a logical constraint or also called objective by the definition of Guest [53]. Additional constraints are more subjective or reasonable as we

call them in this thesis. They cover aspects where domain experts can reasonable argue that the implementation of this combination of option result in higher complexity and development challenges without providing benefit in the metrics of interest. The previous applied constraints about the number of modules as well as the launch from water are illustrations of this type. Another example is a horizontal takeoff without wings. One can think of systems where a horizontal takeoff without a lifting wing may be achievable (e.g. by providing lift with vertical orientated engines). However, we can argue with engineering judgement that this increases complexity without providing a benefit in the cost and risk dimension. We applied a third kind of constraints, a model-limitation constraint. The no-balloon limitation previously mentioned is of this and of the reasonable kind. The model-limitation constraint is a constraint due to limitations of the model to evaluate the metrics for this architecture. This can be for example, the lack of the design framework to evaluate a balloon ascent.

To systematically implement the constraints between the decision and their options from the matrix in Table 2-1, we created a Design Structure Matrix (DSM) with the options as rows and columns. The resulting matrix is shown in Table 2-3. Since the DSM is a symmetrical matrix, we only populated the top-right half. The number 1 with green background stands for no interconnection and constraint between the options. If the background is red, there are constraints and the letter references to the justification in Table 2-4. If there is a dash instead of a letter, this combination is per definition not allowed due to the mutually exclusive requirement of all options for one decision.

We found in total 23 constraints of the three different types: logical, reasonable and model limitation. Table 2-4 shows the justification of these constraints. The column on the left has the ID from the constraints matrix above. The column on the right indicates the type of constraint. The second up to the neigh column contain a pseudocode to describe the field in the constraint matrix where the constraint is applied. The following column contains the justification why this constraint is applied and this combination of option is not allowed in our design space. For example, for the constraint identified with *a*, the table reads:

IF (nModules == 1) *THEN* (RocketEngine1 *!*= No)

Or in text form: if the option for the decision *nModules* is chosen to be *1*, then the *RocketEngine1* decision cannot be *No*. Since the RocketEngine1 decision only has two options, forbidding one option is equal to saying that is must be the other option. In this case, the previous statement is equal to the one saying: if the vehicle has one module,

there must be a rocket engine on the first stage. The justification for this constraint is of the model-limitation kind. We do limit the maximum velocity of jet engines to Ma = 2 and do not consider airbreathing supersonic propulsion like ram- or scramjets. Ma = 2 at absolute ceiling altitude of typical jet engine does not provide enough energy to reach 100 km by pulling up the vehicle to transfer the kinetic into potential energy. The syntax to read the other 22 constraints is equal to the example provided above.

Table 2-3: Constraints matrix

			Module 1												Module 2							
			nModules		TOmode		wing		JetEngine		RocketEngine		LAmode				wing		RocketEngine		LAmode			
			1	2	Hori-zontal	Vertical	No	Yes	No	Yes	No	Yes	Gliding	H Pow-ered	Para-chute	Rocket	No	Yes	No	Yes	Gliding	Para-chute	Rocket	None
Module 1	nModules	1	1	-	1	1	1	1	1	1	a	1	1	1	1	1	1	b	1	c	d	e	f	1
		2		1	1	1	1	1	1	1	1	1	1	1	1	1	1	1	1	1	1	1	1	g
	TOmode	Horizontal			1	-	h	1	1	1	1	1	1	1	1	1	1	1	1	1	1	1	1	1
		Vertical				1	1	1	1	i	j	1	1	1	1	1	1	1	1	1	1	1	1	1
	wing	No					1	-	1	1	1	1	k	l	1	1	1	1	1	1	1	1	1	1
		Yes						1	1	1	1	1	1	1	m	n	1	1	1	1	1	1	1	1
	JetEngine	No							1	-	o	1	1	p	1	1	1	1	1	1	1	1	1	1
		Yes								1	1	1	q	1	1	1	1	1	1	1	1	1	1	1
	RocketEngin	No									1	-	1	1	1	t	1	1	u	1	1	1	1	1
		Yes										1	1	1	1	1	1	1	1	1	1	1	1	1
	LAmode	Gliding											1	-	-	-	1	1	1	1	1	1	1	1
		H Powered												1	-	-	1	1	1	1	1	1	1	1
		Parachute													1	-	1	1	1	1	1	1	1	1
		Rocket														1	1	1	1	1	1	1	1	1
Module 2	wing	No															1	-	1	1	v	1	1	1
		Yes																1	1	1	1	w	x	1
	RocketEngin	No																	1	-	1	1	y	1
		Yes																		1	1	1	1	1
	LAmode	Gliding																			1	-	-	-
		Parachute																				1	-	-
		Rocket																					1	-
		None																						1

Table 2-4: Justification of the constraints

ID	IF	(Decision	==	Option)	THEN	(Decision	!=	Option)	Justification	Type of constraint
a	IF	nModules	==	1	THEN	RocketEngine1	!=	No	A one-module vehicle cannot reach 100 km with jet engines only (jet engines limited to Ma = 2 in the model)	Model limitation
b					THEN	wing2	!=	Yes	The second module does not exist for a single-module vehicle. The *wing2* decision is supposed to be set to *No*	Logical
c					THEN	RocketEngine2	!=	Yes	The second module does not exist for a single-module vehicle. The RocketEngine2 decision is supposed to be set to *No*	Logical
d					THEN	LAmode2	!=	Gliding	The second module does not exist for a single-module vehicle. The *LAmode2* decision is supposed to be set to the default value *none*	Logical
e					THEN	LAmode2	!=	Parachute	The second module does not exist for a single-module vehicle. The *LAmode2* decision is supposed to be set to the default value *none*	Logical
f					THEN	LAmode2	!=	Rocket	The second module does not exist for a single-module vehicle. The LAmode2 decision is supposed to be set to the default value none	Logical
g			==	2	THEN	LAmode2	!=	None	For a two-module vehicle the default option *None* cannot be chosen for the *LAmode2* decision.	Logical
h	IF	TOmode1	==	Horizontal	THEN	wing1	!=	No	Without wings a horizontal launch is not reasonable	Reasonable
i			==	Vertical	THEN	JetEngine1	!=	Yes	There are very few jet aircrafts with a trust/weight ratio over 1, which is necessary to launch vertically. Given the fact that the weight of an additional rocket engine counters against this ratio, it is not reasonable to use jet engines in a vertical launch configuration.	Reasonable
j					THEN	RocketEngine1	!=	No	There are very few jet aircrafts with a trust/weight ratio over 1, which is necessary to launch vertically. Given the fact that the weight of an additional rocket engine counters against this ratio, it is reasonable to use rocket engines for vertical launch configurations	Reasonable

k	IF	wing1	==	No	THEN	LAmode1	!=	Gliding	A horizontal landing requires lift. Without a wings a horizontal landing, specifically gliding is not reasonable.	Reasonable
l					THEN	LAmode1	!=	H Powered	A horizontal landing requires lift. Without wings a horizontal landing, specifically horizontally powered is not reasonable	Reasonable
m			==	Yes	THEN	LAmode1	!=	Parachute	With wings, it is reasonable to use them during landing and land horizontally	Reasonable
n					THEN	LAmode1	!=	Rocket	With wings, it is reasonable to use them during landing and land horizontally	Reasonable
o	IF	JetEngine1	==	No	THEN	RocketEngine1	!=	No	The first module must have either a jet or a rocket engine	Logical
p					THEN	LAmode1	!=	H Powered	A horizontally powered landing must have a propulsion system. It is not reasonable to use a rocket engine during powered landing. Hence, powered horizontal landing requires a jet engine.	Reasonable
q			==	Yes	THEN	LAmode1	!=	Gliding	It is reasonable to land horizontally powered if the vehicle has jet engines since the small fuel consumption outweighs the risk reduction	Reasonable
t	IF	RocketEngine1	==	No	THEN	LAmode1	!=	Rocket	Without a rocket engine, a rocket powered vertical landing is not possible	Logical
u					THEN	RocketEngine2	!=	No	Giving the limit of Ma = 2 for jet engines, either the first or second module must have a rocket engine to reach 100 km. If the first one does not have one, the second module must have one.	Model limitation
v	IF	Wing2	==	No	THEN	LAmode2	!=	Gliding	A horizontal landing requires lift. Without a wings a horizontal landing, specifically gliding is not reasonable.	Reasonable
w			==	Yes	THEN	LAmode2	!=	Parachute	With wings, it is reasonable to use them during landing and land horizontally	Reasonable
x					THEN	LAmode2	!=	Rocket	With wings, it is reasonable to use them during landing and land horizontally	Reasonable
y	IF	RocketEngine2	==	No	THEN	LAmode2	!=	Rocket	Without a rocket engine, a rocket powered vertical landing is not possible	Logical

2.4 Enumeration of the feasible architectures

We have created the morphological matrix and identified all constraints between the decisions' options. With this information, we can now define our design space by enumerating all unconstraint architectures and compare each of them within the constraints matrix. If the architecture contains a set of options which is restricted by one of the 23 constraints, it is no longer included in the list. The approach is automated by a Matlab file. The resulting list covers 33 distinguish feasible architecture out of the 2,048 unconstraint ones. This list of 33 architectures defines our design space.

We have developed a matrix to visually represent these 33-feasible architectures. The matrix shown in Table 2-6 has the concept of the first module as columns and for the second module as rows. There are six possible concepts for the first and the same number for the second module (including the no second module choice). This yields to 36 architecture, but the constraint *a* discussed before excludes three of them. There must be a rocket engine either on the first or on the second module to reach 100 km.

The pictograms in the top row of the first module and the left column of the second module visualize the concepts of the modules and their attributes. A description of the meaning of these pictograms is provided in Table 2-5. We use the decision ID and their options from the morphological matrix displayed in Table 2-1.

Table 2-5: Description of the pictograms used to represent the 33 architectures

1st module			2nd module		
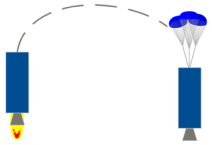	TOmode1: wing1: JetEngine1: RocketEngine1: LAmode1:	Vertical No No Yes Parachute	None	wing2: RocketEngine2: LAmode2:	No No None
	TOmode1: wing1: JetEngine1: RocketEngine1: LAmode1:	Vertical No No Yes Rocket	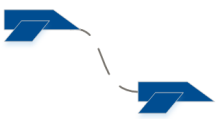	wing2: RocketEngine2: LAmode2:	Yes No Gliding

	TOmode1: wing1: JetEngine1: RocketEngine1: LAmode1:	Vertical Yes No Yes Gliding	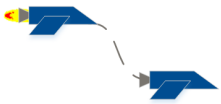	wing2: RocketEngine2: LAmode2:	Yes Yes Gliding
	TOmode1: wing1: JetEngine1: RocketEngine1: LAmode1:	Horizontal Yes Yes No HPowered		wing2: RocketEngine2: LAmode2:	No No Parachute
	TOmode1: wing1: JetEngine1: RocketEngine1: LAmode1:	Horizontal Yes No Yes Gliding	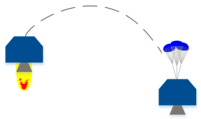	wing2: RocketEngine2: LAmode2:	No Yes Parachute
	TOmode1: wing1: JetEngine1: RocketEngine1: LAmode1:	Horizontal Yes Yes Yes HPowered	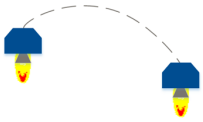	wing2: RocketEngine2: LAmode2:	No Yes Rocket

The 33 architectures are numbered starting from the top left to the bottom right. The three not feasible ones are marked by a *x*. If we screen our database of 37 proposed concepts and match them to one of the 33 architecture, we find that there are just 7 distinguished ones. This means that with our approach we could identify 26 new architectures and describe their main attributes in one matrix together with the existing proposals. One representative of each architecture was chosen and included in the matrix.

Table 2-6: Overview of the 33 architectures defining the design space (* with three propulsive systems, one jet and two rocket engines)

1st module / 2nd module	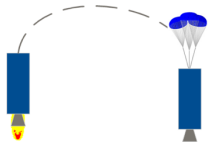	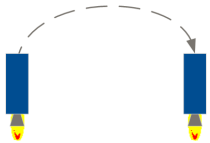			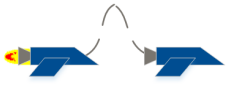	
None	**1** e.g. Copenhagen Suborbital	**2**	**3**	x	**4** e.g. XCOR	**5** e.g. Rocketplane
	**6**	**7**	**8**	x	**9**	**10**
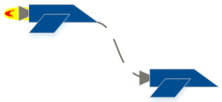	**11**	**12**	**13**	**14** e.g. Virgin Galactic	**15**	**16***
	**17** e.g. ARCA	**18** e.g. Blue Origin	**19**	x	**20**	**21**
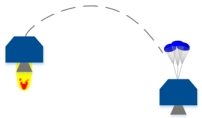	**22** e.g. Canadian Arrow	**23**	**24**	**25**	**26**	**27***
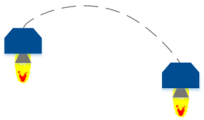	**28**	**29**	**30**	**31**	**32**	**33***

Christopher Frank investigated in his PhD thesis four MSV architectures [20-22]. We can match them into our overview matrix and see that he covers by our notation architecture #1, #4, #5 and #14. Interestingly, they are all part of the Ansari X-Prize design space. With this information, we can visualize the design spaces with ellipses and see how they overlap. This is shown in Figure 2-2. The red ellipse pictures our design space, the blue ellipse the one of the X-Prize proposals and the orange area shows the design space of Frank.

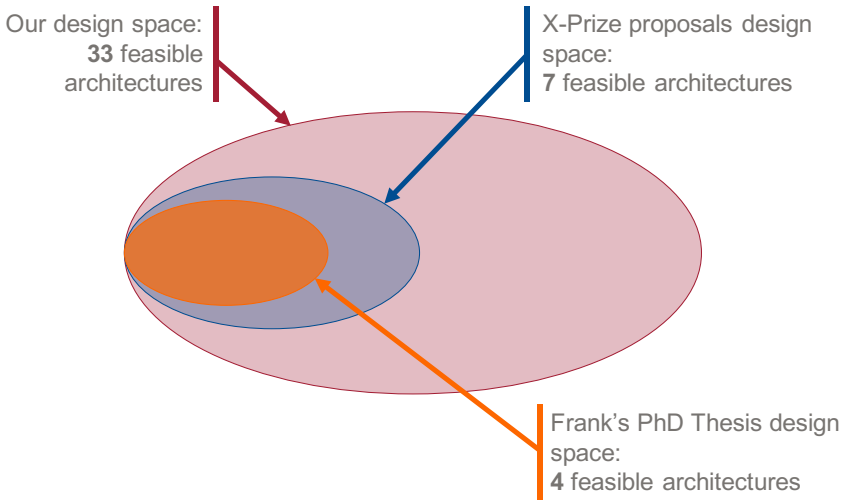

Figure 2-2: Comparison of the different design spaces

With the assumption that a "better" design can be found if the design space is larger, we have laid the foundation to discover new designs to make suborbital space tourism more affordable and safer.

We have shown in this chapter how we generated new architectures by following the four steps of (1) building a database of existing projects and ideas, (2) represent them in a morphological matrix, (3) defining the logical, reasonable and model-limitations constraints and (4) finally, enumerating the feasible architectures. We have visualized the resulting 33 architectures in an unambiguous and understandable way to communicate them to decision makers. We will use the characterization of the architectures in the morphological matrix to generate a set of design variables to optimize each of them with respect to the cost and safety metric defined in chapter 5 and 6, respectively.

3 Design space exploration methodology

We have defined our design space in chapter 2 and describe in this chapter the methodology of how we are going to evaluate this design space. It is followed by a detailed description of the design framework in chapter 4 as well as the used safety metric in chapter 5 and cost metric in chapter 6.

The overall process of the code is shown in Figure 3-1 including a reference to the chapters which describe the design framework as well as the metrics in more detail. We start on the top left with our previously defined design space. An architecture definition class takes the in-decisions-encoded architectures as an input. As all architectures have a different list of design variables, the function extracts the active design variable with their lower and upper boundary as well as the design variable type (continuous or discrete) from a generic design variable list.

These active design variables are then populated with an initial population by the Genetic Algorithm (GA). The design framework sizes the module, calculates the propulsion, the aerodynamic properties and the trajectory. This is an iterative optimization process as all four calculations depend on each other. For example, the trajectory depends on the weight of the module and the weight of module depends on the propellant needed for the trajectory. Depending on the vehicle's number of module, the design framework must be executed once or twice. As a next step, the safety submodule calculates the metric. The total launch mass metric is directly calculated by the design framework. These two metrics are the objective functions of the GA and the new generation is generated by crossover and mutation. The new population is then evaluated again by the design framework until the maximum number of generations is reached. This optimization process is done for all 33 architectures.

After each of the architectures is optimized with respect to their total launch mass and safety, the variables related to the project's operational business such as number of launches per vehicle per year (*nLaunch*) and number of operational vehicles (*numbUnits*) are varied to minimize the Overall Cost Per Participants (OCPP, see chapter 6). The OCPP has a strong dependency on the constraint variable *annualPAX*. One of the basic principles in economics is that with increasing number of flights, the cost per flight and hence per participants drops. This is because the development, production and fixed operation cost

are amortized over more flights. We use a GA to optimize the *nLaunch* and *numbUnits* variables for all pareto designs of all architecture and all number of participants.

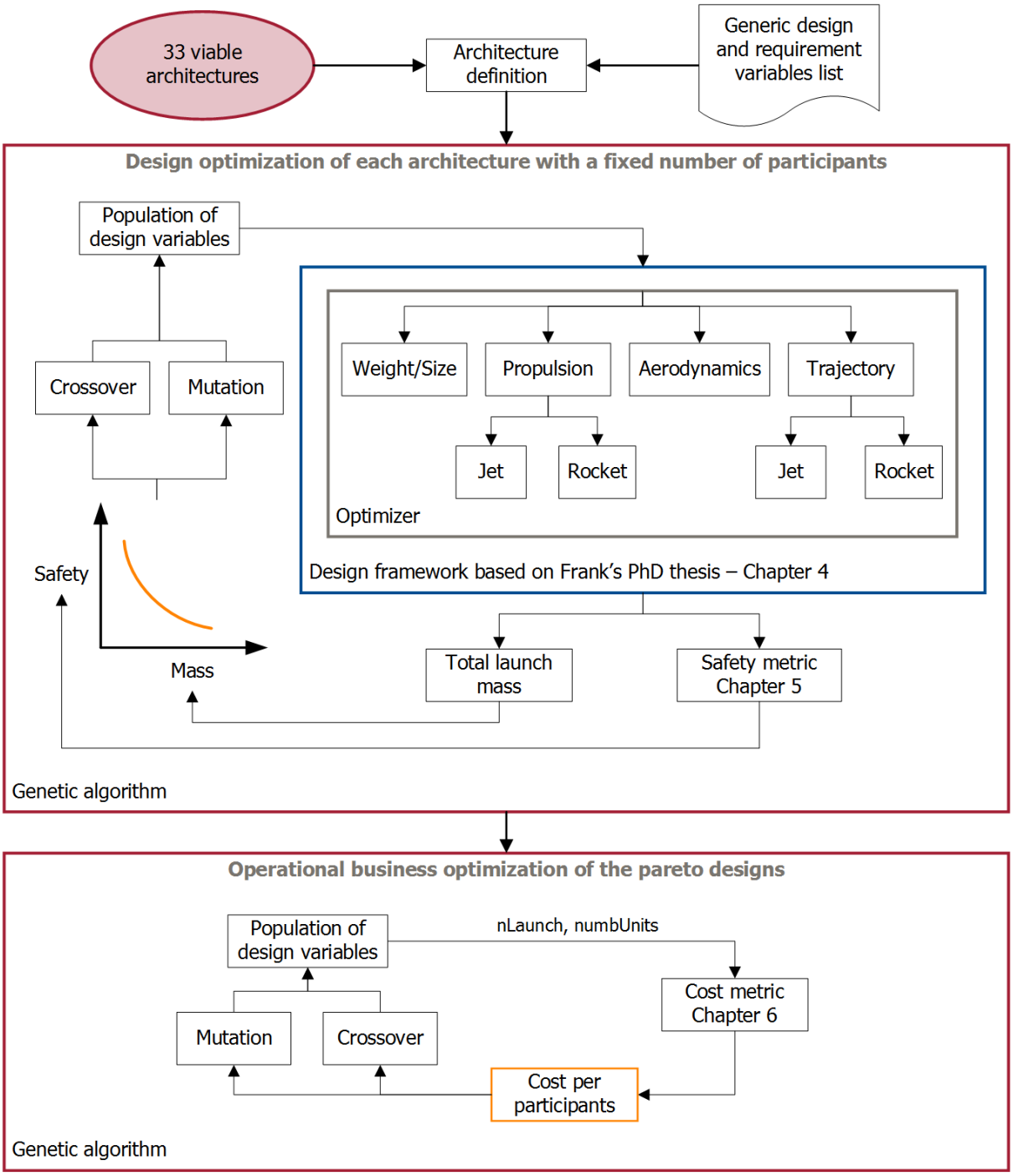

Figure 3-1: Overall process of design space exploration

The following section 3.1 describes our list of design and requirement variables for the design optimization, followed by a description of the variables for the operational business

optimization in section 3.2. The final section 3.3 of this chapter describes some aspects of a two-module vehicle evaluation.

3.1 Architecture design optimization

3.1.1 Design variables

The design variables are the key driver that define the conceptual design of an architecture. Not all architectures have the same set of design variables. We therefore generate a generic list of variables that contains the design variables of all architectures. The design variables are input parameters for the design framework to calculate the outputs needed for the metrics. Based on this connection, our list of design variables is connected to the one made by Frank [20]. If the vehicle consists of two-modules, each module has its own list of design variables.

Table 3-1 shows the generic list of 27 variables used in Matlab including the type, the used lower and upper boundaries as well as a description. They are sorted by categories starting with the variable related to the sizing (nPilots). Those who describe the mission and the distribution of the ascent energy follow (hTransition – vSep). The next set describe the parameters used for the jet engine propulsion type (nJet – TIT), followed by four variables describing the rocket engine characteristic (Propellant – Tr). The sizing parameters of the fuselage are described by diameters and length (dfus – ln). If the module has wings, five variables (Swing – TRwing) parameterize the lifting feature. The last four variables are used to describe the sweep angles and aspect ratios of the vertical and horizontal tails (sweepVTail – ARHTail).

Table 3-1: Generic design variables list

	Variable type	Lower bound	Upper bound	Unit	Description
nPilots	discrete	0	2	-	Number of pilots/crew
hTransition	continuous	1,000	18,000	[m]	Transition altitude from jet engine to rocket engine operation
vTransition	continuous	50	1,500	[m/s]	Transition velocity from jet engine to rocket engine operation
hSep	continuous	8,000	50,000	[m]	Altitude at vehicle separation
vSep	continuous	100	2,000	[m/s]	Velocity at vehicle separation
nJet	discrete	1	4	-	Number of jet engines

Tj	continuous	5,000	100,000	[N]	Maximum thrust per jet engine without afterburner
BPR	continuous	0	6	-	Bypass ratio as defined by Raymer [54]
afterburner	discrete	0	1	-	Afterburner, Yes (=1) or No (=0)
TIT	continuous	1,500	2,500	[K]	Jet engine turbine inlet temperature
Propellant	discrete	1	8	-	Rocket engine propellant type: 1=solid, 2=Lox/Lh2, 3=Lox/Rp1, 4=hypergolic, 5=Lox/HTPB, 6=Lox/Paraffin, 7=N2O/HTPB, 8=N2=/Paraffin
epsilon	continuous	2	100	-	Rocket engine nozzle expansion ratio
pc	continuous	2	12	[MPa]	Rocket engine chamber pressure
Tr	continuous	50,000	700,000	[N]	Rocket engine maximum thrust at sea level
dfus	continuous	2	5	[m]	Fuselage diameter
db	continuous	0.5	1.5	[m]	Fuselage base diameter
la	continuous	0.5	5	[m]	Length of front part: nose
ln	continuous	0.5	5	[m]	Length of back part
Swing	continuous	10	100	[m^2]	Wing surface area
tcWing	continuous	0.08	0.14	-	Wing thickness-to-chord ratio
sweep-Wing	continuous	0	1.4	[rad]	Wing sweep angle
ARwing	continuous	1	6	-	Wing aspect ratio
TRwing	continuous	0	1	-	Wing taper ratio
sweep-VTail	continuous	0	1	[rad]	Vertical tail sweep angle
ARVTail	continuous	0.1	5	-	Vertical tail aspect ratio
sweep-HTail	continuous	0	1	[rad]	Horizontal tail sweep angle
ARHTail	continuous	0.1	5	-	Horizontal aspect ratio

We provide an example set of design variables for the architecture #1 from our matrix in Table 2-6**.** It is a one module vehicle with vertical launch and vertical parachute landing. It has a rocket engine to increase energy and no wings and no jet engines. With these decisions, the architecture definition function would reduce the generic variable list. The result can be seen in Table 3-2. Since the vehicle does only have one module, there is no design variable list for the second module.

Table 3-2: Resulting design variables list for architecture #1

nPilots	discrete	**Propellant**	discrete	**dfus**	continuous
		epsilon	continuous	**db**	continuous
		pc	continuous	**la**	continuous
		Tr	continuous	**ln**	continuous

In opposite to design variables, requirements variables are settled for all architectures and are not optimized by the GA. They are constraints for the conceptual design space and described in the following section.

3.1.2 Requirement variables

The list of requirement variables is static and the values are prescribed for all 33 architectures. Our two metrics to rank the architecture are mass and risk and we optimize by using the isoperformance approach proposed by de Weck [55, 56]. The method argues that for technical system the main metrics are cost, safety and performance. Traditionally, technical system like automobiles, airplanes and spacecrafts have focused on increasing the performance. De Weck argues that the giving up the last digits in performance improvement can lead to a better design summing over all metrics. Indeed, it turns out that technical systems are often build for a certain purpose with performance requirements prescribed. The optimization objectives are then the other metrics, like reducing mass and risk. This approach is called isoperformance and is used in this thesis. The performance of transporting people to 100 km is settled by the definition of MSV we provided in the very beginning (see section 1.1). We then compare architectures that can fulfill this mission and optimize them with respect to mass and safety. The complete list of requirement variables is displayed in Table 3-3.

Table 3-3: Requirement variables list

	Value	Unit	Description
nPAX	1,4,8,16	[-]	Number of participants varied from 1 to 16
hMax	100,000	[m]	Altitude which must be reached
nMax	4	-	Maximum acceptable load factor, in multiple of the gravitational acceleration *g*
seatPitch	1	[m]	Distance between two seats
runway	4,000	[m]	Length of the runway used for horizontal landing

Besides the isoperformance variable *hMax*, there are four more requirements. The third one *nMax* defines the maximum accepted load factor in multiple of *g*. The suborbital experience should be available to a broad spectrum of the world population. NASTAR offers a Federal Aviation Administration (FAA) certified 2-day space training for future suborbital space tourist. Their customer are ages between 18-88 and have shown a pass rate of 94% [57]. The tested g-loads were 3.5 g orientated up-and-down and 6 g orientated front-front [58]. We therefore limit the load factor to 4 g.

The distance between the seats is associated with the quality of the participants' experience. The more space is available, the more the customers can enjoy their weightlessness time. The seat pitch is 1.5 m for Virgin Galactic's SpaceShipTwo, 0.91 m for the Rocketplane XP and 0.74 m for Blue Origin's New Shepard [22, 41, 43, 44, 59, 60]. We set the *seatPitch* length to constant 1 m throughout all architectures.

The *runway* requirement variable is only applicable for horizontally take-off or landing modules. The design framework calculates the required runway length for the module and the GA compares it with the defined maximum length. If the needed length exceeds the defined length, this design is no longer considered for the next generation. We define the maximum length of the runway to be 4,000 m.

3.2 Operational business optimization

3.2.1 Design variables

The operational business design variables are used by the GA to optimize the whole design space with respect to the OCPP. These variables are the same for each architecture and listed in Table 3-4.

Table 3-4: Design variables for operational business optimization

	Variable type	Lower bound	Upper bound	Unit	Description
nLaunch	discrete	2	200	launch/ year/ unit	Number of launches per vehicle per year
numbUnits	discrete	1	20	-	Number of operational vehicles

The capacity of the vehicle as well as the annual number of participants define the required number of launches per year. These number of launches can be achieved by a smaller number of vehicle with a higher launch rate or a larger fleet with a lower launch rate. The vehicles must be maintained and replaced after their lifetime is reached and therefore the production and operating cost affect the two design variables *nLaunch* and *numbUnits*. The annual number of participants is considered as a requirement variable as described in the following section.

3.2.2 Requirement variables

To optimize the operational business aspects of the pareto designs, we must constraint the problem by setting the length of the program as well as the annual demand. We vary in section 7.3 the annual number of participants and optimize for each number the *nLaunch* and *numbUnits* variables.

Table 3-5: Requirement variables for operational business optimization

	Value	Unit	Description
programLength	20	[years]	Length of the program
annualPAX	2…10,000	[-]	Maximum annual available number of participants

The *programLength* is a requirement variable related to the business model of the company. It is the duration of the suborbital program. In the first five years, the vehicle is developed and tested. It starts to be operational after the sixth year. The total duration of the program is of importance as it defines the annual amortization rate of the development costs. To produce comparable results, this variable must be constant for all architectures. We set the length of the program to 20 years.

The *annualPAXdemand* variable describes the maximum annual available number of participants. To find an appropriate value, we must know the overall market demand for a certain ticket price. In 2012 the Tauri Group published a 10-year forecast for the suborbital market (manned and unmanned) [40]. They considered three scenarios: constrained, baseline and growth. All of them have in common that around 80 % of the market is made by commercial human spaceflight (see Figure 3-2).

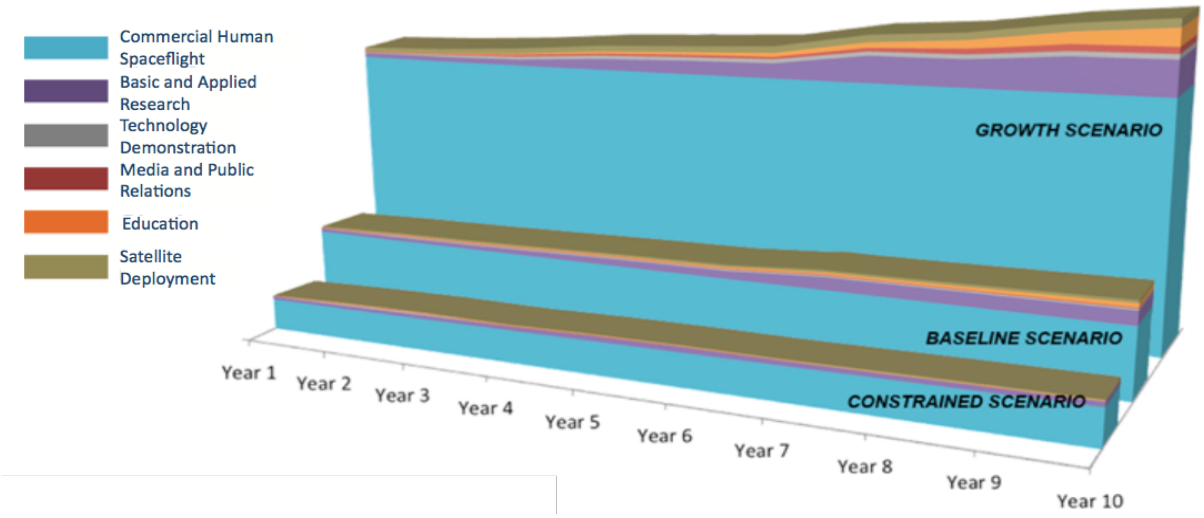

Figure 3-2: 10-year forecast of the Tauri Group [40]

The Futron Corporation conducted a study in 2002 to predicted the annual passenger demand for suborbital space tourism [61]. They surveyed 450 people with an annual income of at least $250,000 about their interest in space tourism and willingness to purchase a ticket for $100,000. Based on this data the report filters the worldwide population to get the fraction of people who are interest in taking these flights once available. A Fisher-Pry curve with a 40-year market maturity was used to model the market diffusion. Assuming 2006 to be the most plausible start year of suborbital flights, they predicted 15,000 passengers for 2021.

Four years later in 2006 the Futron Corporation published an updated report [62]. They lowered their forecast from 15,000 to 13,000 passengers for 2021 as three major changes were made to adapt the prediction to better reflect the state of the suborbital space tourism industry in that year:

- The plausible start date was moved from 2006 to 2008
- The initial ticket price raised from $100,000 to $200,000 (for the first three years, then declining to $50,000 by 2021)
- However, the growth in high net worth population has recovered from 2002 to 2006, resulting in a small increase of target population.

For the last year, 2016, the report predicts an annual passenger demand of 4,400 for a ticket price of $100,000 (see Figure 3-3).

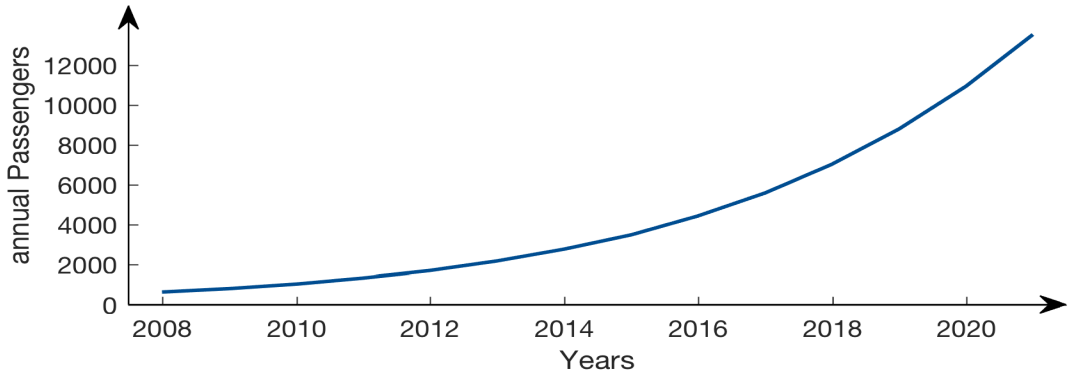

Figure 3-3: Annual passenger demand based on the 2006 Futron study [62]

The 10-year market demand forecast from the Tauri Group has included a price elasticity curve [40]. The relationship was developed for individuals with at least $5 million in investable assets. Figure 3-4 shows the price elasticity curve assuming the predicted demand of 4,400 passengers for a ticket price of $100k. If the ticket price increases, the demand is reduced to a few several hundred participants per year. The opposite effect is true for decreasing ticket prices.

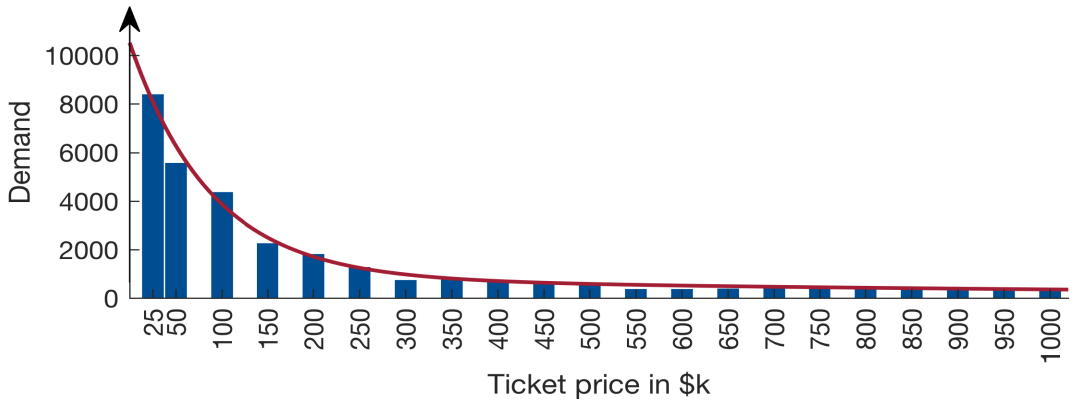

Figure 3-4: Price elasticity based on a 2012 study from the Tauri group [40]

For possible further computational implementation, a double exponential regression is developed (red curve). It reads

$$n_{PAX_i} = 9668 \cdot \exp(-1.135 \cdot 10^{-5} \cdot x_i) + 852.3 \cdot \exp(-8.594 \cdot 10^{-7} \cdot x_i) \qquad (3\text{–}1)$$

with x_i being the ticket price in \$ and n_{PAX_i} the annual passenger in period i. The coefficient of determination is $R^2 = 0.9865$.

Giving the uncertainty and year of these studies, it seems unreasonable to use these data during the optimization. The result would depend on the quality of these predictions. However, we use these studies to determine an annual passenger demand for our requirement variable. Given the fact that Virgin Galactic already sold 700 tickets [8], and Blue Origin plans to be operational 2018 [63], it seems reasonable that the fictive company or project inside a company may have an annual passenger demand of around 1,000. With the assumption of a ticket price of \$100k, this would result in a market share of around 22%.

3.3 Evaluation of a two-module vehicle

To evaluate a two-module vehicle, the design framework must be executed twice for each module and the trajectory split up before the evaluation. The safety and cost metric is calculated afterwards. The separation point of the two modules is defined by the altitude and the velocity as can be seen in Figure 3-5. Both variables are active design variables for a two-module vehicle and optimized by the GA. If there is just a one module vehicle, then this altitude does not exist and is not a design variable during the GA optimization.

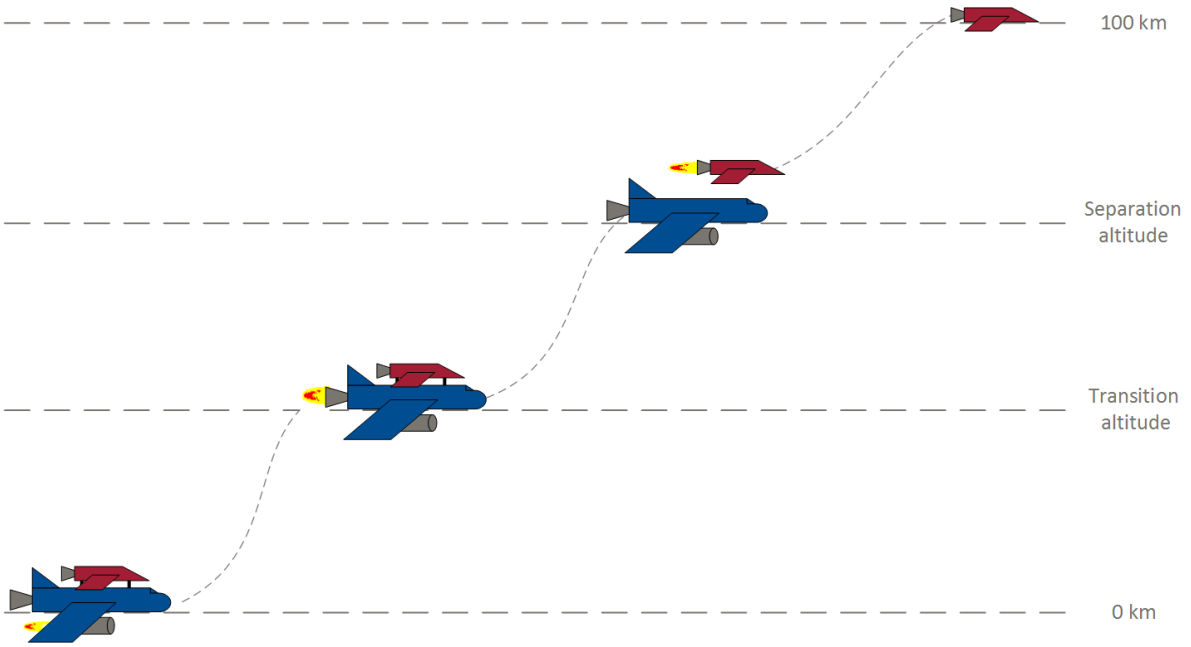

Figure 3-5: Separation and transition altitude for a two-module vehicle

The design framework first evaluates the second module and then the first module. It takes the mass and the aerodynamic parameter of the second module into account during the execution of the first module. If the second module has no propulsion, only the separation altitude is an actives design variable for the GA and the velocity is calculated by the design framework of the second module. In this case, the second module is on a ballistic trajectory and this trajectory is fully defined by the maximum altitude and the separation altitude. The separation velocity is an output variable of this trajectory calculation and an input variable for the first module (together with the mass of the second module and its aerodynamic properties).

Furthermore, if a module has either, a rocket and a jet engine, there is an additional transition velocity and altitude which is optimized. The definition of the corresponding variables is shown in Figure 3-5. It is assumed that if the module has a jet engine and a rocket engine, it launches with just the jet engines until the transition altitude, shuts down the jet engines and uses the rocket engine for the remaining ascent. We do not consider simultaneous operation of both engines types. If the first module only has a jet engine or a rocket engine, there is no active design variable for the transition altitude and velocity.

If the first module does only have jet engines, the upper boundary of the separation velocity is set to the maximum design velocity of jet engines which is Ma = 2 or around v = 600 m/s for an altitude of 12,000 m. This a typical service ceiling altitude of jet engines [64].

4 Design framework

The design framework evaluates the module according to the input design variables. It consists of four submodules, the weight/size, the propulsion, the aerodynamics and the trajectory submodule as can be seen in Figure 4-1. The propulsion as well as the trajectory calculations are further depicted into jet and rocket engine part.

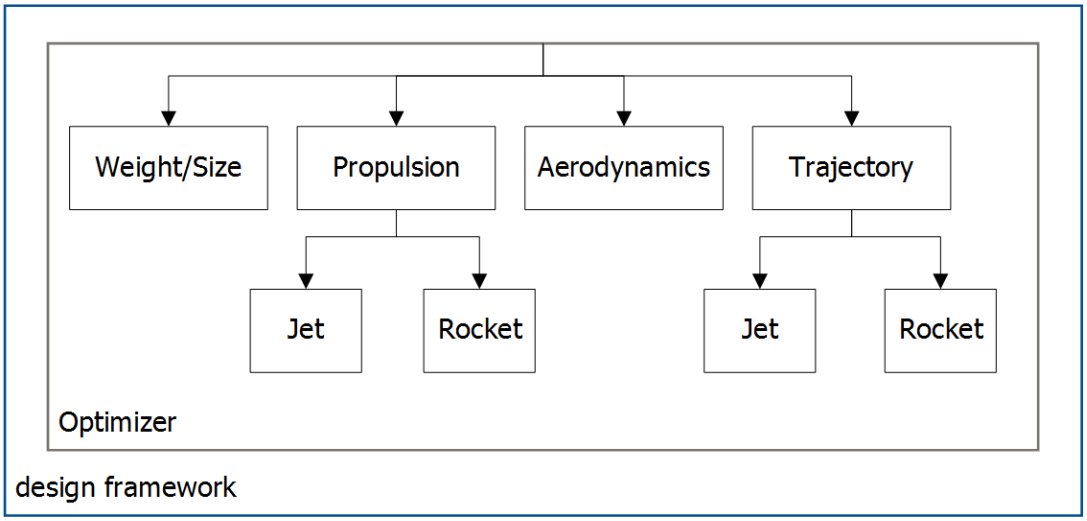

Figure 4-1: Overview design framework

Our design framework is mainly based on Frank's code. The following four subsections aim to describe the main idea behind the submodules. The aspects that differ from Frank's design framework are described in more detail. For a detailed description and validation of the common parts refer to the PhD Thesis of Frank [20].

The optimizer for the design framework varies the propellant/fuel masses and the burn time for the rocket engines until the relative deviations with the previous guesses is below a defined limit.

4.1 Weight and Sizing

Frank based the physical decomposition of the module on Rohrschneider [65]. There are 19 subsystems for the airframe: fuselage, thrust structure, nose, Thermal Protection System, wing, landing gear, horizontal tail, vertical tail, hydraulics, parachute and retrorockets, Reaction Control System, avionics, Environment Control and Life Support System, primary power system, flight control, electrical systems, seats and accessories, parachute, and unused liquids. There are interdependence effects between these subsystems, so that a

loop must be performed to ensure consistency. This process is schematically shown in Figure 4-2 with ϵ being the relative deviation between the total weight from the current loop and the one from the loop before. The maximum allowed deviation is set to 0.1%. The weight and size estimation of the rocket and jet engine is part of the propulsion submodule and is described here in section 4.2.

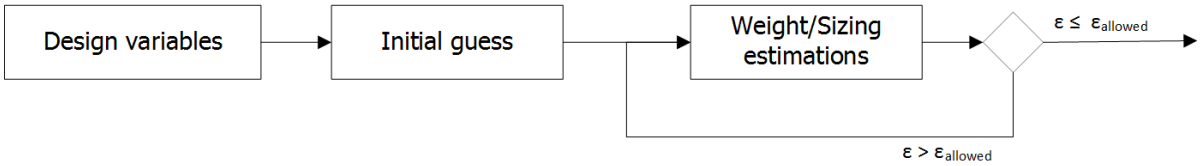

Figure 4-2: Iteration process inside the weight/size estimation submodule [20]

Additional weights depending on landing method

The landing methods can be parachute, rocket powered, gliding and horizontal powered. For the parachute method, the most energy is decimated by the parachute. However, the landing impact must be attenuated by an additional system, e.g. retrorockets, airbags or pneumatic actuators. The weight of this systems is around 2 – 3% of the overall landing weight [24]. We are conservative and reserve 3% for these impact attenuation systems.

In the rocket powered method, a rocket engine is fired in the opposite direction of the flight directions. Usually, the same rocket engine used for ascent is used during landing. The additional propellant needed for the powered landing is calculated as part of the rocket trajectory in section 4.4.2. Until now, two companies, SpaceX and Blue Origin have demonstrated to perform this landing method [4, 43]. Either use additional aerodynamic guiding and aerobrake systems to decimated the initial energy and save propellant. To account for these systems, we reserve 5% of the empty weight of the module.

4.2 Propulsion

4.2.1 Jet engines performance and weight/size

The jet engine submodule models both, the performance and the weight for conceptual design space exploration. Frank based his code on Raymer's [54] series of statistical equations to estimate the empty weight, the length, diameter and the Thrust Specific Fuel Consumption (TSFC). The four main input variables are the take-off thrust, the bypass ratio,

the maximum Mach number and the presence of an afterburner. One additional key parameter is the turbine inlet temperature (TIT). Increasing TIT needs more expensive materials and better cooling techniques, both drives cost. But it also increases the efficiency of the engine and therefore reduces the TSFC [66]. Boggia and Rud [67] have shown the impact of the TIT on the TSFC as a function of the bypass ratio. To integrate this into the Raymers approach, Frank [20] generated a Response Surface Equation (RSE).

4.2.2 Rocket engine performance and weight/size

For the SpaceShipTwo, the weight of the rocket engine accounts for around one third of the module's empty weight [20]. Depending on the architecture and the design parameters the propellant weight can surpass the empty weight. The sensitivity of the propellant weight with respect to the rocket engine performance parameters makes it necessary to develop a more physics-based analysis to increase accuracy. This is done for all three types of rocket engines - solids, liquids and hybrids.

Frank uses the approach of Design of Experiment (DoE) and Response Surface Methodology (RSM) to develop a performance, weight and size estimation tool as depicted in Figure 4-3. Cycle-based or component-based approaches need to many input variables or take too long to run. The points in the interior design space are sampled with the Latin Hypercube method. A least square regression is used to approximate the behavior of the responses using RSM. The surrogated models derived from the DoE represent ideal values and do not account for friction effects, heat transfer, imperfect gases, no axial flow, no uniformity of the fluid and shifting gas composition. By introducing a correction factor the model can be calibrated with existing engines. The value ranges from 0.93 for solid engines, 0.92 - 0.96 for liquid engines and 0.76 – 0.83 for hybrid engines [20, 68-71]. The lower real efficiency of hybrid engines is due to mixing losses of the oxidizer and the solid fuel. A mean relative error for the performance of 2.6 % could be achieved [20]. The weight estimation is done with surrogated and physics based models depending on the engine type. The total rocket engine empty weight includes thrust chamber, tanks and support structure in the case of liquid rocket engines and for hybrid engines additional the weight of the pressuring gas and its tank.

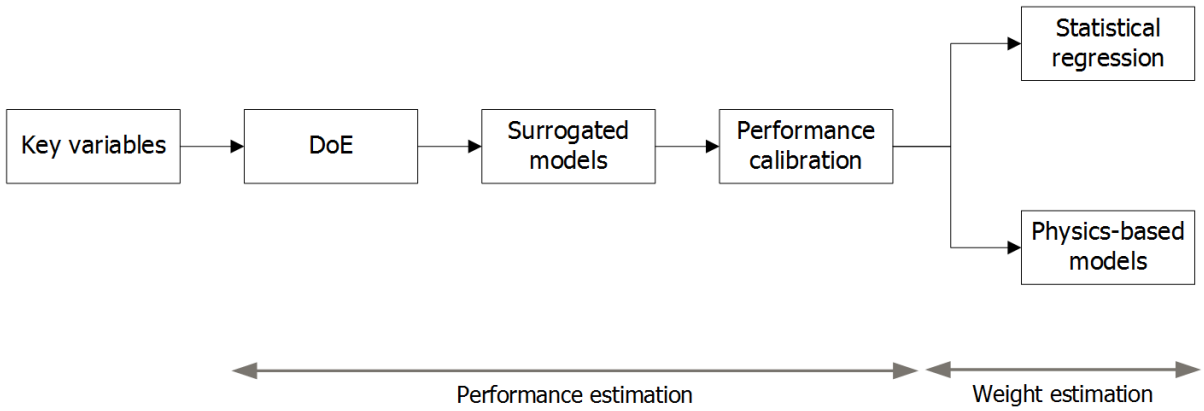

Figure 4-3: Approach for the rocket engine performance and weight/size estimation [20]

4.3 Aerodynamics

The aerodynamic model estimates the drag and lift coefficients for all flight regimes for all possible architectures. Frank built his model upon the one developed by Roskam [72]. These coefficients are particularly difficult to predict for the transonic flow regime compared to the well-known behavior for the subsonic and supersonic regimes. For conceptual analysis, Raymer [54] proposed an approach based on experimental measurements for the transonic flow regime.

Following the approach of Roskam [72], the module drag coefficient is depicted into eleven components: wing drag coefficient, fuselage drag coefficient, empennage drag coefficient, nacelle/pylon drag coefficient, flap drag coefficient, landing gear drag coefficient, canopy/windshield drag coefficient, store drag coefficient, trim drag coefficient, interference drag coefficient and miscellaneous drag coefficient which includes speed brakes, struts, inlets, antennas, gaps and surface roughness. For either, the subsonic and supersonic flow regime Frank [20] developed surrogated models to cover the entire design space. This approach can be seen in Figure 4-4 where he first extracts a data table from the multidimensional plots provided by Roskam [72] and then developed surrogate models to speed up computation.

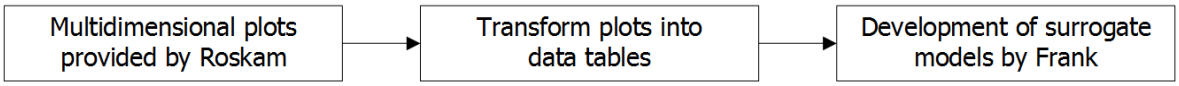

Figure 4-4: Subsonic and supersonic drag estimation process

As suggested by Raymer [54], the subsonic and supersonic lift coefficients are linked by parametric interpolation. This approach has several rules:

- The drag coefficient at Mach 1.2 equals the one at Mach 1.05
- The drag coefficient at Mach 1 is half the one at Mach 1.05
- The drag coefficient has a smooth behavior over the entire regime
- The drag coefficient is linear between Mach 1 and Mach 1.05

Frank used this approach in his code and divided the transonic regime into three ranges: from Mach 0.6 to Mach 1, Mach 1 to Mach 1.05 and Mach 1.05 to Mach 1.2. As the drag coefficient submodule is called during each trajectory optimization step, it appeared to be time a time-consuming approach. Therefore, Frank [20] developed a surrogated model as a function of altitude and Mach number for the considered module. Seven coefficients are necessary to describe the aerodynamic behavior of the module. These coefficients are determined by computing the drag coefficient for five different Mach number and two different altitudes and then passed on to the trajectory optimization submodules.

4.4 Trajectory

The purpose of the trajectory submodule is to calculate the required propellant and fuel for the module to reach the required altitude and velocity. If it is the last module of the vehicle, the required altitude is the maximum altitude of 100 km and the velocity is zero. If it is the first module of a two-module vehicle than the required altitude and velocity is the one of the separation point.

4.4.1 Jet engine Trajectory

A traditional aircraft mission consists of take-off, climbing and landing. For horizontal take-off modules, it is necessary to know the take-off performance to quantify if the module can land on the constraint runway length. Frank [20] implemented the *magic line* approach of Shevell [73] with a 15% margin. A similar approach is proposed by Boiffier [74] for the landing distance if the aircraft is equipped with an Antilock Braking System (ABS). The total fuel consumption during a mission for a jet engine module consist of the climb phase, the required fuel to reach the required separation velocity and the fuel consumption of horizontal powered landing. These three contribution are described hereafter.

4.4.1.1 Climbing phase

The climb phase with jet engine is calculated by assuming it is performed at the maximum climb rate (ROC_{max}). This approach is usually used by commercial aircrafts to minimize the

time spent in the climbing phase. The ROC_{max} is defined by Anderson [64] and depends on the altitude and the weight. An iterative process is performed to calculate the fuel consumption from the initial to the required altitude. The fuel consumption can be calculated by multiplying the TSFC with the duration of the iteration, the thrust per jet engine and the number of engines (see equation (4–5)). As displayed in Figure 3-5, the separation point is defined by both, the altitude and the velocity. With the approach of the ROC_{max} the required altitude can be reached but it is not ensured that also the velocity matched the required separation velocity. To account for this, we developed a model to considered the fuel consumption to accelerate from the velocity at the end of the climb phase to the separation velocity. This approach is described hereafter.

4.4.1.2 Reaching the required separation velocity

Once the required altitude is reached, the module must accelerate to reach its required velocity for separation. This acceleration occurs at a constant altitude which means that the lift forces equal the weight forces as can be seen in Figure 4-5. To accelerate the thrust must be greater than the drag.

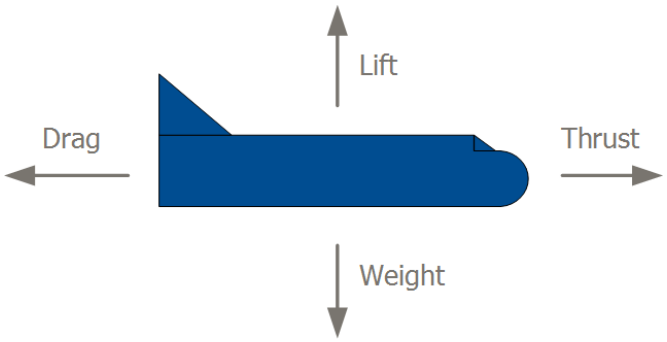

Figure 4-5: Four forces on an airplane

Using Newton's third law, the acceleration of the airplane equals the external forces, thrust T and drag D:

$$m\frac{dv}{dt} = T - D \qquad (4\text{–}1)$$

If we separate the variables we obtain

$$\frac{1}{T-D}dv = \frac{1}{m}dt \qquad (4\text{–}2)$$

Formal integration from the initial point 0 to 1 leads to

$$\int_{v_0}^{v_1} \frac{1}{T-D}\,dv = \int_{t_0}^{t_1} \frac{1}{m}\,dt \qquad (4\text{–}3)$$

If we assume that for small steps the mass, the thrust and the drag is constant we finally have an equation for the duration of the time interval:

$$\Delta t = \frac{m \cdot \Delta v}{T-D} \qquad (4\text{–}4)$$

And the fuel consumption for this time interval is

$$m_{fuel} = c_{TSFC} \cdot \Delta t \cdot T \cdot n_{jet} \qquad (4\text{–}5)$$

Numerically, the velocity difference between the required velocity and the velocity at the end of the climb is broken down into small intervals where the assumption of constant mass, thrust and drag is valid.

4.4.1.3 Fuel consumption for horizontal powered landing

For a horizontally powered landing module, there is additional fuel consumption of the jet engines due to the idle thrust during the approach and flare. If the jet engine is equipped with thrust reversers, additional fuel is needed. They produce a negative thrust of around 40-50% of the maximum thrust [54]. Frank [20] reserves 0.5% of the empty weight of the module for the fuel consumption for horizontal powered landing. We follow this approach.

4.4.2 Rocket Trajectory

During the ascent of a rocket to Low Earth Orbit (LEO), three main losses must be considered, steering losses with $\Delta v \approx 0.05 km/s$, drag losses with $\Delta v \approx 0.4 km/s$ and gravity losses with $\Delta v \approx 1.0 km/s$ [36]. It is the objective of an ascent optimization to reduce the sum of these losses under given constraints and to calculate the required propellant mass.

As can be seen from equation (4–8), the gravity acceleration is integrated over the powered flight time. This means that the resulting losses are proportional to the powered flight time and therefore increase with a slower ascent or decrease with a faster ascent, respectively. Strictly speaking, the drag losses are integrated over the total time of the

ascent including the powered flight time and the unpowered flight time after engine shut-off. Due to the exponential decrease of the air density with increasing altitude and therefore decreasing drag, the drag losses for the unpowered flight are small compared to the other losses [36]. We therefore integrate the drag losses for the powered flight time. As seen in equation (4–10), the drag force depends on the drag coefficient, the area, the density and the velocity. With increasing altitude, the density decreases and the velocity increases. If we consider a slower ascent, then the velocity is smaller and therefore the total drag losses. The vise-versa argument can be made for a faster ascent. Hence, we can general argue that the drag losses increase with a faster ascent whereas the gravity losses decrease.

To solve this ascent optimization problem one solution is to use the gradient based solver *fmincon* from Matlab as proposed by Frank [20]. A run time investigation shows that around 95% of the design framework evaluation are caused by optimizing the trajectory. This is impractical to explore a large architectural design space and seems unnecessary as the main output of the trajectory module is the needed propellant for the ascent to iterate with the sizing and weight module until convergence is accomplished. This section aims to describe a new approach how the propellant mass can be estimated with a fraction of computational effort while remaining accuracy. First, we give a short background on the theory and the needed equations, followed by a description of the assumptions and the proposed approach. The approach is validated as part of the whole design framework in section 4.5.

Background theory

In general, the required propellant mass m_p is given by the rocket equation to

$$m_p = m_F \left(e^{\frac{\Delta v_{tot}}{Isp \cdot g_0}} - 1 \right) \qquad (4\text{–}6)$$

with

m_F: Final mass after engine shut off in [kg]
Δv_{tot}: Total Δv needed to reach the destination in [m/s]
Isp: Specific impulse of the engine [s]
g_0: Standard gravitational acceleration, 9.81 [m/s^2]

The needed delta-v is the sum of the energy difference and the losses. It reads with the specific energy being the sum of the potential and kinetic energy $E_s = g \cdot h + 0.5 \cdot v^2$:

$$\Delta v_{tot} = \sqrt{2 \cdot (E_{s,F} - E_{s,0})} + \Delta v_{tot,losses} \quad (4\text{–}7)$$

with

$E_{s,F}$: Final specific energy at the end of the burn time in [J/kg]

$E_{s,0}$: Specific energy at the start of the burn time in [J/kg]

The total losses are defined by equation (4–8) with all variables except of the thrust depended on the time and altitude, respectively [36].

$$\Delta v_{tot,losses} = \underbrace{F_* \int_0^{t_F} \frac{1 - cos\alpha}{m} dt}_{steering\ losses} + \underbrace{\int_0^{t_F} \frac{D}{m} dt}_{drag\ losses} + \underbrace{\int_0^{t_F} g \cdot sin\gamma\ dt}_{gravitational\ losses} \quad (4\text{–}8)$$

with

t_F: End time of trajectory

F_*: Thrust in [N]

α: Thrust/steering angle [°]

m: Mass of vehicle in [kg]

D: Drag of vehicle in [N]

g: Gravitational acceleration in [m/s^2]

γ: Flight path angle [°]

The gravitational acceleration is indirect proportional to the distance from the surface and is given by equation (4–9) with $r_E = 6378\ km$ being the radius of the earth.

$$g(h) = g_0 \cdot \left(\frac{r_E}{r_E + h}\right)^2 \quad (4\text{–}9)$$

The drag depends on the drag coefficient, the area, the density and the velocity and is given by the succeeding equation. In contrast to the gravitational acceleration, generally no explicit relationship between the drag and the altitude can be given. The drag coefficient has a complex dependency on the Mach number and the altitude.

$$D = 0.5 \cdot C_D(Ma, h) \cdot A \cdot \rho(h) \cdot v^2 \quad (4\text{–}10)$$

with

C_D: Drag coefficient [-]

A: Wetted area [m^2]

ρ: Density of the air [kg/m^3]

v: Velocity of the vehicle [m/s]

Assumptions

It can be interfered from the equation (4–8) that the steering losses are zero if the thrust is in the direction of the flight path ($\alpha = 0$). MSV do not need to perform great changes in the trajectory and therefore the thrust angle will be close to zero. This together with the fact that the overall losses are small compared to the other two justifies that we do not consider steering losses.

Furthermore, common trajectories have a flight path angle $\gamma \approx 90°$ for the first phase of the ascent [36]. The goal is to escape the gravitational field of the earth as quick as possible to reduce the gravity losses. We assume this optimum path for our vehicle and assume a constant flight path angle of 90°. This reduces equation (4–8) to:

$$\Delta v_{tot,losses} = \int_0^{t_F} \frac{D}{m} dt + \int_0^{t_F} g \, dt \qquad (4\text{–}11)$$

Equation (4–8) already implied that the thrust is independent of time or altitude [36], we can therefore calculate the acceleration at the start and end of the rocket engine:

$$a_0 = \frac{F_*}{m_0} \quad \text{and} \quad a_F = \frac{F_*}{m_F} \qquad (4\text{–}12)$$

With the assumption that the acceleration increases linear over the burn time of the engine, we can calculate the acceleration at any given time by

$$a(t) = a_0 + \frac{t}{t_F} \cdot a_F \qquad (4\text{–}13)$$

Proposed approach

Our approach splits the powered flight time into 500 sub steps. The start and final altitude (and therefore the altitude increment) depend on the architecture and the design variables. We can see the drag, mass and gravitational acceleration from equation (4–11) as constant during these time intervals. The integrals can be solved and we obtain for each uniform time interval:

$$\Delta v_{tot,losses_i} = \frac{D_i}{m_i} \cdot \Delta t + g_i \cdot \Delta t \qquad (4\text{–}14)$$

The total losses are then the sum of the individual losses:

$$\Delta v_{tot,losses} = \sum_i \Delta v_{tot,losses_i} \qquad (4\text{–}15)$$

To calculate the losses, we must know the drag, mass and gravitational acceleration. The drag depends furthermore on the velocity and altitude. The following describes how we calculate these variables.

If we integrate equation (4–13) above, we obtain the velocity as a function of the time into flight with the initial velocity v_0:

$$v(t) = \int a(t)\, dt = v_0 + a_0 \cdot t + \frac{t^2}{2 \cdot t_F} \cdot a_F \qquad (4\text{–}16)$$

With this relationship and a known v_F, we can calculate the flight time t_F by rearranging the equation:

$$t_F = \frac{v_F - v_0}{a_0 + \frac{a_F}{2}} \qquad (4\text{–}17)$$

The increment increase in altitude is given by

$$\Delta h = v(t) \cdot \Delta t \qquad (4\text{–}18)$$

The assumption of constant thrust results in a constant propellant mass flow $\dot{m}_P$. This is equivalent to a linear mass decrease of the vehicle which can mathematically written as

$$m(t) = m_0 - \frac{t}{t_F} \cdot \underbrace{(m_0 - m_F)}_{m_P} \qquad (4\text{–}19)$$

Using these equation, we can calculate the total losses of the ascent and have all variables to calculate the total delta-v needed in (4–7). Finally, the rocket equation (4–6) can be used to calculate the needed propellant mass. With the new propellant mass, we can also calculate the new burn time:

$$t_{F,new} = \frac{m_{P,new} \cdot Isp \cdot g_0}{F_*} \qquad (4\text{–}20)$$

The outside sizing loop iterates the burn time and the propellant mass until the relative deviation between the new guess and the guess from the previous iteration is below a defined limit. This approach will be validated as a part of the design framework in section 4.5. The average single execution time for this rocket trajectory calculation is around 0.002s compared to around 0.2s for the fmincon approach of Frank [34]. As 95% of the computational time was used for the rocket trajectory calculation, the time for the overall design framework evaluation could be reduced by a factor of 95.

Implementation of the trajectory optimization

For implementation of this approach, three different cases must be considered. They are described hereafter.

1. The module can have wings or not which influences the gravity and drag losses. In case of wings, the gravity losses are set to zero and the drag losses include the drag due to lift production of the wing. If the module has no wing, the gravity losses are considered and the drag loss is limited to the parasite drag.

2. Depending on the configuration, the drag of the different modules must be considered in the trajectory calculation. An overview flow chart is given in Figure 4-6. If the module is the last module of the vehicle, this can be the first module of a one-module vehicle or the second module of a two-module vehicle, only the drag of the current module must be considered. If it is the first module of a two-module vehicle, we must consider the drag contributions from both modules in the calculations.

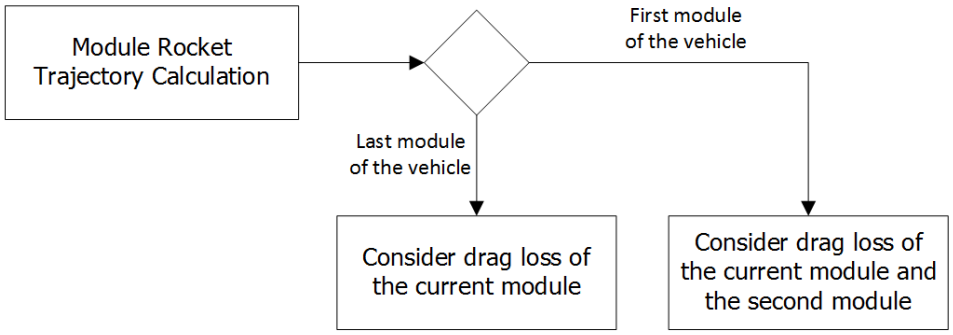

Figure 4-6: Flow chart to assess the consider drag contributions depending on the vehicle configuration

3. If the module is the first module of a two-module vehicle, then the final altitude and velocity are prescribed and optimized by the GA and corresponds to the start values for the second module. In the other case, for the second module of a two-module vehicle or for the first module of a one module vehicle, only the maximum energy needed to reach 100 km is prescribed but no velocity and altitude at burn out time.

4.4.3 Additional propellant for rocket powered vertical landing

This section aims to describe the calculation of the reserved propellant for the final vertical powered landing. We cannot integrate the needed delta-v in the ascent equations since the empty weights can be different. This is for example the case for the Blue Origin architecture. The first module propels both modules during the ascent, but it lands separately from the second module and therefore the rocket equation (4–6) has different masses.

If the rocket powered landing is chosen, we first calculate the needed propellant for the landing and then update the final mass m_F for the rocket trajectory ascent calculation. The landing burn must decimate the kinetic and potential energy. Like the ascent, the gravitational acceleration is a loss, whereas the drag force helps to reduce the energy. As described under the weight and sizing sub-module in section 4.1, we consider additional aerodynamic decelerators to reduce the initial energy. We estimate the required delta-v by analyzing Blue Origin's New Shepard flight #5 [75]. We found that the rocket engine fires at an altitude of 1,500m with a remaining vertical velocity of 160 m/s. The total burn time is 25s with the last few second hovering above the ground. With these data, the specific energy at ignition can be calculated and translated into a delta-v:

$$E_S = g \cdot h_{Ignition} + 0.5 \cdot v_{Ignition}^2 = 27{,}515 \frac{J}{kg} \quad (4\text{–}21)$$

$$\Delta v_{energy} = \sqrt{2 \cdot E_S} = 235 \frac{m}{s} \quad (4\text{–}22)$$

Assuming a constant gravitational acceleration, the gravity losses can be calculated by

$$\Delta v_{G-losses} = \int g \, dt = g \cdot t_{burn} = 245 \frac{m}{s} \quad (4\text{–}23)$$

The total delta-v can be calculated by summing both previous contributions and subtracting the drag part. If we would neglect the energy reduction due to drag, the total landing delta-v would be 480 m/s. To accurately calculate the drag losses, we would have to know the contribution of the aerodynamic decelerators discussed before. Since this thesis focuses on the conceptual design space exploration, this could not be assessed with the data provided by the model. We rather estimate the drag losses to be around 80 m/s for the Blue Origin booster. This results in a total delta-v of 400 m/s for the rocket powered landing:

$$\Delta v_{landing} = \Delta v_{energy} + \Delta v_{G-losses} - \underbrace{\Delta v_{drag}}_{80 \frac{m}{s}} = 400 \frac{m}{s} \quad (4\text{–}24)$$

We use this number throughout the design space for all architectures which have rocket powered landing as the landing method. By using the rocket equation (4–6) with the final mass m_F being the empty weight of the module, we can calculate the required propellant mass for landing. For Blue Origin, assuming an empty weight of 10,000kg and an Isp of 350s, this reads:

$$m_p = m_{Empty} \left(e^{\frac{\Delta v_{landing}}{Isp \cdot g_0}} - 1 \right) = 1{,}236 \, kg \quad (4\text{–}25)$$

This mass does not include any margin as the weight and sizing module account for margins for the propellant. Refer to Frank [20] for further details on the considered margins. The calculated delta-v values and the propellant mass of Blue Origin matches well the estimations from divers online forums [76, 77].

4.5 Validation of the Framework

The three projects of Virgin Galactic, Blue Origin and Rocketplane XP are used to validate the design framework's weight, sizing, jet and rocket trajectory optimization features. We use the take-off mass of these vehicles to compare them with the results from the design framework (see Table 4-1). Due to the lack of funding, no prototype of the Rocketplane XP exists and therefore no measured take-off mass is available. However, the company did a more detailed design study and data is available on their official webpage and other sources. Both, the New Shepard and the SpaceShipTwo are in the test phase but no take-off weights are publicly available. We have provided several sources for each project in the table, they vary from newspaper articles to online forum discussions. The used input design and requirement variables including the references are listed in annex A.7.

Table 4-1: Overview design framework validation

	Reference [kg]	**design framework [kg]**	**relative deviation [-]**
Blue Origin's New Shepard	35,000 [76, 77]	32,710	6.5%
SpaceShipTwo	9,740 - 13,608 [78, 79]	13,495	0.8% w.r.t. 13,608 kg
Rocketplane XP	8,840 - 9,072 [59, 80, 81]	9,641	6.3% w.r.t. 9.072 kg

The table shows relative deviations between 1 and 7% depending on the vehicle. Given the range and uncertainty in the sources, this is a highly accurate result, especially for conceptual design space exploration methods with this variety of features. The next two chapters aim to describe the safety and cost metric.

5 Metric I - Overall Residual Safety-Risk Metric (ORSRM)

The architectural decisions have significant and lasting impact on how safe the system can be build. However, practical methods for quantitative analyzing the safety, like the top-down Fault Tree Analysis (FTA) or the bottom-up Failure Mode and Effect Analysis (FMEA) are hardly applicable in conceptual scenario trades [82-84]. The tragic example of the Space Shuttle's accident *Challenger* shows how the early architectural decision of not including a crew escape system influenced the overall safety of the launch system. There was no cost-effective way to add a crew escape system after the orbiter was already developed [83, 85, 86].

Common assessment methods treat risk as a combination of likelihood and severity, where the operand *x* somehow combines these two factors into a risk metric:

$$c_{Risk} = c_{Severity}\ x\ c_{Likelihood} \qquad (5\text{–}1)$$

In early architectural design exploration, the **severity** can be estimated by considering the worst possible consequences of the hazard. Whereas, **likelihood** is mostly unknown and unknowable for complex new systems, especially without knowing a detailed design.

Therefore, a new approach is defined by Leveson [82-84]. Instead of likelihood, the **hazard mitigation potential** of each architecture is used. It can be computed by following these three steps:

1. Identification of the system-level hazards and associated severities
2. Identification of mitigation strategy and associated impact
3. Calculation of the Overall Residual Safety-Risk Metric (ORSRM) for the given architectures

These steps are described in the following sections 5.1-5.3.

5.1 System-level hazards and associated severities

The identification of hazards in the earliest stages of a program is often called Preliminary Hazard Analysis (PHA) and is updated throughout the development process. It is a two-step process involving:

1. Determining what hazards might exist during operating of the system
2. Quantification their relative magnitude with a severity factor for each category

Dulac et al. discovered four categories for the Safety-Risk analysis of NASA's space exploration architectures [83]. These are (1) Human, (2) Mission, (3) Equipment and (4) Environment. Initially, the environment component was included in the hazard log but left out in the end. The NASA project manager decided to make it a requirement that each architecture must be compliant to the NASA's planetary protection standards. We follow this approach and consider the protection of our environment as a mandatory requirement for all MSV. Furthermore, we do not consider Mission as a separate category, since MSV's main objective is to provide an experience for their passengers. If a human is severely injured, major mission objectives are incomplete. The same reasoning can be applied for the Equipment category. Table 5-1 shows the remaining category human with the scale developed by Leveson [83].

Table 5-1: Hazard severity scale for the categories human

Severity factor s_h	Human (H)
4	Loss of life
3	Severe injury
2	Minor injury
1	Less than minor injury

The first step is to identify the hazards that might occur during operation of the system. For some specific systems, the government agencies have mandated hazards. For example, the U.S. Department of Defense prescribes a minimum baseline of hazard which must be considered when constructing nuclear weapon system [83]. However, in most cases the hazards must be determined by analyst. There are a few structured ways to enable individuals or a group of people to apply their knowledge (e.g. with *what-if* questions). For an extensive list of possible activities refer to *Safeware* [82]. Especially in the space sector there are public available generic hazards lists, which can be used to identify high level system hazards.

Grounded on NASA's generic hazards lists for the Space Shuttle [87] and the Constellation Program [88], we derived a list of system-level hazards. Table 5-2 shows them organized by mission phase, starting with the general applicable hazards and followed by the ascent as well as descent phase. For the second step, we assigned to each hazard a severity factor with the justification provided in Table 5-3. The A2 and D2 hazard has an identical justification reason d).

Table 5-2: System-level hazard list with associated severity factors

ID	Phase	Hazard	s_h
G1	General	Flammable substance in presence of ignition source (Fire + Explosion)	4[a)]
G2	General	Loss of life support (including power, temperature, oxygen, air pressure, CO2, food, water, etc.)	3[b)]
A1	Ascent	Incorrect propulsion/trajectory/control during ascend	3[c)]
A2	Ascent	Loss of structural integrity (due to aerodynamic loads, vibrations, etc.)	4[d)]
A3	Ascent	Failure of stage separation	4[e)]
D1	Descent	Incorrect propulsion/trajectory/control during descent	4[f)]
D2	Descent	Loss of structural integrity (due to inadequate aerodynamic loads, vibrations, etc.)	4[d)]

Table 5-3: Justifications for the severity factor assignment

	Justification
a)	If a fire or explosion on board of the vehicle occurs, this hazard leads most likely to a loss of crew as there is generally no easy escape path.
b)	If the vehicle losses its life support system, the passengers are exposed to the environment without the initial protection. Depending on the mission phase, the environment may severely injure the crew.
c)	Depending on the impact of the propulsion, trajectory or control malfunction, the crew can be severely injured. But the malfunction does not necessary lead to a loss of crew. That is why we assigned a severity factor of 3.

d)	If the vehicle losses its structural integrity, the hazard results most likely into a loss of crew.
e)	If the vehicle has two modules, they separate during ascent and land independently. When this separation fails, the vehicle cannot land and the hazards leads lost likely to a loss of crew.
f)	If there is a malfunction of the propulsion, trajectory or control system during descent, the accident most likely results in a loss of crew.

5.2 Mitigation strategy and associated impact

After building the hazard list and assigning the severity factors, we determine the mitigation potential depending on the architectural decisions. We therefore use the mitigation impact scale developed by Leveson (see Table 5-4).

Table 5-4: Mitigation impact scale [83]

Impact factor	Description
4	Complete elimination of the hazard from the design
3	Reduction of the likelihood that the hazard will occur
2	Reduction of the likelihood that the hazard results in an accident
1	Reduction of damage if an accident does occur

The rows of Table 5-5 are the architectural decision with their options, as well as two important design variables, which impact the safety of the vehicle. These are the number of pilots varying from 0 to 2 and the type of propellant, solid, liquid or hybrid. The columns show the hazards identified in Table 5-2 above. To populate the table, we first decide on whether the decision has a mitigation potential on the hazard or not. For example, the number of modules have no influence on the fire and explosion hazard. Every non-influenced combination was marked by a dash. For the other fields, we discussed on the factors and compared the options inside a decision as discussed in the justification Table 5-6.

Table 5-5: Hazard mitigation database

Decision	Option	Fire + Explo-sion G1	Loss of life support G2	Incor-rect prop/ traj during ascent A1	Loss of structu-ral integrity ascent A2	Incor-rect stage separa-tion A3	Incor-rect prop/ traj during descent D1	Loss of structu-ral integrity descent D2
nModules	1	-	-	-	-	4[k]	-	-
	2	-	-	2[f]	2[f]	-	-	-
TOmode1	Horizontal	-	1[d]	1[d]	1[d]	-	-	-
	Vertical	-	-	-	-	-	-	-
wing1	No	-	-	-	-	-	-	-
	Yes	-	-	2[g]	-	-	2[g]	-
JetEngine1	No	2[a]	-	-	-	-	-	-
	Yes	-	-	1[h]	-	-	2[h]	-
Rocket-Engine1	No	3[a]	-	1[h]	-	-	-	-
	Yes	-	-	-	-	-	-	-
LAmode1	Gliding	3[b]		-	-	-	2[l]	2[m]
	HPowered	2[b]		-	-	-	3[l]	3[m]
	Parachute	3[b]	-	-	-	-	-	1[m]
	Rocket	-	-	-	-	-	2[l]	-
wing2	No	-	-	-	-	-	-	-
	Yes	-	-	2[g]	-	-	2[g]	-
Rocket-Engine2	No	3[a]	-	1[h]	-	-	-	-
	Yes	-	-	-	-	-	-	-
LAmode2	Gliding	3[b]		-	-	-	2[l]	2[m]
	Parachute	3[b]		-	-	-	-	1[m]
	Rocket	-	-	-	-	-	2[l]	-
	None	-	-	-	-	-	-	-
Design Variable	**Value**							
nPilots	0	-	-	-	-	-	-	-
	1	-	1[e]	1[i]	-	-	1[i]	-
	2	-	2[e]	2[i]	-	-	2[i]	-
Propellant	Solid	2[c]	-	-	-	-	-	-
	Liquid	-	-	2[j]	-	-	-	-
	Hybrid	1[c]	-	1[j]	-	-	-	-

Table 5-6: Justifications for the mitigation factor assignment

	Justification
a)	If the module has no jet engines, there is no jet fuel on board. If the module has no rocket engine, no rocket propellant is on board. This reduces the risk of fire in both cases. Compared to the jet engine decision, the risk mitigation in the rocket engine case is higher. We therefore assigned the mitigation factor 2 for the jet engine option and the mitigation factor 3 for the rocket engine option.
b)	The rocket powered landing mode is the most dangerous when it comes to the fire and explosion hazard. The rocket engine fires during landing and therefore the flames reflect from the ground back to the vehicles. This increases the possible risk of fire or explosion during landing. The horizontal landing requires running jet engines with remaining jet fuel in the tanks. The gliding and parachute methods are unpowered and therefore the risk of fire during landing can be fairly mitigated. There is a remaining potential from cable fire, residual fuel/propellant in the tanks and retrorocket landing impact actuators in the parachute case. Hence, we assign the mitigation factor 3 for the gliding and parachute case and slightly lower factor 2 for the horizontal powered option.
c)	For the propellant design variable, the liquid option is the easiest one to ignite. Compared to a liquid, a solid propellant is harder to ignite. The hybrid consists of a solid fuel and a liquid oxidizer and is therefore somewhere in between. Overall the mitigation potential for fire and explosion of a solid propellant is medium. We therefore assigned a factor of 2 for the solid and a mitigation factor of 1 for the hybrid type.
d)	Generally, compared to a vertical launch, a horizontal take-off has softer maneuvers with less vibrations and the ascent time is longer. The crew has more time to check the systems and identify possible malfunction. These factors reduce the risk of loss of life support (G2), incorrect trajectory (A1) and loss of structural integrity (A2) during ascent. We see the mitigation potential to be low and therefore assigned a factor of 1 for all three hazards.
e)	If the number of pilots is 0, the vehicle operated autonomously. To open the suborbital space experience to a broad public, the training is kept to a necessary minimum of a few days for the participants. If the life support system has a malfunction, the life of the passengers relies on this training. Pilots would have more extensive training, especially for emergency situations. They would therefore reduce the risk of a life support failure result in a severe accident. With increasing number of pilots the mitigation potential increases. We therefore assign a low potential of 1 to the one pilot option and a medium potential of 2 for the two-pilot option.

f)	If the vehicle has two modules, the crewed module can separate from the other module. In case of an incorrect propulsion, trajectory or control (A1) or loss of structural integrity (A2) of the unscrewed module, the separation has a medium potential to mitigation these hazards. If these hazards occur in the crewed part, the separation does not mitigate the hazards. We see the mitigation potential to be equal to a factor of 2.
g)	If the module has wings, the risk of an incorrect trajectory or loss of control during ascent (A1) as well as descent (D1) is reduced. It is more likely for a winged module to regain control. The down-range capability can compensate for trajectory misalignments. We see the mitigation potential to be medium with a factor of 2.
h)	For the incorrect propulsion, trajectory and loss of control during ascent (A1), having a jet engine can mitigate the occurrence of this risk, as the thrust usually stabilize the vehicle. The counterargument can be made for the rocket engine as their nature usually add instability. For the decent hazard D1, we see the mitigation potential of the jet engine option higher as a misaligned trajectory is more likely during descent. This results in a mitigation factor of 1 for the jet engine *yes* and rocket engine *no* option and 2 for the descent jet engine *yes* choice.
i)	A similar argument to the **e)** justification can be made for the number of pilot decision for the A1 and D1 hazard. If the vehicle has an autopilot, the pilots can take over control of the system if a malfunction occurs. We assume increasing number of pilots reduces the risk. We assigned the same mitigation factors as for **e)** with 1 for the one-pilot option and 2 for the two-pilot choice.
j)	Generally, a solid rocket engine cannot be throttle, which is the baseline for the A1 hazard. The liquid engine has the best throttle capabilities and the hybrid something in between. In addition, a solid rocket engine cannot be shut down readily, whereas both other types can. We therefore assign a mitigation potential factor of 2 to the liquid propellant and 1 to the hybrid option.
k)	If the vehicle has one module, there is no separation and therefore the hazard of an incorrect stage separation can be eliminated completely. This results in a mitigation factor of 4.
l)	For the incorrect propulsion, trajectory and loss of control during descent hazard (D1), the landing method has an influence on its risk. We see the parachute choice to be worst as the control of the descent trajectory is limited. The horizontal powered option offers the most control of the descent trajectory and for the landing phase. In contrast to the gliding method, a powered horizontal approach has go-around capabilities, which reduces risk. The rocket

	powered vertical landing has a similar mitigation potential as the gliding method. The aerodynamic guiding and drag systems offer downrange capabilities and trajectory adjustments. We therefore assign a mitigation factor of 3 to the horizontal powered method and 2 to the gliding and vertical rocket powered options.
m)	The landing method has influence on the structural integrity during descent, particularly on the amplitude of the final landing impact. The vertical powered rocket landing has the worst mitigation potential as the vehicle is more likely to lose structural integrity during the final ascent. The rocket engine has vibrations that apply stress to the structure. The control descent and landing of the horizontal powered method offers the best risk reduction. In comparison, the gliding method has a bit less mitigation potential. A parachute landing is between the rocket powered landing and the gliding choice. There must be a final impact attenuator to reduce the reminding vertical velocity from the parachute. These can fail or be the source of loss of structural integrity. With this reasoning, we assign a mitigation potential factor of 3 for the horizontal powered option, a 2 for the gliding choice and a 1 for the parachute landing.

5.3 Calculation of the Overall Residual Safety-Risk Metric (ORSRM)

After the hazards are identified, their severity quantified and the architectural decision matched to the hazards with a mitigation impact factor, the ORSRM can be computed by following this procedure:

1. Calculate the Maximum Mitigation Factor (MMF) for each category *c* and each hazard *h* over the Mitigation Factors (MF) for all decision options *d*:

$$x_{MMF_{h,c}} = \sum_{d} x_{MF_{h,c,d}} \qquad (5\text{–}2)$$

2. Calculate the Hazard Mitigation Indices (HMI) for each hazard *h* and each category *c* by summing the MF of the selected architecture:

$$x_{HMI_{h,c}} = \sum_{a} x_{MF_{a,h,c}} \qquad (5\text{–}3)$$

3. Calculate the Relative Residual Risk (RRR) Index for each hazard *h* and category *c*:

$$x_{RRR_{h,c}} = 1 - \frac{x_{HMI_{h,c}}}{x_{MMF_{h,c}}} \qquad (5\text{–}4)$$

4. Check if any hazard is eliminated (Mitigation level = 4) by a chosen option. If so the RRR is set to zero:

$$x_{RRR_{h,c}} = 0 \tag{5–5}$$

5. Calculate a Relative Severity Index (RSI) for each hazard and category with the original hazard severity s_h to the power of *k*. We use a quadratic dependency as proposed by Dulac [84] (k = 2).

$$x_{RSI_{h,c}} = x_{RRR_{h,c}} \cdot s_h^k \tag{5–6}$$

6. Averaging the RSI for each category across the hazards leads to the Relative Risk Metric (RRM):

$$x_{RRM_c} = \frac{\sum_h^N x_{RSI_{h,c}}}{N} \tag{5–7}$$

7. To obtain the Overall Residual Safety-Risk Metric (ORSRM), the RRM for each category must be weighted with subjective factors w_c. As we do only consider one category, this step can be skipped.

$$ORSRM = \sum_c^M x_{RRM_c} \cdot w_c \tag{5–8}$$

6 Metric II - Overall Cost Per Passenger (OCPP)

For costing, we developed an Overall Cost Per Participant (OCPP) metric. It sums the overall cost of the vehicle over its life-cycle and divides it by the number of participant who have flown. The OCPP is a rough indicator of the minimum required ticket price for the company to report no financial loss, in an undiscounted sense. The life-cycle cost of the vehicle is broken down into Research Development Test & Evaluation (RDT&E), production and operating costs. The RDT&E and production cost are specialized for jet or rocket engines and for the airframe. The module related operating costs are accounted for as maintenance, launch operation and fuel costs. The vehicle related operating costs cover pre-launch operation, launch site cost, transportation and insurance costs. It furthermore distributes the cost over the life-cycle of the vehicle for more detailed evaluation of the results.

Note, that we describe the development costs for the jet and rocket engine in this chapter for the sake of completeness, but set them to zero for the financial business optimization. We assume that the engines are bought from other companies or the development costs are financed through other projects.

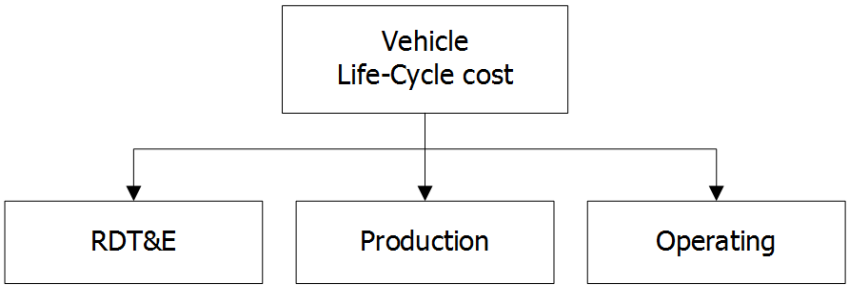

Figure 6-1: Overview life-cycle cost vehicle

The three submodules are described in the following section 6.2 - 6.4 in more detail. Mathematically, the overall cost per passenger is calculated by summing the life-cycle cost for each period i divided by the number of passenger in this period.

$$OCPP = \sum_{i} \frac{C_{tot_i}}{n_{PAX_i}} \qquad (6\text{–}1)$$

For the time distribution, the life-cycle cost module calculates the total cost C_{tot_i} for each period i as

$$C_{tot_i} = C_{RDT\&E_i} + C_{Prod_i} + C_{Oper_i} \quad (6\text{–}2)$$

with

$C_{RDT\&E_i}$: Research, Development, Testing and Evaluation costs

C_{Prod_i}: Production cost

C_{Oper_i}: Operation cost

6.1 Cost conversion value and assessment factors

The Cost Estimating Relationships (CERs) from Koelle [89] and Goehlich [11] are given in Work-Years (WYr) to ensure applicability for different labor costs around the world. For conversion to $ in the American aerospace industry, the cost conversion value d is introduced in equation (6–3) (modified from [11]). For the fiscal year 2017, this cost conversion value is 305,900$ per WYr.

$$d = -7.905 \cdot b^2 + 37{,}308.156 \cdot b - 42{,}784{,}828 \quad (6\text{–}3)$$

with

d: Cost conversion value in [$/WYr]

b: Fiscal year (2017 for this thesis)

Goehlich [11] defined different assessment factors to ensure a satisfactory accuracy of the estimated costs. There are some factors that account for programmatic costs and some for technical derivation from the CERs. The used values for the programmatic costs are summarized in Table 6-1. For a detailed description of each factor refer to [11].

Table 6-1: Summary of used assessment factors values

Factor	Value
Project System Engineering	1.075
Technical Development Factor	1.0
Team Experience Factor	1.0

In addition, there is a Technical Quality Factor which is different for each type of system and depends on the technical features. It is defined in section 6.2.3. To account for learning effects and reduced costs for follow-on manufacturing units, a Cost Reduction Factor f_{CR} is defined with n being the number of units produced during the program length and LC the Learning Curve factor (here 90%) [89] [11]:

$$f_{CR} = 1.004 \cdot n^{\frac{\ln(LC)}{\ln(2)}} \quad (6\text{–}4)$$

As a last factor, we introduce the Commercial Factor f_C. It is different for each type of system and considers the potential of low-cost processes in development and production in the commercial market. The baseline is the aeronautical market covering jet engines and reusable winged subsonic vehicles. The used values can be seen in Table 6-2 with the same commercial factors for the development and production [11]. The cost reduction potential for rocket engines is around 80% for commercial production compared to government programs.

Table 6-2: Values for the commercial factors f_C [11]

Technical system	Development	Production
Rocket Engines	0.2	0.2
Jet Engines	1.0	1.0
Reusable Ballistic vehicles	0.5	0.5
Reusable Winged subsonic vehicles	1.0	1.0
Reusable Winged supersonic vehicles	0.5	0.5

6.2 RDT&E costs

The Research, Development, Testing and Evaluation costs account for the total elaboration of the vehicle. The design framework computes them as a total value for each module. For a two-module vehicle, it is assumed that the development of both modules start at the same time and in the first year of the program. The time distribution is based on ALCCA (Aircraft Life-Cycle Costs Analysis) and taken from Burgaud [23] (see Table 6-3). It is coherent with common RDT&E time distributions in the space sector [90].

Table 6-3: Time distribution of RDT&E costs

Year	1	2	3	4	5	6
Value	5%	20%	20%	20%	20%	15%

For a two-module vehicle, the total RDT&E cost is a sum of the ones for each module m:

$$C_{RDT\&E} = \sum_{m} c_{RDT\&E_m} \quad (6\text{–}5)$$

The development cost for a module is divided into three categories, airframe development cost, rocket engine and jet engine development cost:

$$c_{RDT\&E_m} = c_{D,R} + c_{D,J} + c_{D,AF} \quad (6\text{–}6)$$

with

$c_{D,R}$: Rocket engine development cost

$c_{D,J}$: Jet engine development cost

$c_{D,AF}$: Airframe development cost

This breakdown structure can be seen in Figure 6-2. The airframe is further broken down into winged and ballistic modules. For the latter different costs for modules with and without engines (= capsule) are considered. For the winged airframe two different types, one with jet engines only (= airplane) and the others with rocket engines (= rocketplane).

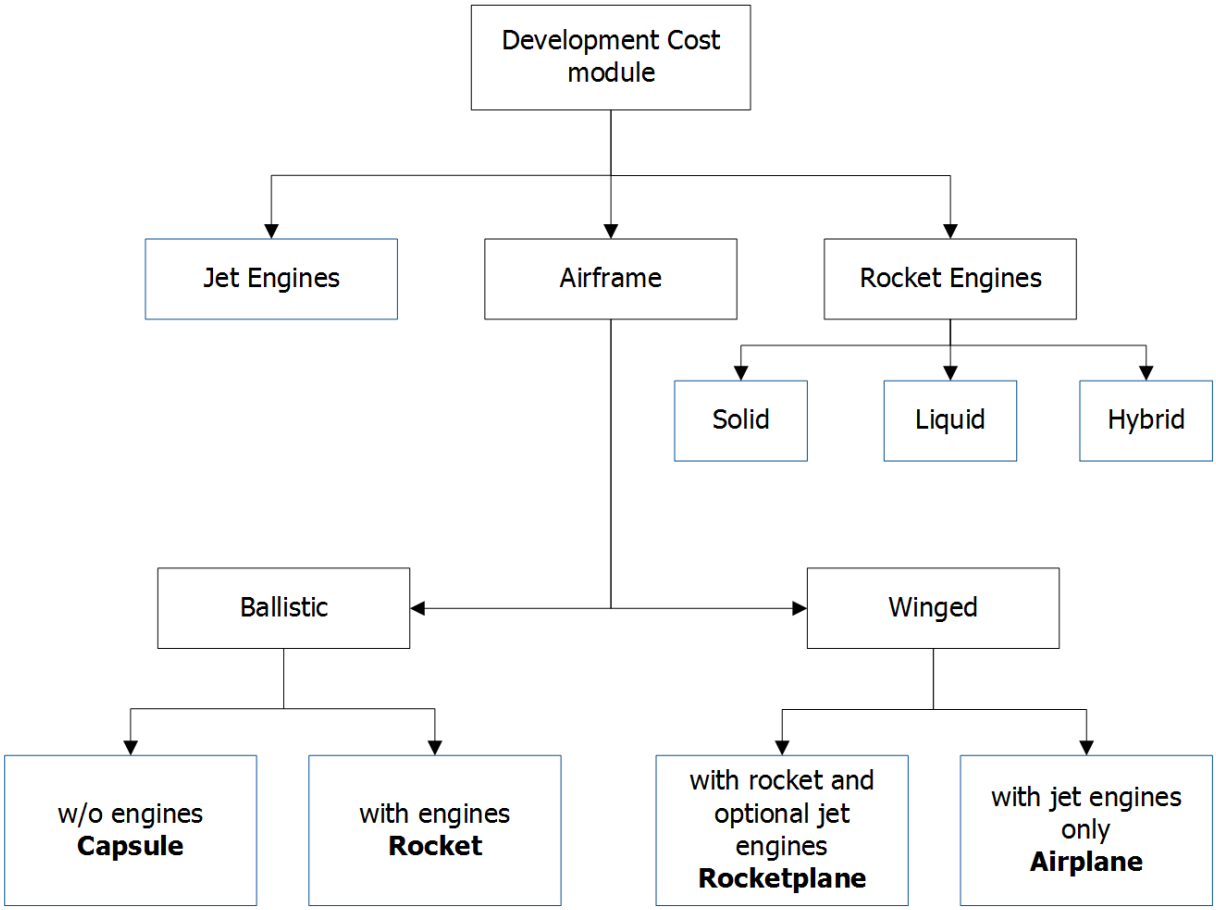

Figure 6-2: Breakdown structure for the development cost calculation

The following three sections describe the CERs for the jet engine, rocket engine and airframe development costs. Jet engines development cost

6.2.1 Jet engine development cost

Frank's [20] code already has an estimation of the jet engine development cost. He used the approach developed by Younossi et al. [91]. Further details are described in section 6.3.1 and the references.

6.2.2 Rocket engines development cost

The development cost calculation for rocket engines is taken from Frank [20]. His approach is based on Morrison [92] with the assumption that the development costs for solid and liquid engines are a function if the number of prototypes and cumulative average cost of 150 engines. These costs are calculated by using the first unit cost and the learning curve effect. The cost for hybrid engines is determined by using the existing relationships for the solid and liquid sub-engines. For further details refer to the provided references.

6.2.3 Airframe development cost

The airframe development costs are derived from Koelle [89]. The technical quality factor f_{TQ} is derived from the technical characteristics and depends on the system. For the rocket and rocketplane airframe architecture this factor considers the relationship between the Net Mass Fraction (NMF) of the module under consideration and the reference NMF for modules with the same dry mass. It avoids for low-tech heavier designs to become more expensive or high-tech design to become less expensive, respectively. Figure 6-3 shows a comparison between both NMF. For the comparison, the payload mass for the reference NMF of the rocketplane airframe is assumed to be zero. The additional mass of wings, control surfaces and actuators with power system result in a higher NMF for the rocketplane. In addition, the figure indicates a greater sensitivity towards increasing dry mass as it may occur during detailed design phase. In this case, the higher sensitivity leads to a much greater reduction in the payload mass for rocketplanes as it would be the case for rocket airframe (or even less for expendable rocket architectures). The solid lines are the areas for which the regression is validated by real data. The dashed lines are extrapolated to cover the design space of manned suborbital vehicles. For example, the Rocketplane XP concept has an estimated propellant mass of around 3 t. The figure illustrated that this is far outside of the range for which reference data exists and therefore the extrapolation becomes less accurate. With the given data from Koelle [89] it is not reasonable to use the

technology factor for this two airframe types. It is set to the default value of 1 which assumes that all architectures have the same technical quality factor.

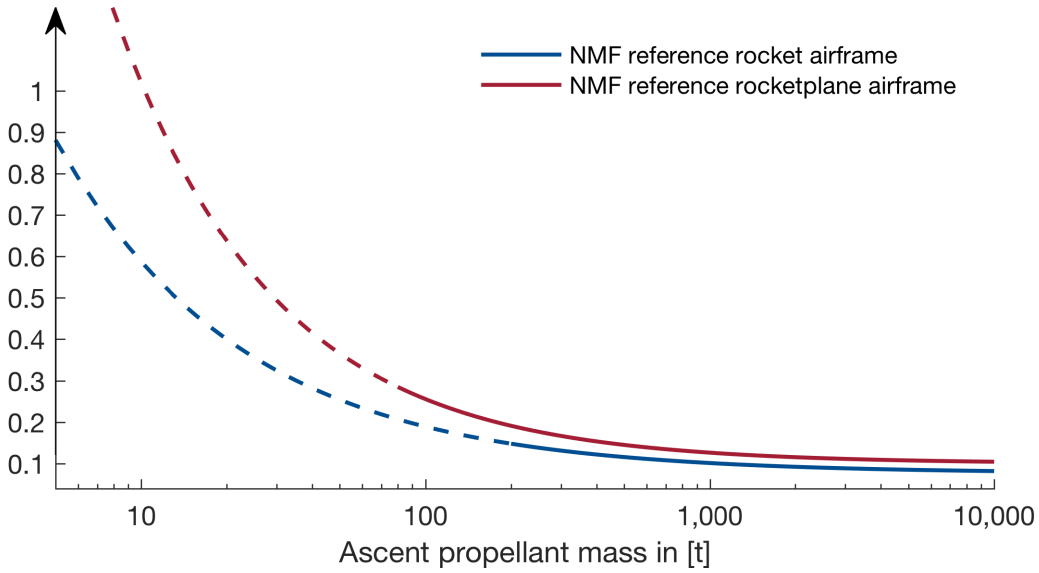

Figure 6-3: Comparison of the reference NMF for the technical quality factor for the rocket and rocketplane airframe architecture

Koelle [89] based his CER regressions on historical data for orbital vehicles with different architectures. The following four subsections describe the results as well as their applicable mass range for the capsule, the rocket, the rocketplane and the airplane airframe. A subsection follows these descriptions and compares the different development costs and their applicable range for suborbital vehicles.

6.2.3.1 Capsule

The capsule airframe features no engines and Koelle [89] based the original regression on the four US re-entry capsules, Mercury, Gemini, Apollo CM and Orion CM . It reads:

$$c_{RDT\&E_{Cap}} = 436 \cdot m^{0.408} \cdot f_{TQ} \cdot f_{C_{Caps}} \cdot d \quad \text{for } m \in [800;\ 10{,}000]\ kg \qquad (6\text{–}7)$$

with

$c_{RDT\&E_{Cap}}$: RDT&E cost for crewed airframe in [$]

m: Mass of capsule in [kg]

f_{TQ}: Technical quality factor [-]

$f_{C_{Caps}}$: Commercial factor for capsule [-]

d: Cost conversion value in [$/WYr]

The technical quality factor f_{TQ} depends on the crew number and lifetime [89]:

$$f_{TQ} = \left(n_{crew} \cdot \frac{t_{mission}}{days}\right)^{0.15} \quad (6\text{–}8)$$

with

n_{crew}: Number of crew consist of passenger and pilots [-]
$t_{mission}$: Max mission design time in [d]

6.2.3.2 Rocket

In contrast to the capsule, a rocket is a ballistic module with engines. The CER is modified from [89]:

$$c_{RDT\&E_R} = 803.5 \cdot m_{dry}^{0.385} \cdot f_{C_R} \cdot d \quad \text{for} \quad m_{dry} \in [25{,}000;\ 700{,}000]\ kg \quad (6\text{–}9)$$

with

$c_{RDT\&E_R}$: RDT&E cost for rocket airframe in [$]
m_{dry}: Dry mass of airframe without engines in [kg]
f_{C_R}: Commercial factor for rocket [-]
d: Cost conversion value in [$/WYr]

6.2.3.3 Rocketplane

The development effort for winged airframe is adapted from Koelle's [89] winged stages with rocket engines and is given to:

$$c_{RDT\&E_{RP}} = 1420 \cdot m_{dry}^{0.35} \cdot f_{C_{RP}} \cdot d \quad \text{for} \quad m_{dry} \in [7{,}000;\ 150{,}000]\ kg \quad (6\text{–}10)$$

with

$c_{RDT\&E_{RP}}$: RDT&E cost for a rocketplane airframe in [$]
m_{dry}: Dry mass of airframe without engines in [kg]
$f_{C_{RP}}$: Commercial factor for rocketplane [-]
d: Cost conversion value in [$/WYr]

6.2.3.4 Airplane

The airplane airframe is derived from airplanes like A380, DC-10, X-30 or Tornado [89]:

$$c_{RDT\&E_{AP}} = 2168.8 \cdot (m_{OWE})^{0.2616} \cdot f_{TQ} \cdot f_{C_{AP}} \cdot d \quad \text{for} \quad m_{OWE} \in [5{,}000;\ 300{,}000]\ kg \qquad (6\text{–}11)$$

with

$c_{RDT\&E_{AP}}$: RDT&E cost for an airplane in [$]
m_{OWE}: Operational Weight Empty (Vehicle dry mass with engines) in [kg]
f_{TQ}: Technical quality factor [-]
$f_{C_{AP}}$: Commercial factor for airplane [-]
d: Cost conversion value in [$/WYr]

The technical factor f_{TQ} depends on the speed capabilities. Therefore, it depends on the Mach number Ma:

$$f_{TQ} = Ma^{0.15} \qquad (6\text{–}12)$$

6.2.3.5 Comparison of the different airframe development costs

The four different architectures with their development cost depending on the dry mass without engines are plotted in Figure 6-4. The CER relation for the airplane is given with the operational weight empty (OWE) which includes the engines. Nevertheless, with the assumption that the dry mass is 0.9 of the OWE (A380: 0.91, Concorde: 0.84), this architecture can be drawn in the same chart. The lines are solid for the area for which data validate the regression. The dashed lines cover extrapolated areas to include the mass ranges needed for suborbital vehicles.

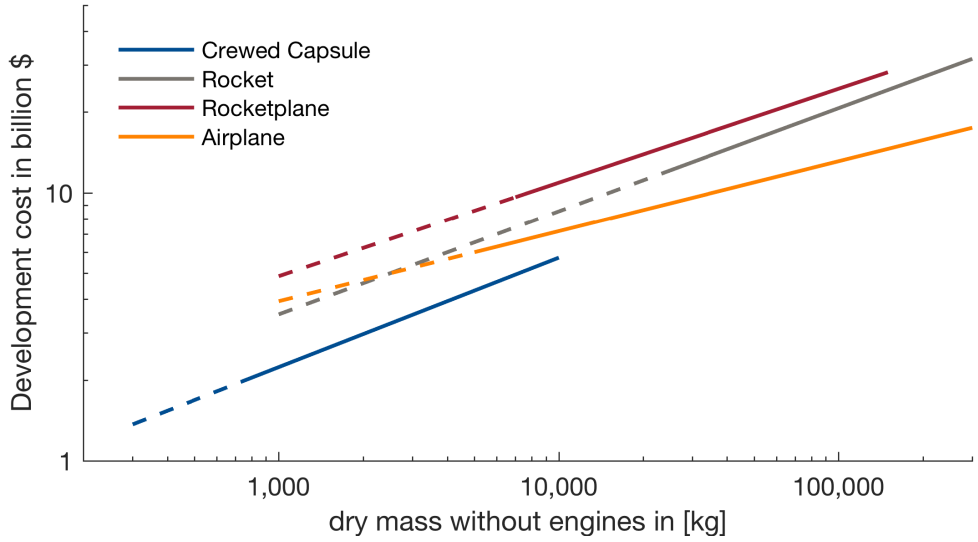

Figure 6-4: Development cost for the different airframes with quality factor of 1

It can be seen from the figure that a crewed capsule is the cheapest airframe per kg, followed by the airplane, the rocket and finally the rocketplane. The slope with respect to the dry mass is similar for all four airframes except with the airplane having a stronger reduction in development cost per kg with increasing dry mass. Generally, the more complex the system becomes, the higher the corresponding development costs. Compared to a rocket, a rocketplane has additional aerodynamics surface, a wing for lifting, some sort of vertical and horizontal stabilizer and rudders. These systems must be developed, tested and verified which adds costs. The capsule has high requirements regarding the Environment Control and Life Support System (ECLSS) for the participants but it does not have as much lift, guiding and control surfaces as the other airframes and do not have tanks to store the fuel. Furthermore, the mass to size ratio is higher for a capsule, this reduces cost for large integration halls and test facilities. These factors result in a lower RDT&E cost per kg for the capsule airframe.

6.3 Production costs

The production cost cover the cost to manufacture, assemble and test the module. According to Burgaud [23] the production starts in year 6 and is limited to 20 spacecrafts per year. 40% of the production costs are charged the year preceding the end of its production and 60% the year it is delivered. Like the development cost breakdown, the production cost of the module consists of the jet engine, the rocket engine and the airframe as shown in Figure 6-5.

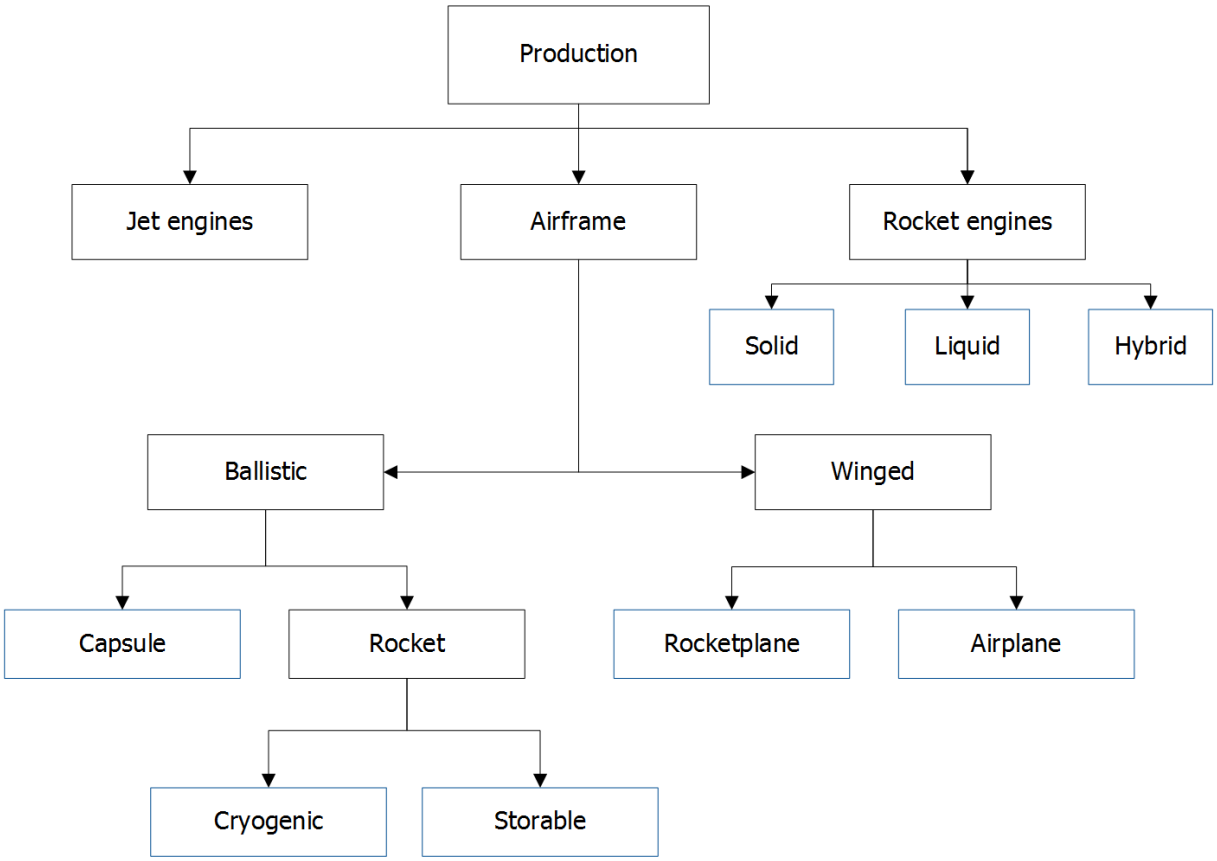

Figure 6-5: Breakdown structure production costs

The production cost of the rocket engine is further broken down into the type of propellant, solid, liquid or hybrid. The decomposition of the airframe follows the development cost approach with the additional differentiation between a cryogenic and storable rocket. Each of the following sections describe the approach of the production cost for the jet engines, rocket engines and the airframe.

6.3.1 Jet engines production costs

The production cost of the jet engines is taken from Frank's code [20]. He uses a four-variable based model developed by Younossi et al. [91]. It considered the learning curve factor, the turbine inlet temperature, the binary variable for the afterburner decision and the engine weight. For details refer to the references.

6.3.2 Rocket engines production costs

Three different production cost CERs for solids, liquid and hybrid rocket engines are used by Frank's code which we use for the cost calculation.

For solid engines, Frank refers to Graver et al. [93] who developed CERs based on the cumulative average cost at total production quantity. Based on this, the first unit cost can be determined if the learning curve factor and the total production quantity is known. The CER relying on the total impulse is considered as the most suitable. Refer to [20] for further details.

For liquid engines, Friedland et al. [94] have found CERs for the first unit cost based on three input variables, the engine dry weight, the vacuum thrust and the mass flow rate.

For hybrid engines, Frank chose a more physics-based approach as no CERs were available. He broke the engine down into four main parts, solid engine, pressurization tank, oxidizer tank and a feed system. The first unit cost is then the sum of the costs for each subsystem. The solid subsystem is based on Graver and Morrison [93] as well as Zandbergen [95]. The cost for the tanks is the sum of the recurring and non-recurring costs, with the input variable being the area of the tank. Refer to Frank [20] and Brown et al. [96] from NASA for a detailed description. According to Meisl [97] the feed system embodies 11% of the total cost for a liquid reusable engine. Using this the cost is a function of the engine weight and the CER developed by Friedland et al. [94] can be used.

6.3.3 Airframe production costs

Airframe production CERs are available for orbital vehicles. The first four subsections aim to describe the four airframe types with their CERs, followed by a subsection that compares the production cost of these four airframes and discuss the applicable range for suborbital vehicles.

6.3.3.1 Capsule

The production costs for capsule are based on the crewed space system CER of Koelle, 2010 [89]. It reads:

$$c_{Prod_{Caps}} = 0.16 \cdot m_{dry}^{0.98} \cdot f_{CR} \cdot f_{C_{Caps}} \cdot d \quad \text{for} \quad m_{dry} \in [1{,}000;\ 70{,}000]\ kg \qquad (6\text{–}13)$$

with

$c_{Prod_{Caps}}$: Production cost for a crew capsule in [$]
m_{dry}: Dry mass of airframe without engines in [kg]
f_{CR}: Cost reduction factor [-]
$f_{C_{Caps}}$: Commercial factor for capsule [-]
d: Cost conversion value in [$/WYr]

6.3.3.2 Rocket

The rocket CER is based on Koelle 2010 [89]. He used 16 reference projects for expendable and reusable rocket modules. Both can be treated with the same equation as the reusable vehicles have around 40% higher dry mass which results in a more expensive production. When it comes to propellant types there are two different CER for cryogenic and storable propellants. The average production cost for one unit reads:

$$c_{Prod_{R-C}} = 1.418 \cdot m_{dry}^{0.646} \cdot f_{CR} \cdot f_{C_R} \cdot d \quad \text{for} \quad m_{dry} \in [600;\ 50{,}000]\ kg \qquad (6\text{–}14)$$

$$c_{Prod_{R-S}} = 1.439 \cdot m_{dry}^{0.593} \cdot f_{CR} \cdot f_{C_R} \cdot d \quad \text{for} \quad m_{dry} \in [600;\ 100{,}000]\ kg \qquad (6\text{–}15)$$

with

$c_{Prod_{R-C}}$: Production cost for cryogenic rocket airframes in [$]
$c_{Prod_{R-S}}$: Production cost for storable rocket airframes in [$]
m_{dry}: Dry mass of airframe without engines in [kg]
f_{CR}: Cost reduction factor [-]
f_{C_R}: Commercial factor for rocket [-]
d: Cost conversion value in [$/WYr]

6.3.3.3 Rocketplane

For rocketplanes the CER is derived from winged orbital detailed concept studies FSSC-9/II and FSSC-1. According to these two studies the production cost is (modified from [89]):

$$c_{Prod_{RP}} = 5.83 \cdot m_{dry}^{0.606} \cdot f_{CR} \cdot f_{C_{RP}} \cdot d \quad \text{for } m_{dry} \in [10{,}000;\ 150{,}000]\ kg \qquad (6\text{–}16)$$

with

$c_{Prod_{RP}}$: Production cost for rocketplane airframes in [$]
m_{dry}: Dry mass of airframe without engines in [kg]
f_{CR}: Cost reduction factor [-]
$f_{C_{RP}}$: Commercial factor for rocketplane [-]
d: Cost conversion value in [$/WYr]

6.3.3.4 Airplane

The cost basis for carrier winged modules with jet engines are commercial airplanes like the F-28, MD-11, 747-400 or A-380. The CER for the production cost of these airframes with engines (OWE) is modified from Koelle, 2010 [89]:

$$c_{Prod_{AP}} = 0.0653 \cdot m_{OWE}^{0.7709} \cdot f_{CR} \cdot f_{C_{AP}} \cdot d \quad \text{for } m_{dry} \in [5{,}000;\ 110{,}000]\ kg \qquad (6\text{–}17)$$

with

$c_{Prod_{AP}}$: Production cost for airplane airframes in [$]
m_{OWE}: Operational Weight Empty (Vehicle dry mass with engines) in [kg]
f_{CR}: Cost reduction factor [-]
$f_{C_{AP}}$: Commercial factor for airplane [-]
d: Cost conversion value in [$/WYr]

6.3.3.5 Comparison of the different airframe productions costs

The CER relation for the airplane is given with the operational weight empty (OWE) which includes the engines. Nevertheless, with the assumption that the dry mass is 0.9 of the OWE (A380: 0.91, Concorde: 0.84), this architecture can be drawn in the same chart. The lines are solid for the area for which data validate the regression. The dashed lines cover extrapolated areas to include the mass ranges needed for suborbital vehicles. A cost reduction factor of 1 is assumed for all airframe architectures. Like the development costs plotted in Figure 6-4, the production cost per unit per dry mass increases with complexity of the airframe. One exception is the crewed capsule which has a lower development cost as the other airframe but a higher production cost. The production cost can be explained by the increased effort which is paid when building a crewed spacecraft. The procedures are more overseen, the inspections are more frequently and the testing is more extensive. This all adds up to a higher production cost. Comparing the production cost of a rocketplane airplane with the cryogenic and storable version of a rocket, there can be seen how complexity drives cost. As described in the development cost section, the rocketplane is a more complex system. The cryogenic rocket propellant must be insulated to reduce boil-off losses and its structure must withstand the temperature differences. This can be achieved by increasing the complexity of the system or by using more enhanced material. Both result in a cost increase.

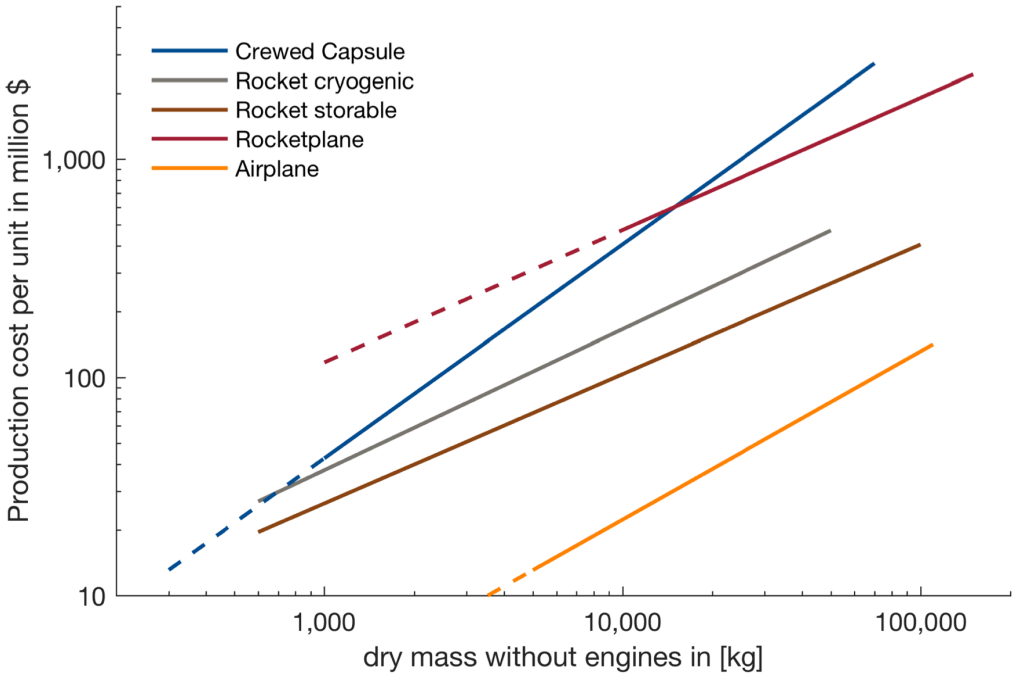

Figure 6-6: Overview of the production costs per unit for the different airframe types

6.4 Operating costs

For each module, the design framework provides the operations cost as cost per flight. Multiplication with the number of flights per year and number vehicles in the fleet leads to the total operation costs in period i with c_{oper} being the operational cost per vehicle per flight.

$$C_{Oper_i} = c_{oper} \cdot n_{vehicles} \cdot n_{flights} \quad (6\text{–}18)$$

The operational cost per vehicle per flight is divided into module and vehicle related costs as depicted in Figure 6-7. The module related operating costs are accounted for as maintenance, launch operation and fuel costs. The vehicle related operating costs cover pre- launch operation, launch site cost, transportation and insurance costs.

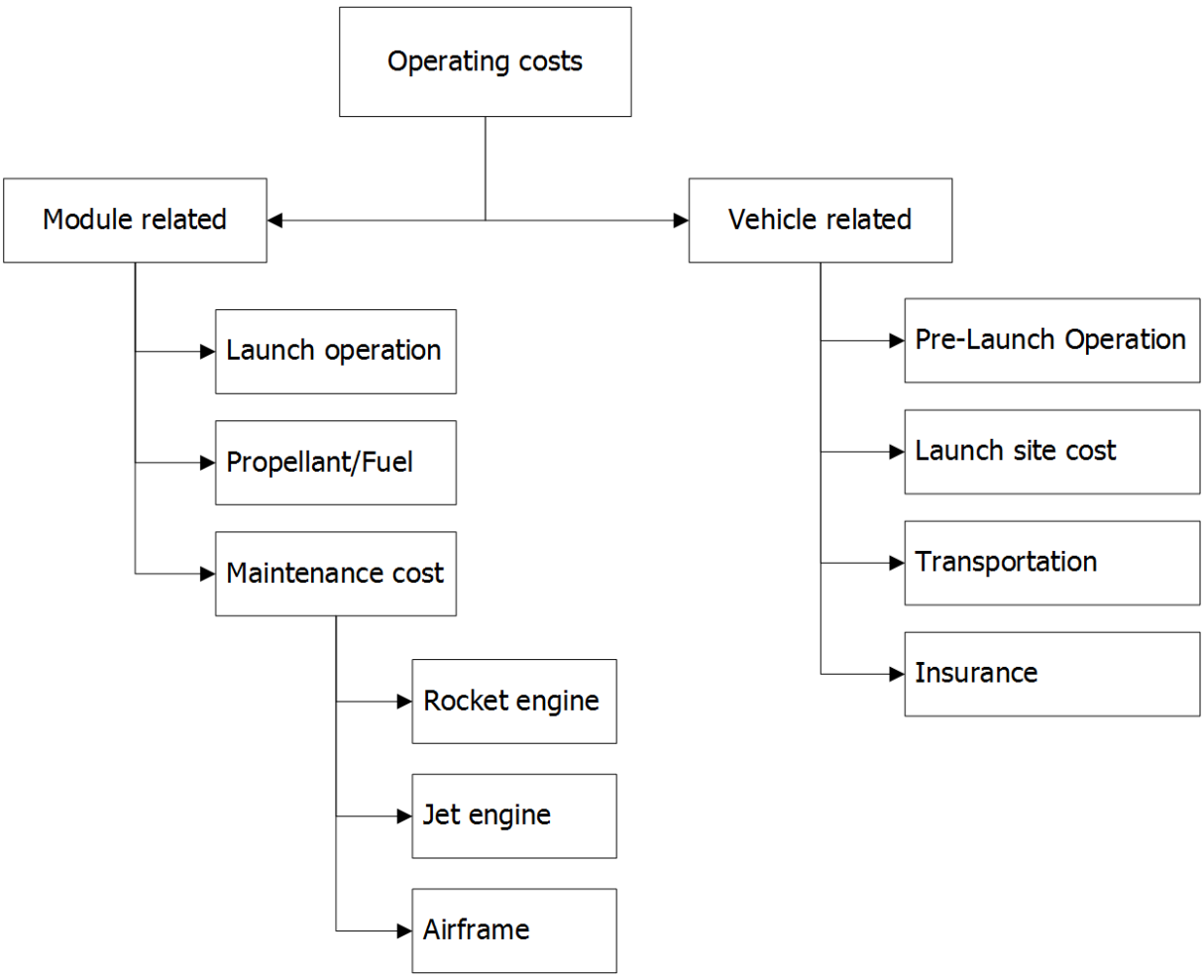

Figure 6-7: Overview operating costs

The following two section describe in more detail the calculation and reference for the cost distributor. Most of the basic code is taken from Frank's [20] with the cost relations developed by Goehlich [11]. To account for a two-module vehicle and the reusability costs, the framing code was adjusted and modified.

6.4.1 Module related

The module related costs are coupled with the module and can be calculated with the outputs of the design framework for each module. Depending on the number of modules there can be one or two module related cost contribution to the overall operating costs. The

6.4.1.1 Launch operation

The launch operation costs include communication related systems and the personnel and software effort of the mission control center. It depends on whether the considered module is the first or second module, on the crew number and on the mission duration.

6.4.1.2 Propellant/Fuel

The costs for the propellant and fuel depend on if the module has engines and which type. It furthermore considers the boil-off factor depending on the propellant/fuel. The main drivers are the propellant mass and the manufacturing prize, which varies by two orders of magnitude between for example, kerosene and liquid hydrogen [98].

6.4.1.3 Maintenance cost

The space shuttle program has shown us that particularly for reusable launch vehicles the maintenance cost can have significant influence on the program cost and therefore on its success [99]. The refurbishment and spares' cost per flight for the space shuttle orbiter was 2.3% of the production cost. This compares to 0.006% for a Boeing 747 and 0.008% for the Concorde [89]. Future reusable suborbital vehicles will have a percentage somewhere between these both extremes. In alignment with the values proposed by Koelle 2010 [89], Goehlich [11] derived the maintenance cost as a percentage of the production cost for the airframe, rocket and jet engine of the module.

Furthermore, we assume that after a certain number of refurbishment the vehicle must be replaced by a new one. These numbers are based on [89] and displayed in Table 6-4

below. This is a very important factor to include in the conceptual design phase, especially if frequent flights are planned and the vehicle is used daily. Without this consideration, the optimization process leads to a fleet with just one vehicle that is used far beyond its expected lifetime.

Table 6-4: Number of maximum flights for each subsystem

Subsystem	Number of maximum flights
Airframe	200
Rocket Engines	50
High speed turbo jet engines	600

6.4.2 Vehicle related

The vehicle related operation cost cover the pre-launch operation, the launch site cost, the transportation and the insurance. These costs are independent of the number of modules and must be just considered ones for each vehicle.

6.4.2.1 Pre-Launch Operation

The pre-launch operation cost of the vehicle depends on the weight of the vehicle, the launch mode (horizontal or vertical) and the frequency of launches. It accounts for the ground transportation, the assembly on-site, checkout, fueling and the launch preparations. For more details the reader is referred to Goehlich [11].

6.4.2.2 Launch site cost

Goehlich [11] estimated the lunch site cost to be 0.1 million WYr which includes the site administration, facilities maintenance, range stations and the safety provisions.

6.4.2.3 Transportation

Lassmann [100] and Goehlich [11] defined the transportation cost which also includes emergency landing sites and ferry flights. The transportation cost depends on the weight of the vehicle.

6.4.2.4 Insurance

The vehicle insurance cost consists of the vehicle loss rate as well as the abort rate. A typical loss rate for commercial aircrafts is in the order of 1 per 1,000,000 flights and 1 out of 14,000 for military aircrafts. For insurance calculation Goehlich assumes a loss rate of 1 per 2,000 flights and a abort rate of 1 per 40 launches [11].

6.5 Limitation cost module

Our cost module is at a far extend based on the approaches of Goehlich [11], Frank [20] as well as Koelle 2010 [89]. There are some limitations that are not implemented in our code:

- No consideration of financing cost for the first loan to finance the RDT&E phase
- Does not consider production improvement costs
- No abolition cost

6.6 Validation cost module

Validation of the cost module is not a trivial task as data from aerospace and defense project are often proprietary and usually not available to the public. There is no active suborbital vehicle with available cost data to validate the whole module. Hence, only validation of the subsystems jet engines, rocket engines and airframe can be made. Some subsystems are taken from Frank's PhD thesis [20] without any modifications. Table 6-5 shows which subsystems are taken from which source.

Table 6-5: Overview of validation of the submodules

Subsystem	Development costs	Production costs
Airframe	Koelle 2010 [89]	Koelle 2010 [89]
Rocket Engines	Frank [20] based on Morrison [92]	Frank [20] based on Graver et al. [93], Friedland et al. [94]
Jet engines	Frank [20] based on Younossi et al. [91]	Frank [20] based on Younossi et al. [91]

Frank validate his cost module and found a mean relative error of 19% for the rocket engines and a R^2 of 0.98 for the jet engine cost [20]. For the subsystems and costs seen in Table 6-5 we used his cost module without any modifications. We can therefore assume that these parts are already validated. In the following we describe the validation of the Airframe development and production costs as well as the jet engines development costs. They are all taken from Koelle 2010 who developed the CERs based on real data. A validation with using these data would make no sense as the relationships are build based on that data. Consequently, we validate the CERs with data that he did not used to generate the relationships.

In accordance to the previous convention, the airframe can have four different configurations, a capsule, a rocket, a rocketplane and an airplane. CERs for both the development and production costs were developed based on Koelle 2010 [89]. In the following four subsections, each of the configuration is validated with data not used by Koelle.

6.6.1 Airframe Capsule cost validation – Dragon 2

We use SpaceX's Dragon 2 crew capsule to validate the CERs from section 6.2.3 and 6.3.3. The development of this and Boeing's CST-100 capsule was funded by NASA's Commercial Crew Development (CCDev) program. In several rounds, they invested around $8.3 billion for the development as well as the first flights to resupply the ISS. Together with its preceding program Commercial Orbital Transportation Services (COTS), these investments aim to stimulate the commercial space industry [101]. NASA provided a total amount of $3.1 billion to SpaceX to develop their human spaceflight capabilities [102-107]. This includes one test flight and two supply flights to the ISS [106]. One seat in the seven seat Dragon 2 capsule should cost around $20 million resulting in a total launch cost of $140 million [108]. Subtracting the three launches from NASA's funding leaves $3.1 billion – 3 · $140million = $2.68 billion for the development costs. In a first approximation, this money is spent on the development of the Dragon, which was the basis for the human-rated Dragon 2. As a comparison, Boeing was awarded $4.82 billion for the CST-100, which results in $4.05 billion excluding the three launches [102-107]. If we subtract the $62 millions launch cost of the Falcon 9 [4], we have a launch cost for the capsule of $78 million.

To evaluate the CERs, we must know the mass of the capsule and the mission time. The mass of the capsule is given by Seedhouse [107] to 4,200 kg. He found a mission time varying from one week to two years. We assume the lower bound of seven days, which result together with seven crew members in a technical quality factor of $f_{TQ} = 1.79$. The commercial factor for development and production is $f_{C_{Caps}} = 0.5$ (see Table 6-2). In addition, a production of ten vehicles with a learning factor of 90% is considered. The results can be seen in Table 6-6.

Table 6-6: Validation of the capsule airframe configuration with the Dragon 2

	Reference	Own CERs
Development costs	$2.68 billion ($4.05 billion for the CST-100)	$3.6 billion
Production costs	$78 million launch cost	$61 million

The development costs for the capsule is estimated to be $3.6 billion compared to the $2.68 billion given in the reference. Boeing received $4.05 billion to develop a similar capsule. Our

estimation is well between both projects. The difference may be due to a different commercial factor for SpaceX compared to Boeing.

To compare the launch cost and the estimated production cost, we assume that one vehicle can be reused ten times as stated by SpaceX [107]. This means the production cost amortization is around $6 million per launch. If we assume a maintenance fraction of 2% like the Space Shuttle [89], we have a cost of around $7 million per flight for the production and maintenance costs. This does not include profit, development cost amortization and operating costs related to the launch. We have no indication on how high the profit of SpaceX is. With further improvements on the Dragon 2, e.g. increasing the number of reuses from 10 to 100, SpaceX things they can reduce the price per seat to a one digit million number [107, 108]. Leaving the launch cost constant and assuming $10 million instead of $20 million per seat, we leave $8 million for the capsule per launch. This would come close to the values we have estimated. This example shows how sensitive the validation of the CERs is without knowing the real cost data. Furthermore, the development costs are already paid by NASA but if we would consider an amortization of these costs among 100 flights (ten vehicles with ten launches each), this would add an additional $27 million for each launch.

To summaries the validation of the capsule airframe CERs, we can say that the development costs are aligned with the reference data. With the production/launch data available it is not possible to validate the production cost CER. However, we have shown that it is at least in the right order of magnitude.

6.6.2 Airframe Rocket cost validation – SLS

The validation of the rocket configuration is made with a heavy expendable launch vehicle, the Space Launch System (SLS) developed by NASA. After the Constellation program was canceled, the SLS aims to replace the Space Shuttle and enables NASA to send humans beyond earth. Its payload capability will be similar to the Apollo Saturn V rocket [109]. The projected development costs are between $7 billion [110] and $35 billion [111, 112]. The cost per launch is assumed to be $500 million [113].

For our CERs a dry mass of 85t for the first core stage and 3.5t for the second stage are assumed. The boosters weight around 100t dry and are mainly derived from the Space Shuttle [114, 115]. We therefore do not consider development costs for them. For the development cost we use equation (6–9) from section 6.2.3 and for the production costs

the cryogenic CER from equation (6–14). For the cost reduction due to learning, we use a learning factor of 90% together with 10 produced units (see equation (6–4)). The obtained costs for both stages in the fiscal year 2017 are shown in Table 6-7. A relative error is not calculated due to unconfirmed reference data.

Table 6-7: Validation of the rocket airframe configuration with the SLS

	Reference	Own CERs
Development costs	$7 - $35 billion	$25 for the first core stage and the second stage without booster
Production costs	$500 million per launch	$530 for the first core stage and the second stage without engines and boosters

Due to the relatively early stage, the reference cost are also estimations and we do not know what the real costs of the programs are. Furthermore, besides the boosters of the SLS, the core stage is also derived from the Space Shuttle's external tank, which means that some parts of the system were already developed previously. The references only list the cost per launch and not the production cost. However, the vehicle production cost accounts usually for a huge amount of the launch costs if the vehicle is not reusable like the SLS. The CER does consider the production of a reusable rocket which results in a higher cost as additional recovery systems must be added.

In summary, the CERs are aligned with the costs provided in the references. Especially for conceptual design space exploration, the relationships provide sufficient accuracy.

6.6.3 Airframe Rocketplane cost validation – Skylon

We validate the rocketplane airframe configuration with the spaceplane Skylon. It is a Single-Stage-To-Orbit (SSTO) vehicle developed by the British company Reaction Engines Limited (REL). The key technology is the Synergistic Air-Breathing Rocket Engine (SABRE) engine, which is a combined air-breathing rocket engine with two modes of operations [116]. It accelerates the vehicle to Mach = 5.4 and 26 km in the air-breathing mode and then switches to rocket propulsion mode for the remaining ascent to LEO [116]. An article published by The Space Review reports that REL estimated the development of the Skylon including the SABRE engines to be at roughly that of the Airbus A380 or about $17-20

billion. According to an assessment report published by ESA [117], this estimation is too pessimistic and ESA calculated the development cost to be $12.3 billion including airframe and engine. The production cost for one spaceplane including the engines is estimated to be £190 million (= $231 million) in 2010 [118].

To calculate the CERs we must know the empty weight without engines, as well as the commercial factor and the cost reduction factor. For the cost conversion value, we use the fiscal year 2011 (273,000 $/WYr). The commercial factor is 0.5 as can be seen in Table 6-2. With the assumption of a production of three units and a learning factor of 90%, the cost reduction factor calculates to 0.85 (see equation (6–4)). The empty weight of the Skylon is given by the Skylon Users' Manual to be 53,000 kg including the engines [116]. We calculate the weight of the engine with using the thrust-to-weight ratio of 14 [119] and the sea level thrust of 1,960 kN [120]. This results in a mass of 14,000 kg per engine and finally 25,000 kg for the Skylon airframe. With these data, we can obtain the estimated development and production costs listed in Table 6-8.

Table 6-8: Validation of the rocketplane airframe configuration with the Skylon spaceplane

	Reference	Own CERs
Development costs	$12.3 - $20 billion with engine	$6.7 billion without engine
Production costs	$231 million with engine	$313 million without engine

For commercial aircrafts, the jet engines account for around one third of the costs [121]. In case of the Skylon, we can assume that the SABRE engine account for a higher fraction due to their more complicated technical systems. We assume that for both, the development and the production, the jet engines account for 50% of the costs. With this assumption, the development costs based on the references are between $6 and $10 billion for the airframe. This compares sufficiently well with our estimation of $6.7 billion.

Using the same assumption, the production cost of the airframe would be $115 million. This differs significantly from our estimation of $313 million. At this point we do not know which estimation is more realistic as no vehicle was built so far.

The validation of the rocketplane airframe CER shows sufficient accuracy of the development costs and is inconclusive for the production costs. However, the production cost number is in the right order of magnitude.

6.6.4 Airframe Airplane cost validation – A320

The validation of the Airplane airframe configuration is done with the A320 family which was produced several thousand times [122]. This family includes short and medium range narrow body commercial aircrafts, numbered from A318 up to A321. Airbus listed an average price of around $100 million for the A320 family with variations depending on the actual aircraft and engine configuration [123]. The Economist reported that the development of an all-new A320 would cost around $10 billion in 2010 [124]. A similar amount was reported by FlightGlobal in 2012 [125]. They reported that the re-engine costs for the A320 are estimated to $1.32 billion or 10-15% of the total development costs as said by Boing CFO James Bell. In addition, he estimated the development of a new 737 would cost around $10-$12 billion. The 737 is the competitor airplane of the A320 and therefore has a comparable cost structure. To use the CERs for the development cost (equation (6–11)) and the production costs (equation (6–17)), we must know the OWE, the maximum design speed, the number of produced units as well as the learning curve. According to Airbus [126] the OWE for a A320 is 42.5t. The maximum design speed is assumed to be Ma = 0.9. For the cost reduction factor, we use 5,000 as the number of units and a learning factor of 90%. This results in $f_{CR} = 0.275$. The obtained costs are compared to the reference data in Table 6-9.

Table 6-9: Validation of the airplane airframe configuration with the A320

	Reference	Own CERs
Development costs	$10 - $12 billion	$11 billion
Production costs	$100 million list price	$20 million without jet engines

The comparison shows a sufficient match for our estimated development cost of the A320. Airbus does not publish their production costs for the A320, so we must use the list price of $100 million to compare it with our estimated production cost of $20 million. The list price is not necessary the price for which the airlines buy the airplanes. The Wall Street Journal reports discounts of 50% and more [127]. If we assume this 50% discount, we end up with a

selling price of around $50 million. The Gross Profit Margin of Airbus is around 10% [128], which means that $45 million of the A320 are production, development cost amortizations and improvement costs. With the assumption that the development costs of $10 billion are equally spread over the 5,000 airplanes, we have a $2 million amortization per airplane for the development costs. If we dedicated $1 million per airplane for continuously improvements and derivatives development, the resulted production cost must be around $42 million for the airframe and the jet engines. The A320 if offered with two engines option, the CFM56 and the IAE V2500. The CFM56 is listed with $10 million [129]. The A320 is a two-engine airplane which results in a total predicted production cost of $40 million ($20 million for the airframe and $20 million for the jet engines). This compares very well with the $42 million we came up from the listed price of $100 million.

In short, the validation with the A320 shows that either the development and the production CERs are sufficiently accurate for conceptual design space exploration.

7 Results and Discussion

We have defined the architectural design space of MSV in chapter 2. The used methodology with the design framework and the two metrics ORSRM and OCPP are described in chapter 3 - 6. This chapter aims to present and discuss the results of the optimization algorithm followed by the conclusions in chapter 8.

As shown in Figure 3-1, the GA optimizes each architecture with respect to their safety and mass objectives. Then, the followed financial optimization calculates the OCPP depending on the annual number of participants. The OCPP metric used to evaluate the architectures does exclude the development costs of the rocket and jet engines. We assume that the engines are bought from other companies or the development costs are financed through other projects. The design optimization uses the number of participants as a prescribed requirement variable. The number of pilots is chosen by the algorithm. We run the optimization four times with a fixed number of participants of *1*,*4*,*8* and *16*. To keep this chapter concisely, we only show and describe the results for four participants. The results of the other three cases are attached in annexes A.8 and A.9.

7.1 Design optimization of each architecture

7.1.1 Pareto architecture for four-participant vehicles

Each architecture was optimized by the GA. The population was set to 2,000 to explore a broad design space. This increases the likelihood that the found optimized designs are global optimums. For each generation, we have calculated the relative deviation of the best individual with respect to the latest generation. This assumes that the latest generation is the one closest to the “real” solution. The relative deviation is calculated for both metrics, ORSRM and total launch mass. It is tracked over the whole optimization and used as a measurement of the level of convergence.

Figure 7-1 shows an example of the XCOR architecture #4 as previously defined in our overview matrix Table 2-6. The title shows the decision that describe the architecture. In this case, we have a horizontal launched plane with no jet engines but rocket engines. There is no second module. The upper of the two plots show the objective metrics, the risk on the ordinate and the mass in metric tons on the abscissa. The dots represent the individuals evaluated during the GA. They are colored by generation with the same color being

individuals from the same generation. The black dashed line connects the design on the pareto front. Interestingly, the results are almost discrete in the risk metric. This is due to the definition of the ORSRM, which is not only based on the architectural decision but also on the two design variables, *nPilots* and *Propellant*. These two variables are chosen and optimized by the GA. There are three choices for the number of pilots and three for the propellant, resulting in nine possible different risk values for one architecture. Some of them are closer to each other than others. For most architectures, they cluster in the three main areas as it is the case in #4 shown by Figure 7-1. As expected, the results are continuous in the mass dimension.

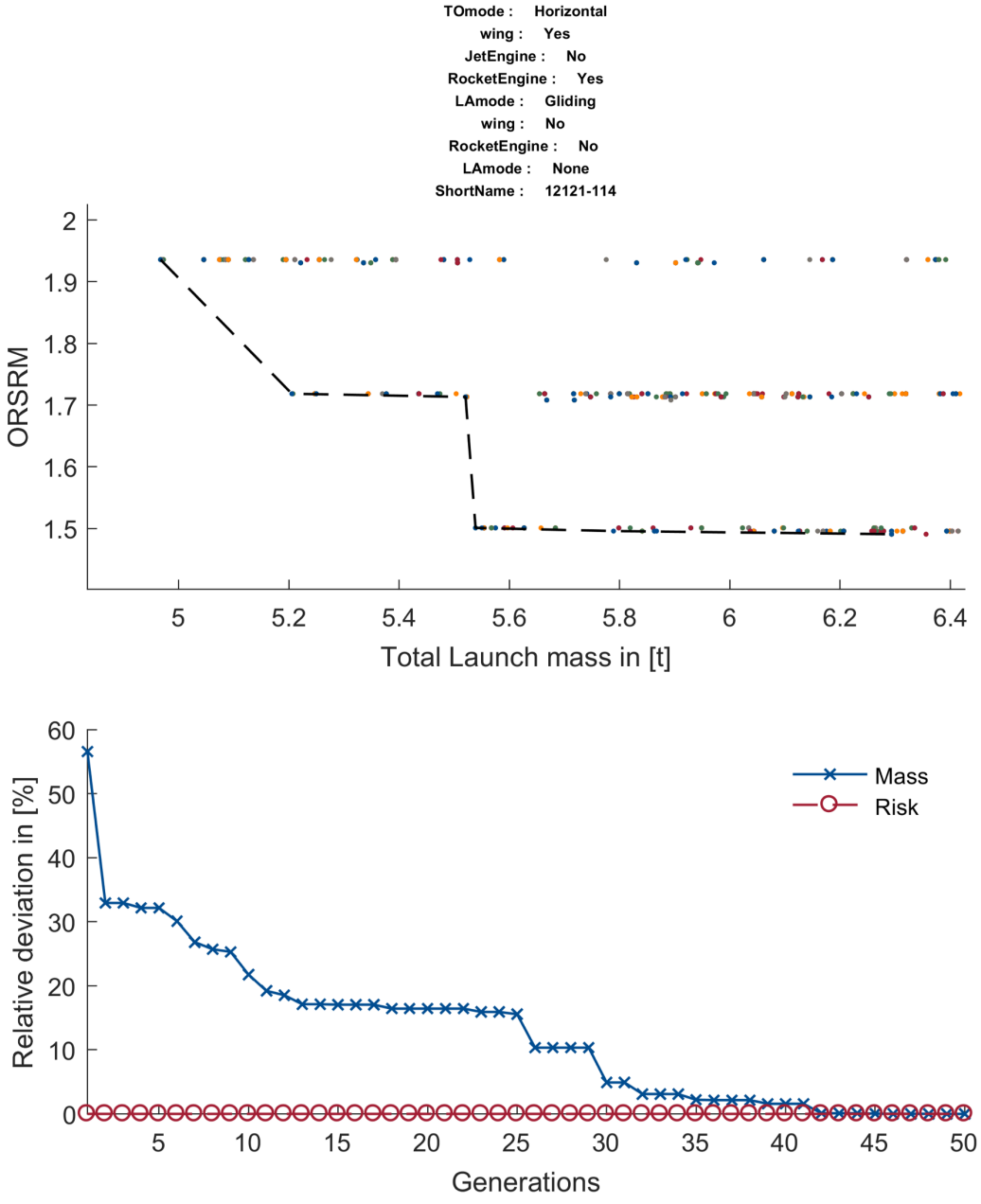

Figure 7-1: Example of the optimized architecture #4 with nPAX = 4

The bottom chart shows the relative deviation in percent versus the number of generations. There are two lines, one for the risk and one for the mass metric. The figure depicts the converged results and we assume that the result of the last generation (here 50) is the one which is closest to the real (unknown) solution. For each generation before, we calculate the relative deviation with respect to this last generation. We can see on the red circled line that compared to the mass objective, the generations show little change in the risk values. Almost during the first iteration, the result is converged in this dimension. The blue crosses show a deviation of around 30% during the first five generations with respect to the last result. As expected, the deviation is reduced with increased generations and during the last 5-10 iterations, no significant change could be observed. The other architectures show a comparable convergence behavior and we can therefore argue that a generation of 50 is an appropriate setting.

Since the optimization of the architectures are not coupled, the problem was parallelized in the very beginning to reduce the computational time. We have broken down the problem into 33 sub problems, with each architecture optimization being one problem. They were executed on a 16-core desktop workstation, achieving a CPU utilization of almost 100% throughout the calculations. The execution time of the whole optimization was around 24 hours. This had to be done four times for the different prescribed numbers of participants.

As mentioned above, to keep this section uncluttered, we only show and describe the results for the four-participant case. For each architecture, we can identify the individuals on the pareto front represented by the dashed black line in Figure 7-1. If we combine these lines of the 33 architectures into one chart, we obtain Figure 7-2 with the ORSRM on the ordinate and the total launch mass on the abscissa. Each pareto front is labeled with the architecture number defined in Table 2-6. The number is plotted to the left of the optimized design of the architecture with the highest ORSRM, i.e. on the top-left of the line. The dashed black line combines the non-dominated solution of all architectures and displays the total pareto front. Furthermore, the architectures are colored depending on their wing attribute. If both modules have a wing, they are colored blue; if only the first module has wings but the second not, they are colored red; if only the second module has wings but not the first, they are colored orange and if neither of the module has wings, they are colored grey. In addition, the four architectures of Blue Origin, Virgin Galactic, XCOR and Rocketplane XP are encoded with markers. The Blue Origin architecture #18 has larger dots (•), the Virgin Galactic architecture #14 has a downward-pointing triangle (▼), the XCOR architecture #4 has crosses (x) and the Rocketplane XP architecture #5 has filled

diamonds as markers (♦). The XCOR architecture is with almost all designs on the pareto front for medium risk and masses. On average, the Rocketplane XP architecture is around 0.5 t heavier but slightly safer. The Blue Origin #18 has around the same mass as the Rocketplane XP but is riskier. Virgin Galactic #14 has almost twice the mass of the XCOR architecture but is the safest. Architecture #17 and #18 differ in the landing mode of the first module, parachute and rocket powered, respectively. As can be seen from the figure, the rocket powered landing increases the mass and slightly the risk of the vehicle. This is due to the additional systems and propellant needed.

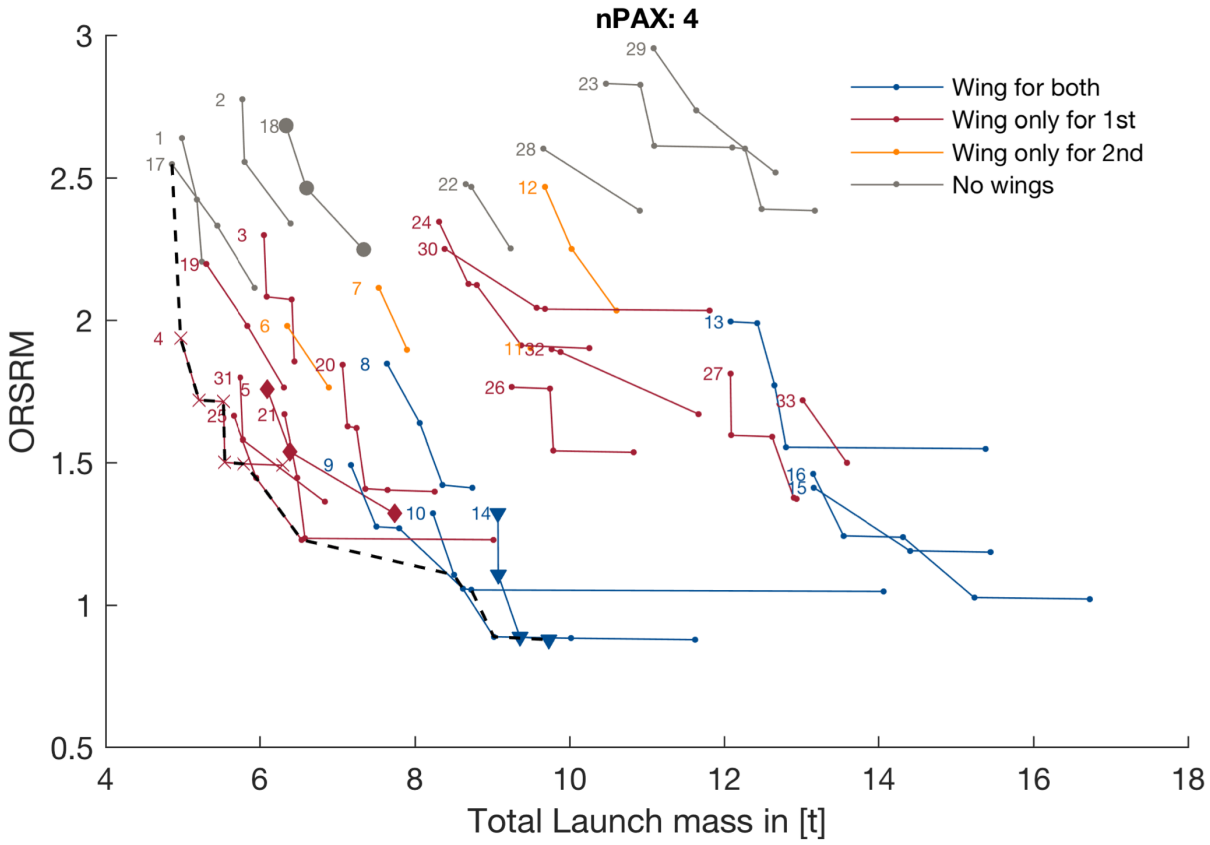

Figure 7-2: Pareto fronts of the 33 architectures with respect to the ORSRM and total launch mass

As shown by the figure, the total launch mass for a vehicle with four participants varies from 4.8 to 17 metric tons. With decreasing mass, the risk increases and vise-versa. This is an expected behavior and true for most technical systems [15]. There is a trade-off between risk and mass (which is often a proxy for cost). The colors show a clear trend from the heavier and safer options on the bottom-right and the lighter and riskier architectures on the top-left. Wings add weight but also reduce risk. The architectures with two wings are the heaviest but the safest. If the vehicles have no wings (grey lines) they are riskier but lighter.

The architectures with either a wing on the first or second modules are in between. According to our reasoning of the risk mitigation factors in Table 5-6, wings have the potential to mitigation trajectory and steering hazards. In addition, they open the possibility to use jet engines instead of rocket engines which are considered safer. It is plausible that wings add weight and reduce risk.

For further discussion, we look at the architectures on the pareto front with the numbers #17, #4, #25, #9, #10 and #14 starting from lighter and riskier to heavier and safer. We display them in Table 7-1 using the pictograms defined in Table 2-5. Three of these six pareto architectures are part of the database we created in the beginning. Four of the seven architectures found in the database are not part of the pareto front for a four-participant vehicle. The architectures #25, #9 and #10 are not proposed yet.

Table 7-1: Overview of the five architecture on the pareto front of four participant's vehicles

Architecture number	Module 1	Module 2
#17 e.g. ARCA	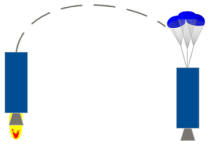	
#4 e.g. XCOR		None
#25	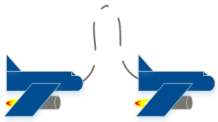	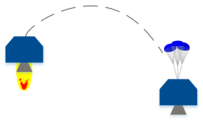
#9		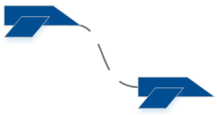
#10	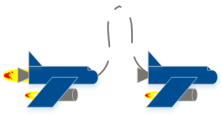	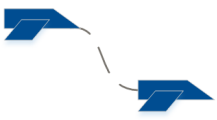
#14 e.g. Virgin Galactic	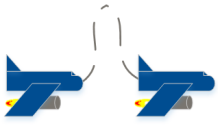	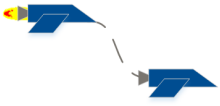

Lighter and Riskier

Heavier and Safer

Since the architectures are ordered from the lighter and riskier to the heavier and safer, the previously discussed influence of the wing on the metrics can be seen graphically. The first architecture has no wings, whereas the last three have wings on both modules. The second and third have wings on the first module but not on the second one (or there is no second module, respectively). Five of the six architectures have a two-module architecture with two of the second modules being powered (#25 and #14). If the landing orientation is vertical and the module has a rocket engine, the preferred decelerating instrument is a parachute. This is the case for the first modules of architecture #17 and for the second module of #25. There is no architecture on the pareto front with a rocket powered landing. None of the six architectures has three engines, the first two lighter and riskier ones and #9 have a rocket engine on the first module and no additional engine on the second module. The heavier and safer three architectures #25, #10 and #14 have jet engines on the first module and an additional rocket engine either on the first module (#10) or as part of the second module (#25 and #14).

7.1.2 Pareto fronts of all four number of participant cases

In the previous section, we described the pareto architectures for a four-participant vehicle. We have defined a new pareto front containing the six non-dominated architectures. The dashed black line in Figure 7-2 combines those. The equivalent figures for the other three number of participants are attached in annex A.8. If we plot these four pareto fronts into one chart, we obtain Figure 7-3.

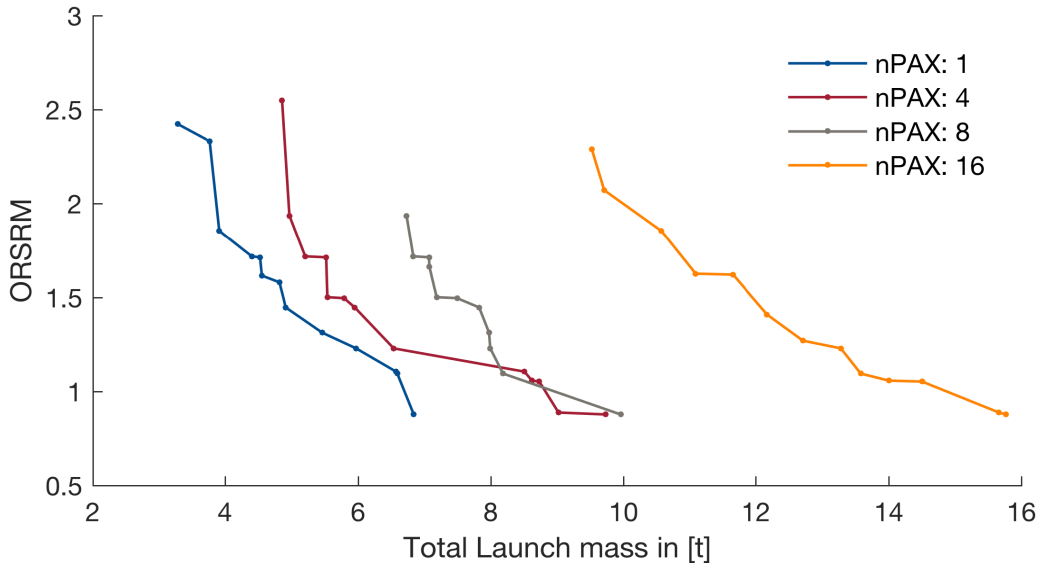

Figure 7-3: Pareto fronts of all pareto architecture for 1, 4, 8 and 16 participants

All four pareto fronts show an equal behavior with respect to the two-metrics risk and mass. The heavier architectures are safer and the lighter ones are riskier. With increasing number of participants, the vehicles are heavier as the payload mass increases and likewise the structural support mass. The pareto curves are shifted to the right. The ORSRM of the safest architecture remains almost constant at around 0.88 with the riskiest architecture being between 2 and 2.5.

It is apparent that the vehicles become heavier with increasing number of participants. But as the bar graph in Figure 7-4 shows, the average launch mass per person decreases. A person can be both, a participant or a pilot. With this definition, there can be between four and six people on a four participants' vehicle since the number of pilots can vary from zero to two. The same is true for the 1, 8 and 16 participant vehicles. The average number of pilots across all architectures and number of participants is 1.25.

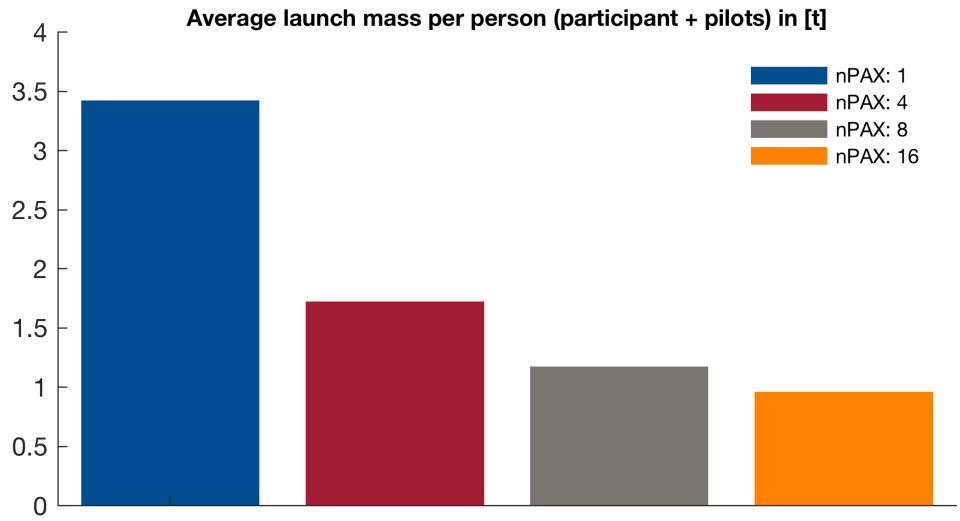

Figure 7-4: Comparison of the average launch masses per person (participants and crew) for the four different cases

For the one-participant vehicle, the average mass per person is around 3.5 metric tons. For a four-participant vehicle this value is almost halved and decreases further for increasing number of participants. This makes sense due to scaling effects. Like for the costs, there are fixed and variable mass contributions. The former is not a function of the payload mass and is distributed among the participants. With increasing number of participants, the fixed mass contribution decreases. For an infinite number of participants, only the variable mass contributions would remain. The effect is more pronounced for smaller number of participants as shown by the Figure 7-4. For the 16-participant architectures, the average mass per person is around 1 metric ton.

7.2 Financial optimization with fixed annual demand

7.2.1 Pareto architecture for four-participant vehicles

As described in chapter 3 and depicted in Figure 3-1, the architectures are optimized by the GA with respect to the ORSRM and total launch mass. The results were shown in the previous section. This section presents the results after another GA optimizes the operational business variables, which are the number of launches per vehicle and year as well as the size of the fleet, i.e. the number of operational vehicles. The ORSRM and the cost metric OCPP are the two objective functions. The requirement variables are the length of the program and the annual demand of number of participants. The program length is fixed to 20 years, with operation starting in year 6. We reasoned in section 3.2.2 that an annual participant demand of 1,000 is reasonable for a ticket price of $100k (assuming 22% market share). With these constraints, we optimized the pareto designs of all 33 architectures. The resulting plot for a four-participant vehicle is shown in Figure 7-5. Annex A.9 shows the figures for the other three cases.

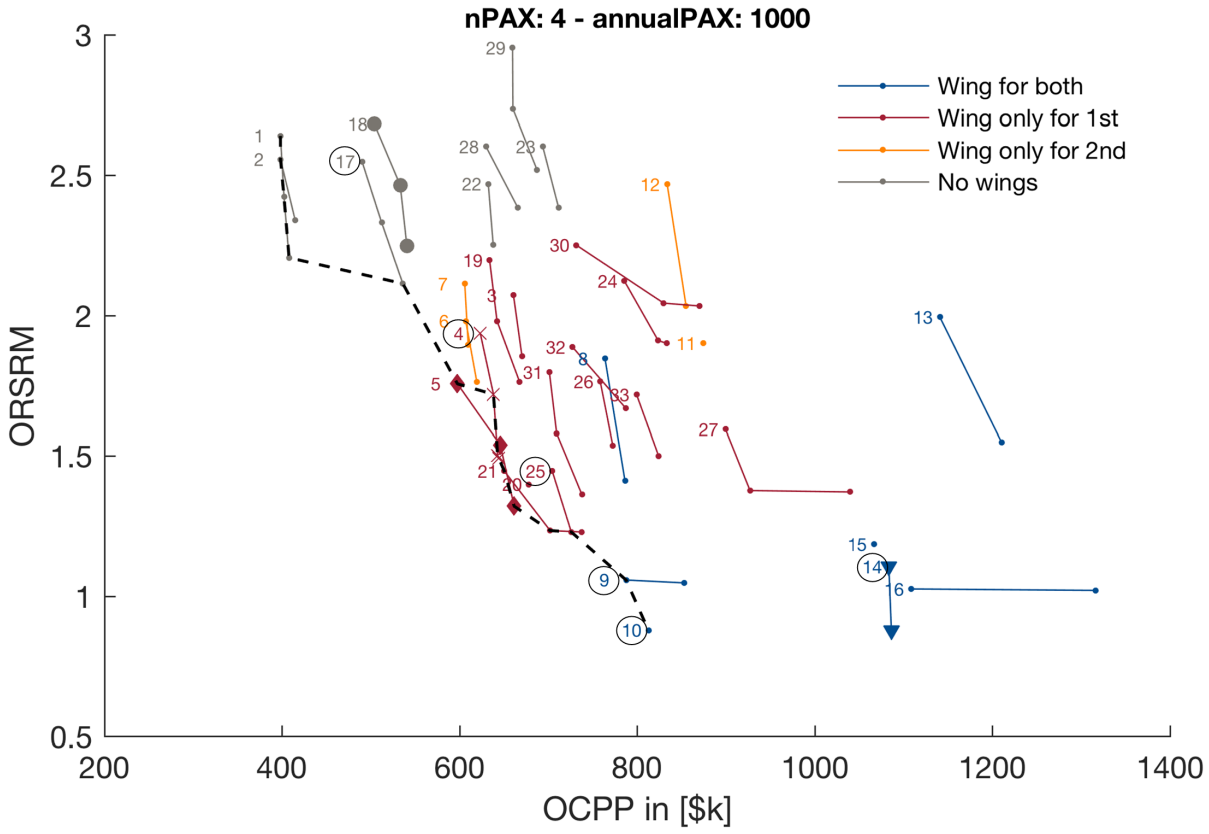

Figure 7-5: Architectures with optimized business variables for four-participant vehicles

Like Figure 7-2, the architectures are labeled with their number and colored by the wing attribute. The dashed black line connects the non-dominated architectures. The similar effect of the wings can be observed. Wings decrease risk but add cost. We marked the six pareto architectures #17, #4, #25, #9, #10 and #14 with a black circle. Except of the Virgin Galactic architecture #14, all of them are on the pareto front after the operational business optimization.

The four architecture of XCOR (x), Rocketplane XP (♦), Blue Origin (●) and Virgin Galactic (▼) are shown as well. The XCOR #4 is still on the pareto front with medium risk and cost. Blue Origin has shifted to the left closer to the pareto front. It is the cheapest of these four but the riskiest. The Rocketplane XP architecture is still safer than XCOR but slightly more expensive. Virgin Galactic #14 is the safest but around twice as expensive as the other three.

In addition to the previous non-dominated architectures, there are #1, #2, #5 and #21 on the pareto front (shown in Table 7-3). These are single-module rockets (#1, #2), the Rocketplane XP (#5) and a jet equipped rocketplane architecture with an unpowered capsule (#21). The first module of #1 lands with a parachute whereas the landing mode for #2 is rocket powered (see section 2.4). This shows that the rocket powered landing increases the risk and slightly reduces the cost. In comparison with architecture #21, #5 has higher risk but lower cost. The second module adds safety to the system but increases the cost.

As discussed above, some architectures have shifted closer or further away from the pareto front after the financial business optimization. The problem is setup in a way that the risk dimension does not change. In Figure 7-2, the grey architecture #1, #2 and #17, #18 are in the same mass region. After the financial optimization, #1 and #2 have shifted away from #17 and #18 to the left. If we compare #1 and #17, we observe a similar contribution of the RDT&E, production and operating costs. However, since #17 is a two-module vehicle all three costs are higher compared to a one-module vehicle. It is cheaper to develop, produce and operate a one-module vehicle than a two-module one with the same total launch mass. This makes sense since the CERs are defined this way that with increasing mass the cost per mass unit decreases.

Next, we discuss the one winged vehicles. The orange architectures have not significantly moved after the business optimization. #6 and #7 were farer of the pareto front in Figure 7-2 and are now closer. However, this change is small compared to the other shifts. The order

inside this group is the same. The Rocketplane XP architecture #5 has moved towards the pareto front inside the red group. It almost matches XCOR #4 but is slightly riskier and cheaper on average. #5 compared with #4 has an additional jet engine. There are no development costs associated with the jet engine, resulting in almost equal RDT&E cost of around $3.5 billion on average for both architecture. The jet engine adds weight as shown by Figure 7-2 but together with a rocket engine on one module it is riskier than a rocket engine only.

The Virgin Galactic architecture #14 has the same minimum ORSRM value as the architecture #10 but a higher OCPP. These two architecture are similar, but #10 has the rocket engine on the first stage together with the jet engine, whereas #14 has the rocket engine on modules two. Figure 7-2 already showed that the Virgin Galactic's architecture is heavier with a slightly benefit in the safety domain. The heavier weight can be explained by scaling effects of the vehicle and the wings. If the rocket engine is part of the second module, the fuselage and wings must be sized to support the additional weight. If the rocket engine is part of the first module, the airframe size must be increased as well, but due to the inherently higher weight, the additional weight can be support with a lower increase. This results in a lower total launch mass for the same number of participants. Since in general, the mass is correlated with the cost of the vehicle, the observation in Figure 7-5 can be explained. Table 7-2 shows the summed, not discounted costs for the 20 operational years in comparison. #14 has 33% higher total costs, which is around the same percentage the OCPP is higher. Architecture #14 was almost dominated by #10 after the design optimization and is completely dominated after the financial business optimization.

Table 7-2: Comparison of the costs summed across the program length from architecture #10 and #14

	#10	**#14**
RDT&E	$6.6 billion	$8.7 billion
Production	$1.7 billion	$2.1 billion
Operation	$3.1 billion	$4.3 billion
Total	$11.4 billion	$15.1 billion

We can say that #1, #2, #17, #4, #5, #21, #25, #9, #10 are the pareto architectures after financial optimization. They are ordered from cheaper and riskier to more expensive and safer and listed in Table 7-3.

Table 7-3: Overview of all pareto architecture after financial optimization

Architecture number	Module 1	Module 2	nLaunch	numb-Units
#1 e.g. Copenhagen Suborbital	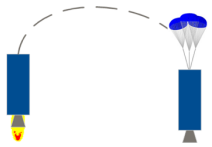	None	10-25	10-25
#2	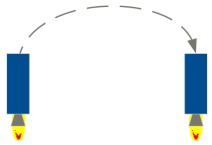	None	10	25
#17* e.g. ARCA	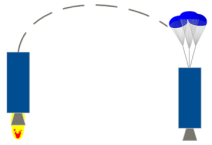		10-25	10-25
#4* e.g. XCOR		None	12	20
#5 e.g. Rocketplane XP	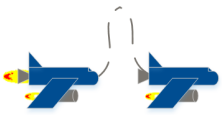	None	12-50	5-20
#21	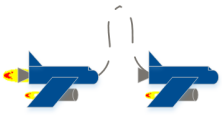		12-25	10-20
#25*	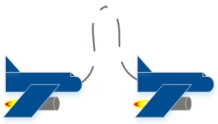	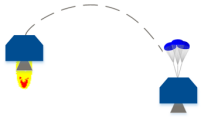	13	19
#9*		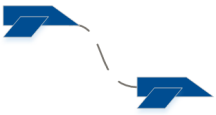	10-25	10-25
#10*	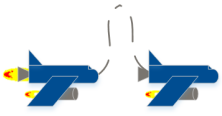	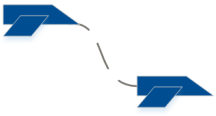	25	10

Cheaper and Riskier

More expensive and Safer

* pareto architectures after design optimization

In addition to the pictograms, the columns nLaunch and numbUnits show the optimized design variables. Each architecture has up to three designs. Each design is one dot on the pareto line in Figure 7-5. Table 7-3 above shows the range of these variables. With the

annual demand of 1,000 participants and a vehicle size of four participants, the product of nLaunch and numbUnits must be smaller than 250. Both variables have similar values. They range from minimum 5 to maximum 50. For some jet engine equipped architectures, we can observe a trend towards higher launch frequency and smaller fleets (#5, #21, #10). This makes sense since jet engine have a higher lifetime than rocket engines and therefore the vehicle can be launch more often until it must be replaced. This goes along with a smaller fleet to meet the demand requirement. A launch frequency of 10-50 equals a turn-around time between five and one week. This goes along with statements of current suborbital companies.

The influence of the wing can be observed in Table 7-3 graphically as well (previously discussed in section 7.1.1). The first three architecture have no wings, the next two have one wing on the final module, the following two have a wing on the first module and the last two have wings on both modules. There are several additional observations which can be made:

- A powered vertical rocket landing of the first module results in a slightly cheaper but riskier vehicle (compare #17 and #18). For a one-module rocket this effect is less pronounced (#1 and #2).
- Adding a second module lead to a more expensive but safer architecture (#1 vs. #17, #4 vs. #9, #5 vs. #21).
- If the second module has wings, this adds costs but reduces risk (#21 vs. #10).
- Compared to rocket engines, jet engines increase the cost of the architecture but add safety to the system. (#9, #10)
- There is no architecture with a rocket powered vertical landing of the second module

Furthermore, there is a correlation between the number of features and costs – parts attract cost [15]. This can be observed on the pareto architectures as well. As Table 7-3 shows, the more expensive architectures have more features than the cheaper ones. These features result in increased development and production costs. Table 7-4 depicts a comparison of the cost distributions with the riskiest and cheapest pareto architecture #1, a medium concept #5 and the safe and more expensive #10. For #1, the operation costs are 52% of the total cost with 42% of development costs. #5 has a similar development cost percentage, but the absolute amount increases from $2.3 billion to $3.4 billion. The more complex two-module architecture #10 has three times the development costs of #1. With 58% it is also the greatest contribution to the total costs. The operational cost influence

dropped to 27% with an absolute amount around the other architectures. In total, #10 is twice as expensive as #1 with #5 being in the middle.

Table 7-4: Cost distribution of the riskiest & cheapest pareto architecture #1, a medium concept #5 and the safe and more expensive #10 for a 4-participant vehicle

#1	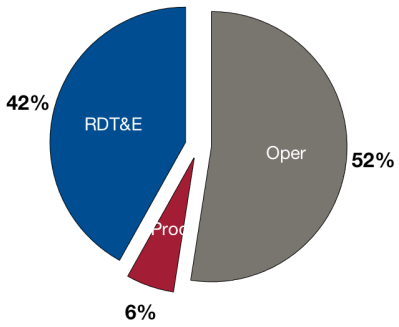	**RDT&E**	$2.3 billion
		Production	$0.3 billion
		Operation	$2.8 billion
		Total	**$5.4 billion**
#5	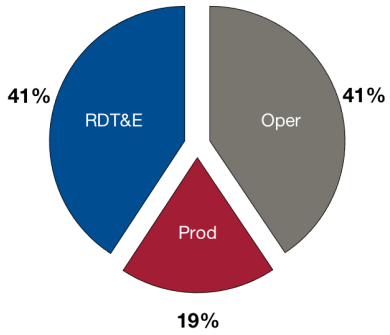	**RDT&E**	$3.4 billion
		Production	$1.6 billion
		Operation	$3.4 billion
		Total	**$8.4 billion**
#10	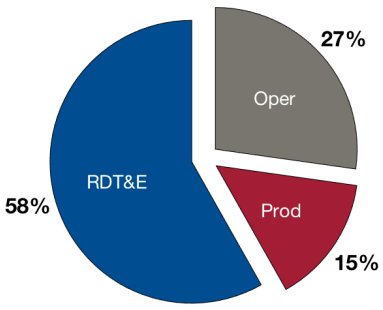	**RDT&E**	$6.6 billion
		Production	$1.7 billion
		Operation	$3.1 billion
		Total	**$11.4 billion**

This data implies that the increased development costs do neither reduce the amount of the operational nor the production costs. The more complex architectures do not economically profit from the investment in the higher development costs in the beginning. Even with a higher demand the variable costs (which are basically the operational and production costs) are the same or even higher. Compared to #1, the higher RDT&E costs of #10 are an investment to reduce the risk of the architecture, but not an investment to reduce the operational costs. For any demand, the more complex architecture will have a disadvantage in the cost dimension.

7.2.2 Pareto fronts of all four participant cases

Like in the previous section 7.1, we have described and discussed the results for the four-participant vehicle first and have identified the pareto architectures. Then, we have compared the resulting new pareto front with the other three cases, 1, 8 and 16 participants. Following this structure, Figure 7-6 shows the pareto front for each number of participant.

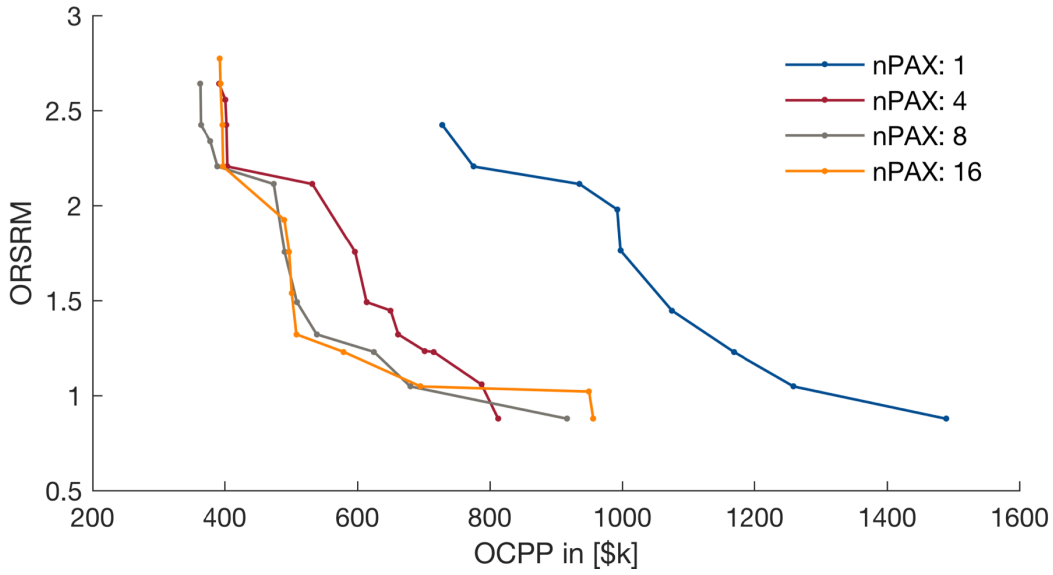

Figure 7-6: Pareto fronts of all pareto architecture for 1, 4, 8 and 16 participants

The coloring is equal to Figure 7-3, with blue for one, red for four, grey for eight and orange for 16 participants. The other three lines follow the global trend with cheaper architectures being riskier and more expensive ones being safer. The have the same value for the lowest ORSRM as well as a similar one for the highest. The global trend is that with increasing size of the vehicle, the OCPP drops. The architectures with one-participant have around twice the OCPP than the other three cases. For bigger vehicles, the cost reduction is less pronounced. The reduction between 4 and 8 participants is on average around $50k, and between 8 and 16, almost no reduction can be observed.

To understand this scaling effect, we investigate the cost distribution of architecture #1 for all four sizes. As shown latter in Table 7-6, this in one of three architectures that is on the pareto front for the four sizes. This architecture is on the riskier but cheaper branches of the four lines. The cost distributions together with the absolute numbers are shown in Table 7-5. The summed not discounted development costs are shown in blue, the summed production costs in red and the summed operation costs are the grey regions. The absolute amounts are summed over the program length of 20 years. Annex A.10 shows the equivalent tables for architecture #9 and #21. They illustrate the same trends.

Table 7-5: Cost distribution of architecture #1 for 1, 4, 8 and 16 participant vehicles

nPAX = 1 total mass: 3,280 kg	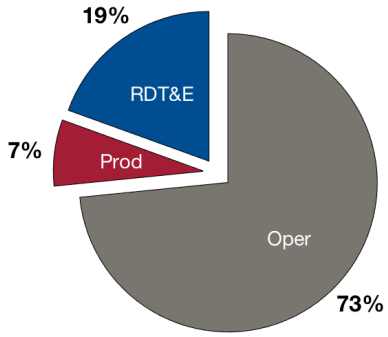	**RDT&E** **Production** **Operation** **Total**	$2.0 billion $0.7 billion $7.4 billion **$10.1 billion**
nPAX = 4 total mass: 4,981 kg	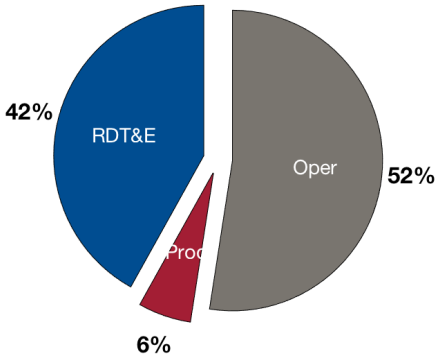	**RDT&E** **Production** **Operation** **Total**	$2.3 billion $0.3 billion $2.8 billion **$5.4 billion**
nPAX = 8 total mass: 6,774 kg	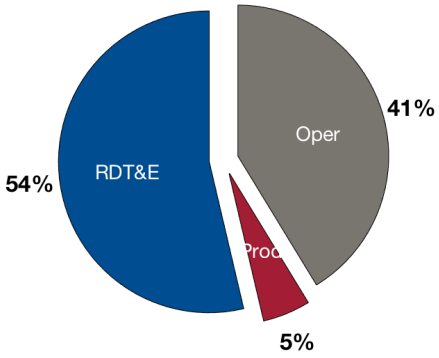	**RDT&E** **Production** **Operation** **Total**	$2.7 billion $0.3 billion $2.1 billion **$5.1 billion**
nPAX = 16 total mass: 11,866 kg	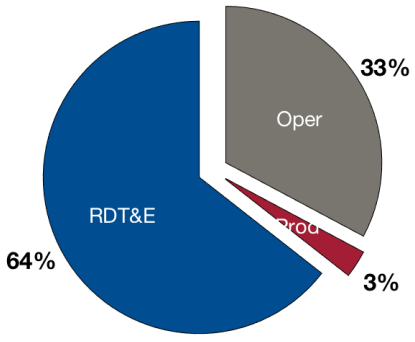	**RDT&E** **Production** **Operation** **Total**	$3.4 billion $0.1 billion $1.7 billion **$5.2 billion**

The absolute total costs from Table 7-5 go along with the OCPPs from Figure 7-6. The smallest vehicle has twice the total costs than the bigger ones and the difference between 4, 8 and 16 participants is little. The contribution of the development costs increases from 19% to 64%, the productions costs decrease from 7% to 3% and the operational proportion decreases from 73% to 33%. The absolute numbers behave equivalent. As shown by the table above and by Figure 7-3, the total launch mass of the vehicle increases with the number of participants. According to the CERs' fundamentals, the development costs increases with the mass of the vehicle. This explains the increase of the RDT&E costs.

With increasing mass, the production and operation costs per vehicle rise accordingly. The numbers shown in Table 7-5 are the summed costs for the whole program. This means that the costs per vehicle are multiplied with the number of launches per year and the operational years. The latter is constant for all sizes, but the launches per year vary with the number of participants that can fly with one launch. With the demand of 1,000 annual participants, the smallest vehicles need 1,000 launches, the four-participant vehicle a quarter of that, 250 launches, and so on. The result implies that the increased cost per vehicle is less than the decrease due to less launches. This is a typical scaling effect that can be observed throughout the industries.

These results do not consider the discounting of the development costs. If we consider the cost of capital, this would be a drawback for larger vehicles. Their higher development costs would result in higher discounting costs. However, we assume that this effect does not change the global trend.

To provide an overview of which architectures are on the pareto front for which sizes, we made a list for all four cases. It is the same as displayed in Table 7-3 for the four-participant vehicles. The figures are attached in annex A.9. This list for all four cases is shown in Table 7-6. The rows are the pareto architectures and the columns show the four different cases. The *x* indicates that the architecture is on the pareto front. There are 12 out of the 33 architectures which are at least on one of the pareto fronts. Three architectures, #1, #9 and #21 are on the pareto front in all four cases.

Table 7-6: 12 pareto architectures for the four-different number of participants

Architecture #	nPAX=1	nPAX=4	nPAX=8	nPAX=16
1	x	x	x	x
2		x	x	x
4		x	x	x
5		x	x	x
6	x			
9	x	x	x	x
10	x	x		
14			x	x
16				x
17	x	x	x	
21	x	x	x	x
25	x	x		
Total number	7	9	8	8

A different representation of the same result is shown in Table 7-7. The 21-dominated architectures are greyed out and have a strikethrough font style. For the remaining architectures, the number of participants is written in grey and brackets for which the architecture is on the pareto front. We can see that there are concepts which perform well for smaller vehicles, i.e. lower number of participants, and vise-versa. Non-dominated architectures with participant numbers of one to four are #10 and #25. The Virgin Galactic architecture #14 and the three-engine vehicle #16 are on the pareto front for eight and 16-participant vehicles. A powered vertical landing of the second module is not part of any of the pareto architectures.

There is no general set of pareto architectures which is non-dominated for all four number of participant's cases. It depends on the size of the vehicle. To answer the research question which architecture offers the best combination of safety and economic return, the decision-makers first must decide on the number of participant or the sizing of the vehicle, respectively. The discussion suggests that architectures with four participants offer a "good" combination of prospect of viability and fundable development costs. We further discuss the conclusion in chapter 8.

Table 7-7: Overview of the 12 remaining pareto architectures (* with three propulsive systems, one jet and two rocket engines)

1st module / 2nd module	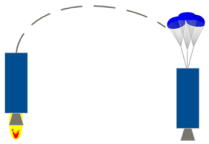				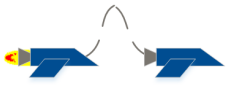	
None	**1** (1,4,8,16) e.g. Copenhagen Suborbital	**2** (4,8,16)	~~**3**~~	x	**4** (4,8,16) e.g. XCOR	**5** (4,8,16) e.g. Rocketplane
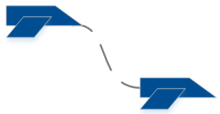	**6** (1)	~~**7**~~	~~**8**~~	x	**9** (1,4,8,16)	**10** (1,4)
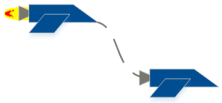	~~**11**~~	~~**12**~~	~~**13**~~	**14** (8,16) e.g. Virgin Galactic	~~**15**~~	**16*** (16)
	**17** (1,4,8) e.g. ARCA	~~**18**~~ e.g. Blue Origin	~~**19**~~	x	~~**20**~~	**21** (1,4,8,16)
	~~**22**~~ e.g. Canadian Arrow	~~**23**~~	~~**24**~~	**25** (1,4)	~~**26**~~	~~**27***~~
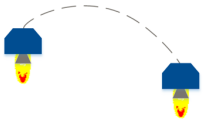	~~**28**~~	~~**29**~~	~~**30**~~	~~**31**~~	~~**32**~~	~~**33***~~

7.3 Profitability - Financial optimization with variable annual demand

The previous section described a relative comparison of the architectures and we defined a set of non-dominated concepts. This section aims to make a statement about the absolute OCPP values compared with the market demand, i.e. if the company or project can be profitable. In doing so, we calculate a demand elasticity curve for each architecture and design. This curve is generated by running the operational business for various demands.

In the foregoing, the demand was fixed to 1,000 annual participants. We estimated this demand based on the reports of the Futron and Tauri group discussed in section 3.2.2. We further assumed a ticket price of $100k and a market share of around 22%. The demand has significant influence on the OCPP since development, production and fixed operating costs can be amortized over more participants. With infinite participants, the OCPP would represent the variable operating costs plus the production amortization cost.

To investigate the influence of the annual number of participant on the OCPP, we have run the operational business variable optimization seven times with 100, 250, 500, 1,000, 5,000 and 10,000 annual participants. This was done for all architectures with their designs and for all four cases. The OCPP from 0 to $1,500k is displayed on the abscissa and the annual number of participants from 0 to 5,000 on the ordinate of Figure 7-7. Lines connect the calculated points of the seven different demand numbers. The global behavior is like the price elasticity curve from Figure 3-4. The cost decreases with increasing demand and convergences to a value which is the variable cost amount. On the other extreme, if the demand decreases to a few participants per year, most of the OCPP is the amortization of the development, production and fixed operating costs. Depending on the size, the OCPP increases significantly below an annual participant number of 750 for the smallest and 250 for the largest vehicles. Above this spot, the price drops and more people are willing to purchase a ticket. The black line is the demand elasticity curve. It is based on equation (3–1) but considers a 22% market share. Consistent with the discussion in section 3.2.2, we find an annual participant demand of 1,000 for a ticket price of $100k. The green demand curve assumes that the fictive company has 100% market share. If we assume that the OCPP equals the ticket price, the regions below the demand curves are the profitable regions. Any design below the demand line has a lower OCPP than the participants are willing to pay.

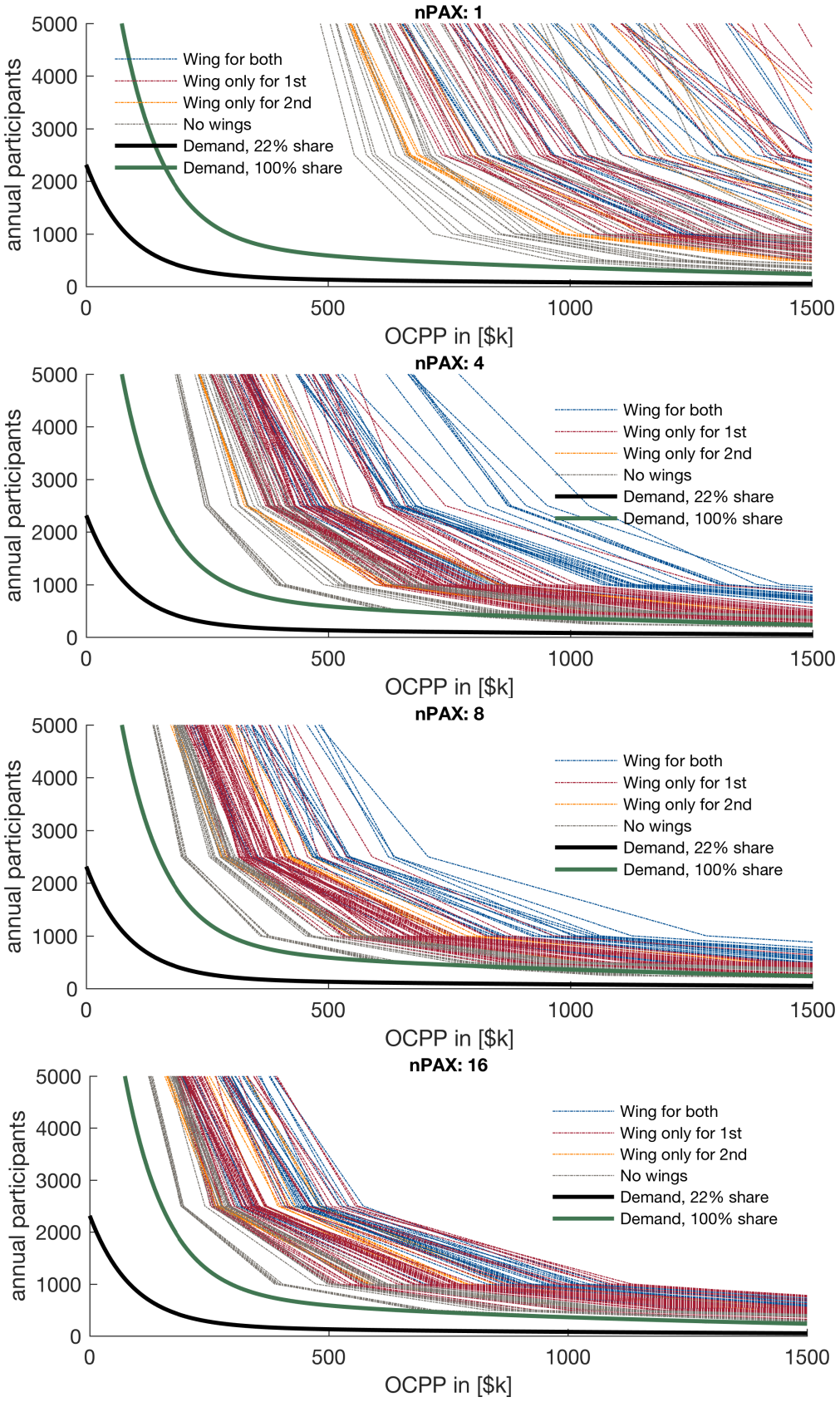

Figure 7-7: Comparison of supply elasticity with demand elasticity assuming the OCPP equals the ticket price

In alignment with Figure 7-6, the OCPP decreases with larger vehicles for all demands between 100 and 10,000 annually. Except of some individuals, all architectures show a similar supply elasticity. For none of the cases, any of the architecture is in the profitable zone for 22% market share. If the company can get the complete market, there may be some architectures that touch the profitable region for low demands. Notice, that the demand elasticity was not defined for a ticket price above $1,000k and we extrapolated the curves. This means that there is a particularly high uncertainty for high ticket prices and low demands. Interestingly, with increasing size, the distance between the cheapest and the most expensive architecture decreased. The lines are closer to each other. The more expensive architectures with two wings move closer to the pareto front. For example, as can be seen from Table 7-6 and Table 7-7, the Virgin Galactic architecture #14 is on the pareto front for larger vehicles with 8 or 16 participants, but not for the smaller ones. This means that for larger vehicles, safer architectures have less price penalty and the additional costs to add safety decreases.

7.4 Sensitivity of the architectural decision options

According to Battat [130] and Simmons [131], decisions can be characterized in two dimensions, the degree of sensitivity and the degree of connectivity. The former is a measurement of how strong a change in a certain decision influences the objective function (the metrics). The degree of connectivity is a measurement of how the decision are coupled between each other. There are four regions with (I) being sensitive and strongly connected, (II) sensitive but weakly connected, (III) insensitive but strongly connected and (IV) insensitive and weakly connected (see Figure 7-9).

The sensitivity of the decisions with respect to the two metrics, OCPP and ORSRM, is calculated by plotting all architectures with all four number of participant's cases in the risk vs. cost charts. Then, the optimized pareto front of the architecture are colored by the chosen option. This is repeated for each decision. The nine plots are attached in annex A.11. In a next step, the average OCPP and ORSRM for each chosen option, i.e. for the lines with the same color, is calculated. The maximum distance between those values is computed for one decision. This difference indicated how much the choice of this decision can influence the metrics. These numbers are calculated for both metrics and all nine decision. Finally, they are normalized to make them comparable. The resulting plot is shown in Figure 7-8. The horizontal bars represent the normalized distance between the average OCPP and ORSRM for the decision's options. The red bars are the sensitivity in the risk

and the blue bars in the cost dimension. One red and one blue bar relates to one decision displayed on the left of the figure. The decisions are ordered according to the morphological matrix from Table 2-1.

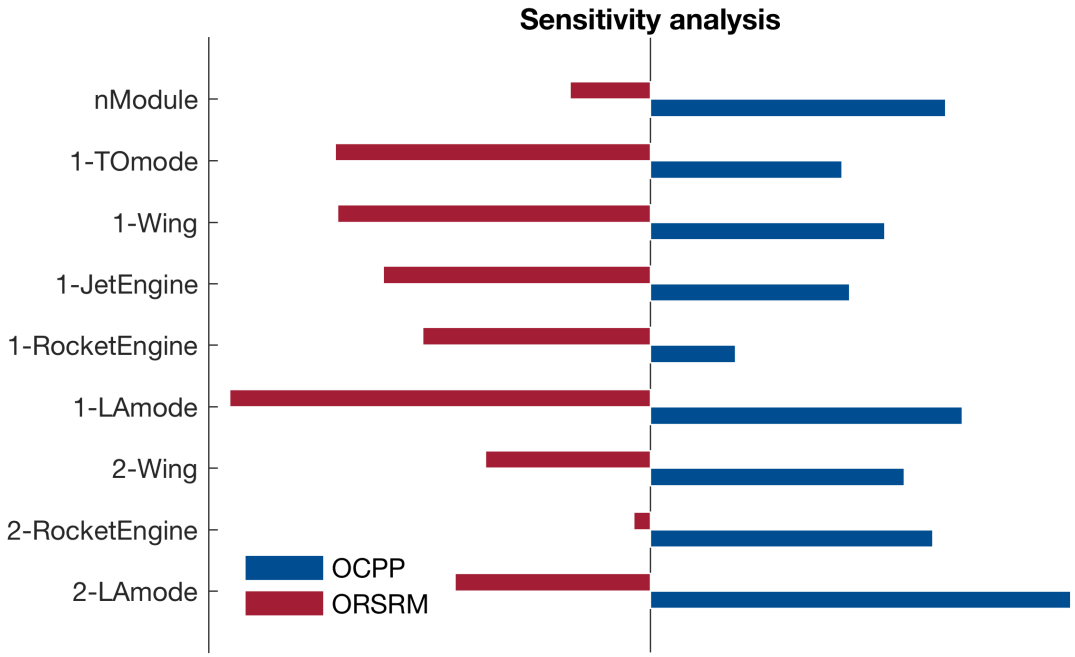

Figure 7-8: Sensitivity analysis of the architectural decisions

A short bar specifies that the decision is less sensitive to the metric, or in other words that the metric is less dependent of the chosen option for this decision. For example, the decision about the rocket engine of the second module (2-RocketEngine) is the least sensitive one in the risk dimension. If the vehicle has a rocket engine on the second module or not, does not influence the ORSRM as much as other decision do. However, it has slightly above average influence on the OCPP. In opposite, the decision about the landing mode of the first module (1-LAmode) has the highest influence on the total risk of the vehicle and the second highest on the cost. The combined sensitivity, which is the sum of the one for OCPP and ORSRM, is the highest for this decision. Decisions-maker must be particularly careful with high sensitive decisions. Their choice has great influence on the achievable risk and cost metrics. Interestingly, the sensitivities of the decision about the same feature for module one and two are different. The 1-RocketEngine decision has more influence on the risk than on the costs. The opposite is true for the 2-RocketEngine decision. The same can be observed for the landing mode decision. On average, module one decisions have higher influence on the ORSRM than on the OCPP and vise-versa for module two decisions. The risk level is more defined by module one and the costs are more

a result of the module two architecture. The choice if the vehicle has one or two modules has moderate influence on the ORSRM but the third highest sensitivity on the OCPP.

To order the decisions into the four regions as defined by Battat [130] and Simmons [131], the connectivity between the decision is calculated. We use the constraint matrix from Table 2-3 and count the number of constraints the decisions have between each other. The resulting matrix is shown in annex A.12. The connections vary between two and five with most decisions having three as their degree of connectivity. With these numbers and the combined sensitivity from Figure 7-8, we can categorize the decision in the two dimension as shown in Figure 7-9. The degree of connectivity is depicted on the abscissa with increasing values to the right and the degree of sensitivity on the ordinate with higher values towards the top. The quadrants (I) – (IV) identify the four regions with (I) being sensitive and strongly connected, (II) sensitive but weakly connected, (III) insensitive but strongly connected and (IV) insensitive and weakly connected.

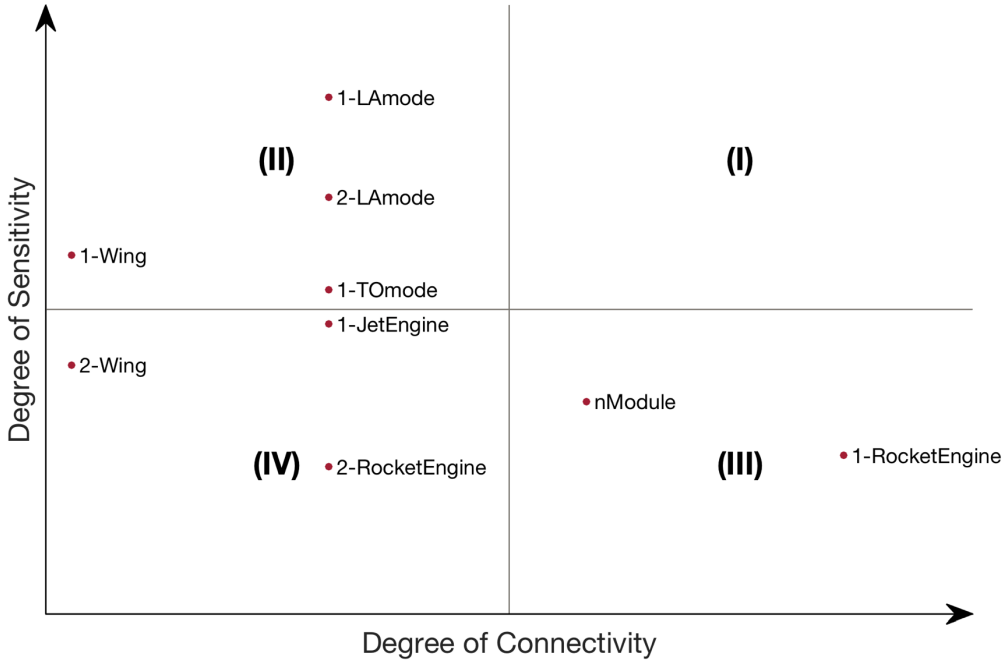

Figure 7-9: Characterization of the architectural decision with the degree of sensitivity and degree of connectivity

Battat [130] and Simmons [131] argue that decisions in the area (I) should be made first, followed by (II), (III) and (IV). The high sensitive decisions have the greatest influence on the achievable metrics. High connected decisions influence the scope of the design space.

If these decisions are made early on, the design space can be reduced significantly to enable a deeper analysis of the remaining possibilities. The high connected decisions influence the design space in a greater way since they have more constraints with other decisions and may reduce the number of decisions needed to be made. For example, if the take-off mode is chosen to be horizontally, the decision of the wing must be yes (compare constraint h) from Table 2-4). The choice of the one option has resulted in a decision about the option of another decision. If we would choose a vertical take-off, the decision about the wing remains undefined. The module could have a wing or not, we do not have defined any constrain for this option.

None of the decisions are in the region (I), four are in (II), two are in (III) and three are in (IV). Two of the three module-two decisions are in region (IV). The ones about the architecture of module one are across all three regions (II), (III) and (IV). The number of modules decision is part of the area (III). If we use the same ordering of decisions from top-right to top-left to bottom-right and bottom-left, we can list all decision according to their chronological recommended order (see Table 7-8).

Table 7-8: Ranking of the nine-architectural decisions

Rank	Region	Decision
1	(II)	1-LAmode
2	(II)	2-LAmode
3	(II)	1-TOmode
4	(II)	1-wing
5	(III)	1-RocketEngine
6	(III)	nModule
7	(IV)	1-JetEngine
8	(IV)	2-Wing
9	(IV)	2-RocketEngine

The first three decisions are about the conops of the vehicle, the landing of the first and second module as well as the take-off mode of the vehicle. The choice about the wing and rocket engine attributes of vehicle one follows. These decisions of the second module are the last two in the chronologic order. In between there are the decisions about the number of modules as well as the jet engine attribute of the first module.

8 Conclusion

We have defined the plausible design space in chapter 2 by creating a decision matrix and applying constraints. The 33-feasible architectures can be represented in a one-side graphical representation. Our design space includes 26 new and never proposed concepts, making it likely to find better solutions.

We have described the exploration methodology in chapter 3 with the used design and requirement variables. The approach breaks down the optimization into two steps, the design optimization and the operational business aspects. We have shown which aspects must be considered when evaluating a two-module instead of a single-module vehicle.

The design framework to optimize the architectures is described in chapter 4. We provided a short description of the four submodules, weight and sizing, propulsion, aerodynamics and trajectory. The jet and rocket trajectory had to be adopted from Frank's [20, 22] design framework. An approach to calculate the fuel needed to reach the separation velocity after the climbing phase was developed. We redesigned the rocket trajectory optimization resulting in a reduction of the design framework execution time of almost 100 times. This reduction made it possible to optimize our larger design space with reasonable computational effort. A model to calculate the propellant needed for vertical powered landing was implemented. The validation of the design framework with Blue Origin's New Shepard, Virgin Galactic's SpaceShipTwo and the Rocketplane XP showed relative deviations of the take-off mass of less than 7%.

The explanation of the GA's two objective functions, the ORSRM and the OCPP metric are presented in chapter 5 and 6, respectively. The risk metric is based on a list of seven hazards. A severity factor was assigned to each of these hazards. Then, the mitigation potential with respect to each hazard was defined. This was done for each option for each decision as well as for the two design variables, number of pilots and propellant type. With these information, the Overall Residual Safety-Risk Metric could be calculated. It depends on the architecture and on the designs within an architecture. The cost metric is broken down into the development, production and operational aspects. The first two contributions are assessed for the jet engine, rocket engine and airframe. The operational costs are divided into those related to the module and those applicable for the vehicle. We have taken the CER for the jet and rocket engine development and production costs from Frank and have adopted the CER from Koelle to fit our model. Frank has validated the CERs in his

PhD thesis [20]. We have validated the four adopted CERs for the airframe types with using Dragon 2 for the capsule, the SLS for the rocket airframe, the Skylon for a rocketplane and the A320 for an airplane. The used CERs show reasonable accuracy.

We have shown and discussed the results in the previous chapter 7. First, the results for a four-participant vehicle after the design optimization are depicted. The six non-dominated pareto architecture were described. We have shown how the other three cases relate in the ORSRM vs. mass chart. The trend of the average launch mass per person for the four different cases is discussed. Second, we displayed the results of the same four-participant's architectures after the financial business optimization with a fixed annual participant demand of 1,000. Five of the six previous pareto architecture remain on the pareto front. Four additional architecture can be found on the pareto front. We compared the results of the other three cases in the ORSRM vs. OCPP chart and found that architectures with four participants offer a "good" combination of prospect of viability and fundable development costs. 12 out of the 33 architecture are part of the pareto front at least in one of the cases. Third, the financial optimization was run for different demand numbers from 100 to 10,000. We have compared the resulting supply elasticity with the demand elasticity generated from the Futron [61, 62] and Tauri group [40] studies. We found that with a market share of 100% architectures with low demand and high OCPP may provide a profitable business. Finally, we conducted a sensitivity analysis of the architectural decisions and calculated their connectivity based on the constraint matrix. The sensitivities were calculated for each metric and each decision. The decision about the architecture of the first module have higher influence on the ORSRM and the ones for the second module effect the OCPP more. We could categorize the decisions into four regions from sensitive and strongly connected to insensitive and weakly connected. With the approach that the sensitive and highly connected decisions should be made first, we ordered the nine decision chronologically.

This chapter 8 aims to present the conclusion of the thesis with their main findings in section 8.1, the contribution of our work in section 8.2 and an outlook on future work in section 8.3.

8.1 Main Findings

The research question of this thesis was defined in the general thesis objective section 1.2:

What system architecture of MSV will provide the best combination of safety and economic return?

As discussed in the result chapter, there is no single set of architectures which are the non-dominated solutions. It rather depends on the number of participants. We have shown that architectures with four participants may offer the best combination of prospect of viability and fundable development costs. Since the set of pareto architectures depend on the size of the vehicle, the decision about the number of participants on the vehicle has the highest priority and should be made before an architecture is chosen.

We could reduce the design space to 12 architectures which are at least on the pareto front for one vehicle size. Furthermore, we can make these six statements about the architectures independent of the size of the vehicle:

1. Winged modules are safer but heavier and more expensive
2. A powered vertical rocket landing of the first module results in a slightly cheaper but riskier vehicle
3. There is no pareto architecture with a rocket powered vertical landing of the second module
4. Adding a second module leads to a more expensive but safer architecture
5. Jet engines increase the cost of the architecture but add safety to the system
6. Vehicles with three propulsive systems shift towards the pareto front with increasing size of the vehicle

The financial business optimization with different numbers of annual participants have shown that vehicle may be economically feasible for low demand and high cost cases. This conclusion assumes that

- the studies of Futron from 2002 and 2006 [61, 62] and Tauri group from 2012 [40] are applicable in 2017 and the demand and price elasticity have not changed since then,
- either the jet and rocket engines can be purchased from the market and the cost of adapting them to the airframe is negligible or the engine development costs are amortized by another project inside the company,

- and the ticket price equals the OCPP (no consideration of sales, general and administrative costs which is usually around 15% of the revenues [23]).

In addition, we found that higher development costs in the beginning of the program for more complex vehicles do not reduce the production and operational costs latter on. The higher costs of the more complex system result in a safer vehicle. For larger vehicles, this price penalty is less pronounced and there is less additional cost to make the system safer.

The sensitivity analysis has shown that not all decisions have the same influence on the risk and cost metric. First-module decisions have greater sensitivity on the risk of the vehicle whereas the ones for the second-module effect the cost more. Furthermore, decisions about the conops of the vehicle appear to be in the sensitive and weakly connected region and should be made first.

In sum, we propose to follow these three steps to guide the decision-making process:

1. Decisions-maker should first agree on the size of the vehicle. The financial optimization with fixed demand informs this decision. We showed that four-participant architecture offer a “good” combination of prospect of viability and fundable development costs. There may be other aspects that plead for another size. They may come from marketing strategy, product commonality, reuse of existing systems or reuse of systems in the future, availability of jet and rocket engines with the appropriate thrust, or technology demonstration and development.
2. After the vehicle’s size is determined, the set of pareto architectures can be extracted as we have shown for the case with four-participants. If the company or team has experience with specific features or airframe types, architecture that are on the fuzzy pareto front should be included as well. The experience reduces the development and production cost and may shift the architecture towards the pareto front.
3. The defined set of pareto architectures can be clearly communicated to decisions-maker with the developed pictograms. They can be ordered from cheaper but riskier to more expensive but safer. The six general statements above and the conclusions from the sensitivity analysis inform this decision. They help to identify which decisions should be made first from the risk and cost perspective. The decisions may have additional constraints from e.g. the company’s team experience, product portfolio, existing infrastructure, geography, geopolitical situation, expanding plans, business model or regulations.

8.2 Thesis Contribution

The objective of this thesis was to identify the architectures for MSV with the best combination of safety and economic return. We have done this by defining a plausible design space, building a parametric model to optimize each architecture and visualize the result and make sense of them to support the decision-making process. The main contributions are:

- **Contribution 1:**
  A one-side matrix shows all 33 MSV architectures graphically. The information of the morphological matrix was encoded in clear pictograms. 26 new and never proposed architectures were discovered.

- **Contribution 2:**
  Frank's [20, 22] design space exploration methodology and framework was extended to be able to optimize two-module vehicles. The new approach for the rocket trajectory reduced the design framework execution time by almost a factor of 100. This allowed us to optimize the broader design space with reasonable computational effort.

- **Contribution 3:**
  A hazard based quantitative risk assessment was used to evaluate the safety-risk level of the designs. The cost metric allows to compare architectures with different number of participants. Both metrics can be extended to orbital launch vehicles with manageable changes.

- **Contribution 4:**
  A three step process was proposed to guide the decision-making process towards an MSV architecture. The results of the design space exploration inform these decisions in the technical, risk and cost domains.

8.3 Future work

Like every time constraint work, also this thesis had a limited scope and there are related unexplored questions that are worth investigation. They may be part of follow-on work or separate research. Possible future investigations in this area may cover:

- Defining the architectural decision matrix for orbital vehicles and development of a similar compact representation of the feasible architectures

- Investigation of how the design space exploration methodology and design framework can be adopted to orbital vehicles

- Research on how the different architectures can be scaled to orbital launch vehicles with development of a quantitative model

- Implementation of the heritage metric developed by Hein [132]

- Expanding the design framework to include airbreathing engines like ram and scramjet as well as balloon ascents

A Annex

A.1 Reference list

[1] W. J. Abernathy and J. M. Utterback, "Patterns of industrial innovation," *Technology review,* vol. 80, pp. 40-47, 1978.

[2] J. D. Anderson, *The airplane, a history of its technology*. Reston, VA: American Institute of Aeronautics and Astronautics, 2002.

[3] SpaceX, "SpaceX to send privately crewed Dragon spacecraft beyond the moon next year," ed, 2017.

[4] SpaceX. (Mar 15). *Capabilities & Services*. Available: http://www.spacex.com/about/capabilities

[5] R. Becker, "How much are SpaceX tourists actually paying to fly around the Moon?," in *The Verge*, ed, 2017.

[6] Reuters, "Singer Sarah Brightman calls off tourist flight to International Space Station," in *The Guardian*, ed, 2015.

[7] M. Belfiore, *Rocketeers: how a visionary band of business leaders, engineers, and pilots is boldly privatizing space*: Harper Collins, 2007.

[8] "More than 700 Virgin Galactic ticket holders are left wondering what's next," in *Mashable*, ed, 2014

[9] D. E. Wagner, "Karman line, now boarding: public access to sapce," ed. New Space Age Conference, 2017.

[10] J. Foust, "Virgin Galactic relaunches its smallsat launch business," in *NewSpace Journal*, ed, 2012.

[11] R. A. Goehlich, *Space tourism : economic and technical evaluation of suborbital space flight for tourism*. Osnabrück: Der Andere Verlag, 2002.

[12] (Oct 30 2016). *Ansari Xprize*. Available: http://ansari.xprize.org/teams

[13] (Oct 30 2016). *The Student Aerospace Challenge*. Available: http://www.studentaerospacechallenge.eu/

[14] M. W. Maier, *The art of systems architecting*: CRC press, 2009.

[15] E. Crawley, B. Cameron, and D. Selva, *System architecture : strategy and product development for complex systems*. Hoboken, NJ: Pearson Higher Education, Inc., 2016.

[16] D. Dori. (2002). *Object-Process Methodology A Holistic Systems Paradigm*. Available: SpringerLink http://dx.doi.org/10.1007/978-3-642-56209-9 MIT Access Only

[17] D. Dori. (2016). *Model-based systems engineering with OPM and SysML*. Available: http://dx.doi.org/10.1007/978-1-4939-3295-5 MIT Access Only

[18] M. S. Net, "Architecting Space Communication Networks," Master of Science, Department of Aeronautics and Astronautics, Massachusetts Institute of Technology, 2014.

[19] W. Simmons, B. Koo, and E. Crawley, "Architecture Generation for Moon-Mars Exploration Using an Executable Meta-Language," 2005.

[20] C. P. Frank, "Design Space Exploration Methodology to Support Decisions Under Evolving Uncertainty in Requirements and Its Application to Advanced Vehicles," PhD, School of Aerospace Engineering, Georgia Institute of Technology, 2016.

[21] R. A. M. Christopher P. Frank, Olivia J. Pinon-Fischer, and Dimitri N. Mavris, "An Evolutionary Multi-Architecture Multi-Objective Optimization Algorithm for Design Space Exploration," presented at the San Diego, California, USA, 57th AIAA/ASCE/AHS/ASC Structures, Structural Dynamics, and Materials Conference, 2016.

[22] M. F. A. Christopher P. Frank, Olivia J. Pinon-Fischer, Dimitri N. Mavris, "A Conceptual Design Framework for Performance, Life-Cycle Cost, and Safety Evaluation of Suborbital Vehicles," presented at the 54th AIAA Aerospace Sciences Meeting, San Diego, California, USA, 2016.

[23] C. P. F. Frederic Burgaud, Dimitri N. Mavris, "A Business-Driven Optimization Methodology Applied to Suborbital Vehicle Programs," presented at the AIAA SPACE 2016, Long Beach, California, 2016.

[24] N. S.-K. Marti Sarigul-Klijn, "Flight Mechanics of Manned Sub-Orbital Reusable Launch Vehicles with Recommendations for Launch and Recovery," presented at the 41st Aerospace Sciences Meeting and Exhibit, Reno, Nevada, 2003.

[25] M. Buckley, K. Fertig, and D. Smith, "Design sheet-An environment for facilitating flexible trade studies during conceptual design," in *Aerospace design conference*, 1992, p. 1191.

[26] X. Huang and B. Chudoba, "A Trajectory Synthesis Simulation Program for the Conceptual Design of a Suborbital Tourism Vehicle," 2005.

[27] J. D. Mattingly, *Aircraft engine design*: Aiaa, 2002.

[28] T. Nam, "Introduction to FLOPS Modeling," U. Lecture, Ed., ed, 2012.

[29] A. S. T. rep., "ASTOS, Aerospace Trajectory Analysis Tool for Launch, Reentry and Orbit Vehicles," G. Tech, Ed., ed, 2008.

[30] F. Villeneuve and D. Mavris, "A new method of architecture selection for launch vehicles," in *AIAA/CIRA 13th International Space Planes and Hypersonics Systems and Technologies Conference*, 2005, p. 3361.

[31] D. O. Stanley, T. A. Talay, R. A. Lepsch, W. Morris, and K. E. Wurster, "Conceptual design of a fully reusable manned launch system," *Journal of Spacecraft and Rockets,* vol. 29, pp. 529-537, 1992.

[32] J. R. Olds, "Multidisciplinary Design Techniques Applied to Conceptual Aerospace Vehicle Design," PhD, School of Aerospace Engineering, North Carolina State University, 1993.

[33] D. Kinney, J. Bowles, L. Yang, and C. Roberts, "Conceptual Design of a'SHARP'-CTV," in *35th AIAA thermophysics conference*, 2001, p. 2887.

[34] R. D. Braun, A. A. Moore, and I. M. Kroo, "Collaborative approach to launch vehicle design," *Journal of spacecraft and rockets,* vol. 34, pp. 478-486, 1997.

[35] C. Frank, J.-G. Durand, H. Evain, C. Tyl, F. Mechentel, A. Brunet*, et al.*, "Preliminary Design of a New Hybrid and Technology Innovative Suborbital Vehicle for Space Tourism," 2014.

[36] U. Walter, *Astronautics the physics of space flight*, 2., enl. and improved ed. Weinheim: Wiley-VCH, 2012.

[37] A. A. f. C. S. T. AST, "Reusable Launch Vehicle Programs and Concepts," 1998.

[38] J. C. Martin, G. W. Law, and United States. Office of Space Commercialization. (2002). *Suborbital reusable launch vehicles and applicable markets*. Available: http://purl.access.gpo.gov/GPO/LPS34272

[39] T. T. Group, "The U.S. Commercial Suborbital Industry: A Space Renaissance in the Making," Federal Aviation Administration2011.

[40] T. T. Group, "Suborbital Reusable Vehicles: A 10-Year Forecast for Market Demand," Federal Aviation Administration2012.

[41] E. Seedhouse. (2014). *Suborbital industry at the edge of space*. Available: SpringerLink http://dx.doi.org/10.1007/978-3-319-03485-0 MIT Access Only

[42] (Oct 20 2016). *ARCA*. Available: http://www.arcaspace.com/en/haas2b.htm

[43] (Oct 20 2016). *Blue Origin*. Available: https://www.blueorigin.com/technology

[44] (Oct 20 2016). *Virgin Galactic*. Available: https://en.wikipedia.org/wiki/SpaceShipTwo

[45] (Oct 20 2016). *XCOR*. Available: http://spaceexpeditions.xcor.com/spacecraft/

[46] (Oct 20 2016). *Copenhagen Suborbital*. Available: https://copenhagensuborbitals.com/roadmap/spica/

[47] (Oct 20 2016). *Dassault-Aviation*. Available: http://www.dassault-aviation.com/en/space/our-space-activities/aerospace-vehicles/suborbital-vehicles-vehra-vehicule-hypersonique-reutilisable-aeroporte-family/

[48] (Oct 20 2016). *EADS*. Available: http://www.space-airbusds.com/en/dossiers-ea0/the-spaceplane-rocketing-into-the-future.html

[49] (Oct 20 2016). *Cosmocourse*. Available: http://www.cosmocourse.com/sxema-polyota/

[50] (Oct 20 2016). *Scaled Composites*. Available: https://en.wikipedia.org/wiki/SpaceShipOne

[51] F. Zwicky and F. Zwicky, "Discovery, invention, research through the morphological approach," 1969.

[52] G. Pahl and W. Beitz, *Engineering design: a systematic approach*: Springer Science & Business Media, 2013.

[53] A. N. Guest, "Multi-level Decision-based System Architecting," Master, Department of Aeronautics and Astronautics, Massachusetts Institute of Technology, 2011.

[54] D. P. Raymer, *Aircraft design : a conceptual approach*, 4th ed. Reston, Va.: American Institute of Aeronautics and Astronautics, 2006.

[55] O. L. de Weck and M. B. Jones, "Isoperformance: Analysis and design of complex systems with desired outcomes," *Systems Engineering,* vol. 9, pp. 45-61, 2006.

[56] O. L. De Weck, "Multivariable isoperformance methodology for precision opto-mechanical systems," Ph D, Massachusetts Institute of Technology, 2001.

[57] B. L. Henwood, "National AeroSpace Training & Research Center," NASTAR, Southampton, PA2010.

[58] NASTAR, "NASTAR Center Completes First ATSA Suborbital Scientist Observatory Training," ed, 2011.

[59] R. G. Inc. (20 Feb). *Rocketplane XP*. Available: http://rocketplane.ca/spec_and_description.html

[60] E. Seedhouse. (2015). *Virgin Galactic : the first ten years*. Available: http://dx.doi.org/10.1007/978-3-319-09262-1 MIT Access Only

[61] Futron, "Space Tourism Market Study," 2002.

[62] Futron, "Suborbital Space Tourism Demand Revisited," 2006.

[63] "Jeff Bezos' Blue Origin Will Take Tourists to Space by 2018," in *Fortune*, ed, 2016.

[64] J. D. Anderson, *Aircraft performance and design*. Boston: McGraw-Hill, 1999.

[65] R. Rohrschneider, "Development of a mass estimating relationship database for launch vehicle conceptual design," *AE8900 Special Project, School of Aerospace Engineering, Georgia Institute of Technology,* 2002.

[66] H. Rick, *Gasturbinen und Flugantriebe Grundlagen, Betriebsverhalten und Simulation*. Berlin u.a.: Springer Vieweg, 2013.

[67] S. Boggia and K. Rüd, "Intercooled recuperated aero engine," technical report, Advanced Project Design, MTU Aero Engines, Munich, Germany2004.

[68] H.-L. Besser, R. E. Henderson, and P. Kuentzmann, "Propulsion and Energy Issues for the 21st Century."

[69] Y.-S. Chen, T. Chou, and J. Wu, "Hybrid rocket propulsion technology for sounding rocket development," *Rep. No. AASRC,* vol. 9, 2008.

[70] T. Ishiguro, K. Sinohara, K. Sakio, and I. Nakagawa, "A Study on Combustion Efficiency of a Paraffin-based Hybrid Rockets," in *47th AIAA/ASME/SAE/ASEE Joint Propulsion Conference & Exhibit*, 2011, p. 5679.

[71] C. E. Rogers, "The solid rocket motor–part 4, Departures from ideal performance for conical nozzles and bell nozzles, straight-cut throats and rounded throats," *Tech Series, High Power Rocketry magazine, Orem,* 2004.

[72] J. Roskam, "Preliminary Calculation Of Aerodynamic, Thrust And Power Characteristics," *Airplane Design Part Vi–2000,* 1987.

[73] R. S. Shevell, *Fundamentals of flight*, 2nd ed. Upper Saddle River, N.J.: Prentice Hall, 1989.

[74] J.-L. Boiffier, "Dynamique de vol de l'avion," *SupAéro, Départements des Aéronefs, Toulouse-Novembre,* 2001.

[75] B. Origin, "Replay of In-flight Escape Test Live Webcast," ed, 2016.

[76] saabstory88. (2015, March). *Estimated masses and dimensions of the New Shepard PM. Estimates based on Thrust and Volume*. Available: https://redd.it/3u8m2h

[77] mlindner. (2015, March). *Blue Origin - New Shepard second developmental test flight and landing*. Available: https://forum.nasaspaceflight.com/index.php?topic=38873.280

[78] G. Norris. (2009, September 7) Galactic. *Aviation Week & Space Technology*.

[79] P. Vis. (Feb 20). *SpaceShipTwo Specifications*. Available: http://www.petervis.com/interests/published/Spaceshiptwo/Spaceshiptwo_Specifications.html

[80] I. Adventures. (March). *Suborbital Space Flights: The Space Plane*. Available: http://www.incredible-adventures.com/rocketplane-xp.html

[81] M. Wade. *Rocketplane XP*. Available: http://www.astronautix.com/r/rocketplanexp.html

[82] N. Leveson, *SafeWare : system safety and computers*. Reading, Mass.: Addison-Wesley, 1995.

[83] N. Leveson, *Engineering a safer world : systems thinking applied to safety*. Cambridge, Mass.: MIT Press, 2011.

[84] N. Dulac and N. Leveson, "Incorporating Safety Risk in Early System Architecture Trade Studies," *Journal of Spacecraft and Rockets,* vol. 46, pp. 430-437, Mar-Apr 2009.

[85] H. E. McCurdy, "Inside NASA: High technology and organizational change in the US space program," *New Series in NASA History, Baltimore: Johns Hopkins University Press,| c1993,* 1993.

[86] R. Godwin, *Columbia accident investigation report* vol. 39: Burlington, Ont.: Apogee Books, 2003.

[87] NASA, "Methodology for Conduct of Space Shuttle Program Hazard Analyses," 1993.

[88] NASA, "Constellation Program Hazard Analyses Methodology," 2009.

[89] D. E. Koelle, *Handbook of cost engineering for space transportation systems*, Revision 3 ed. Ottobrun, Germany: TransCostSystems, 2010.

[90] W. J. Larson, J. R. Wertz, and B. D'Souza, *SMAD III : Space mission analysis and design, 3rd edition : workbook*. El Segundo, CA.: Microcosm Press, 2005.

[91] O. Younossi, Rand Corporation., and Project Air Force (U.S.), *Military jet engine acquisition : technology basics and cost-estimating methodology*. Santa Monica, CA: Rand, 2002.

[92] Institute of Cost Analysis. National Conference (1989 : Washington D.C.), T. R. Gulledge, and L. A. Litteral, *Cost analysis applications of economics and operations research : proceedings of the Institute of Cost Analysis National Conference, Washington, D.C., July 5-7, 1989*. New York: Springer-Verlag, 1989.

[93] C. A. Graver and D. C. Morrison, "Cac (q) cers for solid rocket motors," DTIC Document1993.

[94] J. S. Nieroski and E. I. Friedland, "Liquid rocket engine cost estimating relationships," in *AIAA Second Annual Meeting*, 1965.

[95] B. T. C. Zandbergen. (March 5). *Mass data for solid propellant rocket motors*. Available: http://www.lr.tudelft.nl/en/organisation/departments/space-engineering/space-systems-engineering/expertise-areas/space-propulsion/system-design/analyze-candidates/dry-mass-estimation/chemical-systems/srm-mass-data/

[96] L. D. Brown, M. J. Martin, B. J. Aleck, and R. Landes, "Composite-Reinforced Propellant Tanks," DTIC Document1975.

[97] C. J. Meisl, "Life-cycle-cost considerations for launch vehicle liquid propellant rocket engine," *Journal of Propulsion and Power,* vol. 4, pp. 118-126, 1988.

[98] H. Adirim, J. Lassmann, and T. U. B. I. f. L.-u. Raumfahrt, "Investigation into a Payload Propulsion Module System as an Alternative to Upper Stages for Future Reusable Sub-Orbital Launch Vehicles," ed: ILR-Mitteilung, 1998.

[99] M. Cegłowski. *A Rocket To Nowhere*. Available: http://www.idlewords.com/2005/08/a_rocket_to_nowhere.htm

[100] J. Laßmann, *<<Ein>> Modell zur Simulation der Personentransportkosten im cislunaren Bereich*, Als Ms. gedr. ed. vol. 74. Düsseldorf: VDI-Verl., 1994.

[101] NASA, "Selection Statement For Commerical Crew Development," 2009.

[102] G. Hautaluoma, "NASA Selects Commercial Firms to Begin Development of Crew Transportation Concepts and Technology Demonstrations for Human Spaceflight Using Recovery Act Funds," ed, 2010.

[103] M. Braukus, "NASA Awards Next Set Of Commercial Crew Development Agreements," ed, 2011.

[104] NASA, "NASA Announces Additional Commercial Crew Development Milestones," 2013.

[105] C. Thomas, "NASA Awards Contracts In Next Step Toward Safely Launching American Astronauts From U.S. Soil," ed, 2012.

[106] S. Schierholz, "NASA Chooses American Companies to Transport U.S. Astronauts to International Space Station," ed, 2014.

[107] E. Seedhouse. (2016). *SpaceX's dragon : America's next generation spacecraft*. Available: http://dx.doi.org/10.1007/978-3-319-21515-0 MIT Access Only

[108] S. Anthony, "SpaceX unveils Dragon V2, the world's first commercial manned reusable spaceship," in *ExtremeTech*, ed, 2014.

[109] P. B. Rehmus and R. Hall, "Alternatives for Future US Space-launch Capabilities," 2006.

[110] W. Harwood, "NASA commits to $7 billion mega rocket, 2018 debut," in *CBS News*, ed, 2014.

[111] A. Pasztor, "White House Experiences Sticker Shock Over NASA's Plans," in *The Wall Street Journal*, ed, 2011.

[112] NASA, "ESD Integration, Budget Availability Scenarios," 2011.

[113] M. Wall, "NASA's huge new rocket may cost $500 million per launch," in *NBC News*, ed, 2012.

[114] Braeunig. (March 12). *Space Launch System Specifications*.

[115] E. Kyle, "NASA's Space Launch System," 2016.

[116] M. Hempsell, "Skylon Users' Manual," 2010.

[117] ESA, "Skylon Assessment Report," 2011.

[118] A. Bond, "Travelling at the edge of space: Reaction Engines and Skylon in the next 20 years," ed, 2010.

[119] H. Webber, A. Bond, and M. Hempsell, "The sensitivity of precooled air-breathing engine performance to heat exchanger design parameters," *Journal of the British Interplanetary Society,* vol. 60, p. 188, 2007.

[120] R. Engines. *SABRE: How it works*. Available: http://rel.space/sabre_howworks.html

[121] "Gearing up for a fight," in *The Economist*, ed, 2014.

[122] Airbus. (2017). *Order & Deliveries*. Available: http://www.airbus.com/company/market/orders-deliveries/

[123] Airbus. (2016). *New Airbus aircraft list prices for 2016*. Available: http://www.airbus.com/presscentre/pressreleases/press-release-detail/detail/new-airbus-aircraft-list-prices-for-2016/

[124] "Airbus to launch a new A320 version," in *The Economist*, ed, 2010.

[125] S. Hamilton, "Boeing disputes 737 Max development cost report," in *FlightGlobal*, ed, 2012.

[126] Airbus, "All about the A320 Family - Technical appendices," 2009.

[127] D. Michaels, "The Secret Price of a Jet Airliner," in *The Wall Street Journal*, ed, 2012.

[128] YCharts. (2017). *Airbus Historical Gross Profit Margin Data*. Available: https://ycharts.com/companies/EADSY/gross_profit_margin

[129] CFM. (2015). *CIT selects CFM56-5B for new A321 aircraft*. Available: https://www.cfmaeroengines.com/press-articles/cit-selects-cfm56-5b-for-new-a321-aircraft/791/

[130] J. A. Battat, "Technology and Architecture: Informing Investment Decisions for the Future of Human Space Exploration," M.Sc., Aeronautics and Astronautics, Massachusetts Institute of Technology, 2012.

[131] W. L. Simmons, "A Framework for Decision Support in Systems Architecting," PhD, Department of Aeronautics and Astronautics, Massachusetts Institute of Technology, 2008.

[132] A. M. Hein, "Heritage Technologies in Space Programs - Assessment Methodology and Statistical Analysis," PhD, Chair of Astronautics, Technical University Munich, 2016.

[133] W. W. A. Tai, "Virgin Galactic presentation Oshkosh Theater in the Woods 2007," 2007.

A.2 Definition of form, object, structure, function, operand, process, context and concept

Form

"Form is the physical or informational embodiment of a system that exists or has the potential for stable, unconditional existence, for some period of time, and is instrumental in the execution of function. Form exists prior to the execution of function." [15]

Object

"An object is that which has the potential for stable, unconditional existence for some period of time." [15]

Structure

"Formal relationships, or structure, are the relationships between objects of form that have the potential for stable, unconditional existence for some duration of time and may be instrumental in the execution of functional interactions." [15]

Function

"Function is the activity, operation, or transformation that causes or contributes to performance. In designed systems, function is the actions for which as system exist, which ultimately lead to the delivery of value. Function is executed by form, which is instrumental in function. Function emerges from functional interaction between entities." [15]

Operand

“An operand is an object and therefore has the potential for stable, unconditional existence for some period of time. Operands are objects that need not exist prior to the execution of function and are in some way acted upon by the function. Operands may be created, modified, or consumed by the process part of function.” [15]

Process

“Process is a pattern of transformation undergone by an object. Processes generally involve creation of, destruction of, or a change in an operand.” [15]

Context

“Context is what surrounds the system. It is the entities that are “just on the outside of the system” but are relevant to it.” [15]

Concept

“Concept is a product or system vision, idea, notion, or mental image that maps function to form. It is a scheme for the system and how it works. It embodies a sense of how the system will function and an abstraction of the system form. It is a simplification of the system architecture that allows for high-level reasoning.

Concept is not a product/system attribute but a notional mapping between two attributes: form and function.” [15]

A.3 OPM: Building blocks, links, states

The Building Blocks

	Visual Representation	Textual Form	Definition	Description
Entities	Object	Nouns; capitalized first letter in every word; if ending with "ing", "Object" is placed as a suffix	*An **object** is a thing that has the potential of stable, unconditional physical or mental existence.*	Static things. Can be changed only by processes.
	Process(ing)	Nouns in gerund form; capitalized first letter in every word; if not ending with "ing", "Process" is placed as a suffix	*A **process** is a pattern of transformation that an object undergoes.*	Dynamic things. Are recognizable by the changes they cause to objects.
	Object (state)	Nouns, adjectives or adverbs; non-capitalized	*A **state** is a situation an object can be at.*	States describe objects. They are attributes of objects. Processes can change an object's state.
OPL Conventions	**Non-Reserved Words**	Arial bold by default	*Names of entities.*	Words used by the system architect, unique to the system.
	reserved words	Arial by default; non-capitalized	*Object-Process Language (OPL) words.*	Words or phrases used by OPL, the same in every sentence of a certain type.

Links: The Mortar

Tagged Structural Links

Generally used between objects, but may also be used between processes.
Cannot be used to link an object to a process.

Link Name	Object Process Diagram (OPD) Symbol	OPL Sentence	Description
Tagged	R Object — refers to → S Object	**R Object refers to S Object.**	Relation from source object to destination object; relation name is entered by architect, and is recorded along link.
(Null)	R Object → S Object	**R Object** relates to **S Object.**	Relation from source object to destination object with no tag.
Bi-directional Tagged	R Object — precedes / follows — S Object	**R Object precedes S Object. S Object follows R Object.**	Relation between two objects; relation names are entered by architect, and are recorded along link.
(Null) Bi-directional	R Object ↔ S Object	**R Object** and **S Object** are related.	Relation between two objects with no tag.

Links: The Mortar (continued)

The Four Fundamental Structural Relations

Shorthand Name	Aggregation	Exhibition	Generalization	Instantiation
Symbol				
Meaning	Relates a whole to its parts	Relates an exhibitor to its attributes	Relates a general thing to its specializations	Relates a class of things to its instances

A fundamental structural relation can have many descendants.
The different OPL sentences and OPD pictures are listed below.

Structural Relation Name and **Shorthand Name**	Number of Descendants						Description
	One		Two		Three or more		
	OPD	OPL	OPD	OPL	OPD	OPL	
Aggregation- Participation	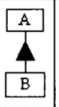	**A** consists of **B.**	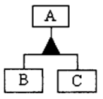	**A** consists of **B** and **C.**	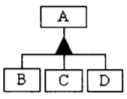	**A** consists of **B, C,** and **D.**	B, C and D are parts of the whole A.
Exhibition- Characterization	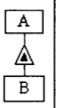	**A** exhibits **B.**	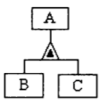	**A** exhibits **B** and **C.**	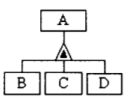	**A** exhibits **B, C,** and **D.**	B, C and D are attributes of A. If B is a process, it is an operation of A.
Generalization- Specialization	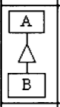	**B** is an **A.**	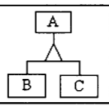	**B** and **C** are **A**s.	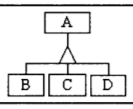	**B, C,** and **D** are **A**s.	B, C and D are types of A.
Classification- **Instantiation**	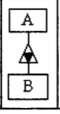	**B** is an instance of **A.**	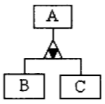	**B** and **C** are instances of **A.**	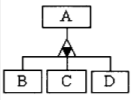	**B, C,** and **D** are instances of **A.**	B, C and D are unique objects of the class A.

The four fundamental relations are also applicable to processes. Only exhibition can link objects with processes. Instantiation cannot generate a hierarchy while the other three can. Any number of things can be linked to the root.

	Aggregation	Exhibition	Generalization	Instantiation
Object	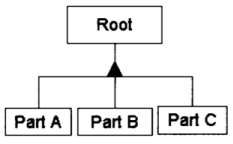	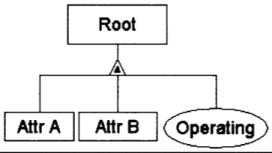	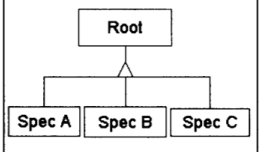	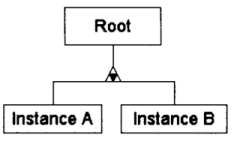
Process	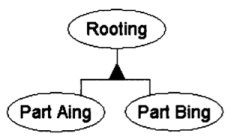	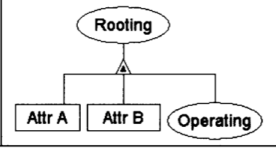	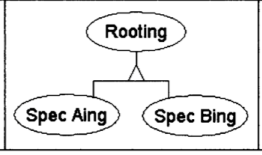	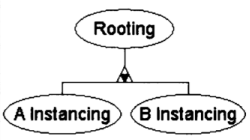

Links: The Mortar (continued)

Procedural Links

These links are generally used between an object and a process. They cannot be used to link objects together.

Link Name	OPD Symbol	OPL Sentence	Description
Consumption	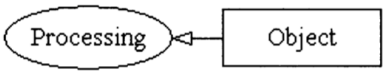	**Processing** consumes **Object.**	Process uses object up entirely during its occurrence.
Result	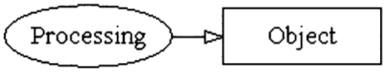	**Processing** yields **Object.**	Process creates an entirely new object during its occurrence.
Effect	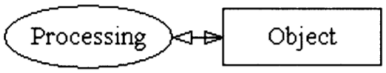	**Processing** affects **Object.**	Process changes the state of the object in an unspecified manner.
Input and Output	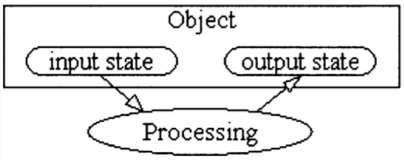	**Processing** changes **Object** from **input state** to **output state.**	The object is at input state prior to the process occurrence, and at output state as a result of its occurrence.
Agent	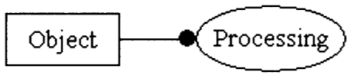	**Object** handles **Processing.**	Object is a human that is not changed by the process; process needs the agent object in order to occur.
Instrument	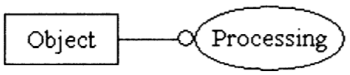	**Processing** requires **Object.**	Object is a non-human that is not changed by the process; process needs the instrument object in order to occur.
Invocation	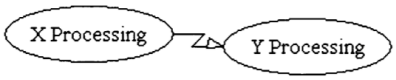	**X Processing** invokes **Y Processing.**	First process directly starts up a second process, without an inter-mediate object.

States

State sentences and images

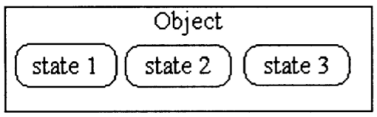

Object can be **state 1, state 2,** or **state 3.**

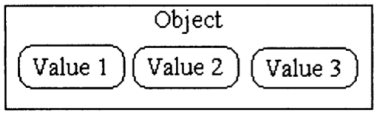

Values of **Object** are **Value 1, Value 2,** and **Value 3.**

States (continued)

State-related Links

Link Name	OPD Symbol	OPL Sentence	Description
Condition	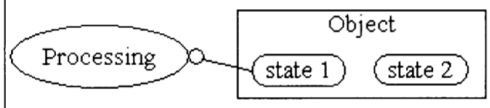	**Processing** occurs if **Object** is **state 1.**	Object is an instrument. It must be at a specific state in order for the process to occur.
Agent Condition	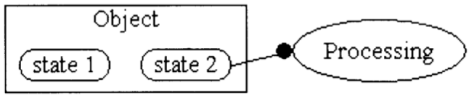	**Object** must be at **state 2** for **Processing** to occur.	Object is an agent. It must be at a specific state in order for the process to occur.
Qualification	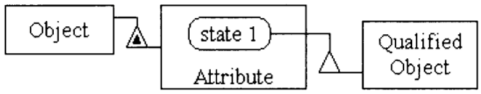	**Qualified Object** is an **Object,** the **Attribute** of which is **state 1.**	Qualified Object is a type of Object. It must be at a particular state of Object's Attribute.
Instance Qualification	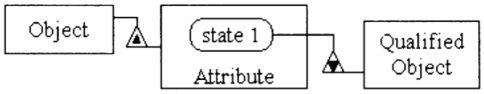	**Qualified Object** is an instance of an **Object,** the **Attribute** of which is **state 1.**	Qualified Object is an instance of class Object. It must be at a particular state of Object's Attribute.
State Specificied Consumption	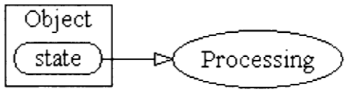	**Processing** consumes **state Object.**	Process consumes object only if it is at a certain state.
State Specificied Result	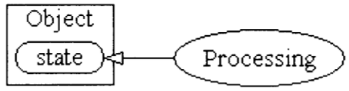	**Processing** yields **state Object.**	Process creates object at a certain state.

Boolean Objects

Specialized informatical objects. Boolean objects are questions, and they always have two states (the answers): yes and no.

Link type	OPD Symbols	OPL Sentence	Description
Determination (a Result Link)	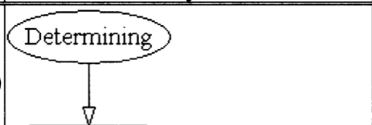	**Determining** determines whether **Object** is **proper.**	Process yields a Boolean object that poses a "yes or no" question. The process then determines the answer.
Condition link	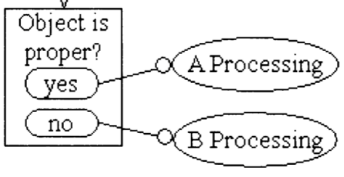	**A Processing** occurs if **Object** is **proper.**	If the answer is "yes," a certain process occurs. If the answer is "no", a different process occurs.
Negative condition link		**B Processing** occurs if **Object** is not **proper.**	
Both condition links	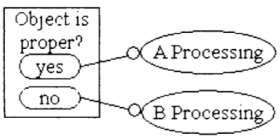	**A Processing** occurs if **Object** is **proper,** otherwise **B Processing** occurs.	Compound sentence: if the answer is "yes," a certain process occurs, otherwise a different process occurs.

A.4 Overview of the manned suborbital market

#	Name of the company	Type of vehicle	Ascent method	Ascent method specifics	Landing method	Landing method specifics	# of passengers	# of engines	Time in Weight-less, sec	Total duration, min	Takeoff weight, kg	1st module Pro-pulsion	1st module Oxidizer	1st module Fuel	2nd module Pro-pulsion	2nd module Oxidizer	2nd module Fuel
1	Acceleration Engineering	Single module rocket	Vertical	Ground	Vertical	Ground	3	Not disclosed	200	12	2540	Rocket	Liquid Oxygen	Liquid Methane			
2	Advent Launch Services	Single module rocket	Vertical	Water	Horizontal	Water	3	1	220	13	5700	Rocket	Liquid Oxygen	Liquid Methane			
3	Aeronautics and Cosmonautics Romanian Association	Two modules rocket and capsule	Vertical	Ground	Vertical (Parachute recovery)	Water	3	1	120	Not disclosed	7000	Rocket	Hydrogen Peroxide	Kerosene			
4	Armadillo Aerospace	Single module rocket	Vertical	Ground	Vertical (Parachute with crushable nose cone)		3	4	Not disclosed	15	6350	Rocket	Hydrogen Peroxide	-			
5	American Astronautics Corporation	2 module rocket and booster	Vertical	Ground	Vertical (Parachute recovery)	Water	7	1 (booster) 3 (capsule emergency system)	Not disclosed	Not disclosed	9900	Rocket	Liquid Oxygen	HT Kerosene			
6	Bristol Spaceplanes	Single module rocketplane	Horizontal	Ground	Horizontal	Ground	4	3 total 2 turbojets	120	30	4500	Rocket	Liquid Oxygen	Hydrogen			
7	Canadian Arrow	Two module rocket	Vertical	Ground	Vertical (Parachute recovery)	Water	3	1 (1st module) 4 (2nd module)	240	45	14000	Rocket	Liquid Oxygen	Alcohol	Rocket	Perchlorate	Asphalt, special oil, etc.
8	The Da Vinci Project	Two module balloon/ rocket	Vertical (Balloon)	Air	Vertical (Parachute recovery)	Ground	3	2	210	110	3300	Helium Balloon	-	-	Rocket	Liquid Oxygen	Kerosene
9	Pablo de Leon & Associates	Two modules rocket/capsule	Vertical	Ground	Vertical (Parachute recovery)	Water	3	4	240	17	8000	Rocket	Liquid Oxygen	HTPB			
10	Flight Exploration*	Two modules rocket/ capsule	Vertical	Ground	Vertical (Parachute recovery)	Ground					20000	Rocket	Hydrogen Peroxide	Kerosene			

11	Fundamental Technology Systems	Two modules rocket	Horizontal	Ground	Horizontal	Ground	3	1	240	30	4800	Rocket	Hydrogen Peroxide	Kerosene			
12	HARC*																
13	IL Aerospace Technologies	Two module balloon/rocket	Vertical	Ground or Ocean	Vertical	Parachute land or ocean	3	1 for rocket module	720	240	3370	Balloon	-	-	Rocket	Liquid Oxygen	HTPB
14	Interorbital Systems	Single module rocket	Vertical	Ground or Ocean	Horizontal	?	?	?	480	?	145	Rocket	WFNA	Turpentine			
15	Kelly Space and Technology	Two module plane/rocket	Horizontal	Ground	Horizontal	Ground	?	?	?	?	?	Airbreathing	Air	Kerosene	Rocket	Not Disclosed	Not Disclosed
16	Lone Star Space Access Corporation	Single module rocketplane	Horizontal	Ground	Horizontal	Ground	?	?	?	?	?	Airbreathing	Air	Kerosene	Rocket	Not Disclosed	Not Disclosed
17	Micro-Space Inc.	Single module rocket	Vertical	Ground	Vertical	Ground	3	6	240	15	2268	Rocket	Hydrogen Peroxide	Methyl Alcohol			
18	Panaero Inc.	Single module rocketplane	Horizontal	Ground	Horizontal	Ground	11 for unmodified aircraft configuration	7 for rocket module	180	40	11900	Airbreathing	Air	Kerosene	Rocket	Not Disclosed	Not Disclosed
19	Pioneer Rocketplane	Single module rocketplane	Horizontal	Ground	Horizontal	Ground	4	1	240	60	8165	Airbreathing	Air	Kerosene	Rocket	Liquid Oxygen	Kerosene
20	Starchaser Industries	Two module rocket with strap-on boosters	Vertical	Ground	Vertical	Ground	3	4 strap-on boosters, 1 for first module, 1 for second module	270	23	20000	Rocket	Liquid Oxygen	Not Disclosed	Rocket	Liquid Oxygen	Not Disclosed
21	Suborbital Corporation	Two module plane/rocket	Horizontal	Ground	Horizontal	Ground	?	?	?	60	?	Airbreathing	Air	Kerosene	Rocket	Ammonium Perchlorate	Polymer Binder
22	TGV Rockets	Single module rocket	Vertical	Ground	Vertical	Ground	1000 kg payload	6	200	10	27818	Rocket	Liquid Oxygen	Kerosene			

23	Vanguard Spacecraft	Three module rocket	Vertical	Ground	Vertical	Ground	270 kg payload	16 (12 liquid, 4 solid)	300	30	133000	Rocket	Nitrogen Tetroxide	Hydrazine	Rocket module 2 and 3	Nitrogen Tetroxide	Hydrazine
24	Discraft Corporation	Single module Saucer	Horizontal	Ground	Horizontal	Ground	?	?	?	?	?	Blast-Wave Pulse Jets	?	?			
25	ARCA	Two module rocket	Vertical	Ground	Vertical	Ground	5	1	?	?	14120	Rocket	Liquid Oxygen	Kerosene			
26	Blue Origin	Two module rocket	Vertical	Ground	Vertical	Ground	6	1	?	10	?	Rocket	Liquid Oxygen	Liquid Hydrogen			
27	Virgin Galactic	Two module plane/rocket	Horizontal	Ground	Horizontal	Ground	8	1	?	?	9740	Airbreathing	Air	Kerosene	Rocket	Nitrous oxide	Polyamide
28	XCOR	Single module rocketplane	Horizontal	Ground	Horizontal	Ground	2	4	?	?	?	Rocket	Liquid Oxygen	Kerosene			
29	Copenhagen Suborbital	Single module rocket	Vertical	Ground	Vertical	Ground	1	1	?	?	4000	Rocket	Liquid Oxygen	Ethanol			
30	Dassault-Aviation	Two module plane/rocket	Horizontal	Ground	Horizontal	Ground	6	1	?	?	?	Rocket	?	?			
31	EADS	Single module rocketplane	Horizontal	Ground	Horizontal	Ground	?	?	?	?	?	Airbreathing	Air	Kerosene	Rocket	?	?
32	Cosmocourse	Two module rocket	Vertical	Ground	Vertical	Ground	7	?	330	15	?	Rocket	?	?			
33	Scaled Composites	Two module plane/rocket	Horizontal	Ground	Horizontal	Ground	3	3 (2 for the 1st module, 1 for the 2nd module)	210	90	3600	Airbreathing	Air	Kerosene	Rocket	Nitrous oxide	HTPB
34	Vela Technology Development	Two module plane/rocket	Horizontal	Ground	Horizontal	Ground	8	1st module: 2 JT8D/F100; 2nd module: 3 rocket, 2 JT15D	?	?	18000 dry	Airbreathing	Air	Kerosene	Rocket/ Airbreathing	Oxide	Propane

35	David L. Burkhead - Spacecub	Single module rocket	Vertical	Ground	Vertical	Ground	4	4	?	?	?	Rocket	LOX	Kerosene			
36	Andrew Space and Technology	Single module rocketplane	Horizontal	Ground	Horizontal	Ground	Proprietary	?	?	?	123000	Rocket	LOX	RP-1			
37	Myasishchev Design Bureau	Two module plane/rocket	Horizontal	Ground	Horizontal	Ground	1st module: 2 PS-30V12; 2nd module: 1 rocket	2	?	?	?	Airbreathing	Air	Kerosene	Rocket	Solid	

A.5 Decision matrixes representing Virgin Galactic and Rocketplane XP

Table 8-1: Virgin Galactic

shortID			Option 1	Option 2	Option 3	Option 4	number of options
nModules			1	2			2
Module 1	Launching	TOmode1	Horizontal	Vertical			2
	Flying	wing1	No	Yes			2
		JetEngine1	No	Yes			2
		RocketEngine1	No	Yes			2
	Landing	LAmode1	Gliding	HPowered	Parachute	Rocket	4
Module 2	Flying	wing2	No	Yes			2
		RocketEngine2	No	Yes			2
	Landing	LAmode2	Gliding	Parachute	Rocket	None	4

Table 8-2: Rocketplane XP

shortID			Option 1	Option 2	Option 3	Option 4	number of options
nModules			1	2			2
Module 1	Launching	TOmode1	Horizontal	Vertical			2
	Flying	wing1	No	Yes			2
		JetEngine1	No	Yes			2
		RocketEngine1	No	Yes			2
	Landing	LAmode1	Gliding	HPowered	Parachute	Rocket	4
Module 2	Flying	wing2	No	Yes			2
		RocketEngine2	No	Yes			2
	Landing	LAmode2	Gliding	Parachute	Rocket	None	4

A.6 Morphological matrix including those architectures which are very likely to be dominated

	shortID	Decision	Option 1	Option 2	Option 3	Option 4	Option 5	Option 6	Option 7	Option 8	Option 9	number of alternatives
System												
	NrModul	Number of modules	1	2	3							**3**
Launching	LaunchO	Attribute of launching for the system - Orientation	Horizontal	Vertical								**2**
	LaunchP	Attribute of launching for the system - Place	Ground	Water								**2**
											Number of total combinations on system level	**12**	**O(2)**
					1 ... 3							
Modules												
Crew	NrPilot	Number of pilots	1	2							None	**3**
	NrPass	Number of passengers	1	1	3	3	5	6	7	8	None	**9**
Flying	Inc	Instrument of increasing energy of module	Jet engines	Rocket engines	Helium Balloon	Jet + Rocket engines					None	**5**
	Lift	Instrument of lifting	Wings								None	**2**
	Guid	Instrument of guiding	Aerodynamic surfaces	Rocket engines	Aerodynamic surfaces + Rocket engines						None	**4**
	Dec	Instrument of decreasing energy of module	Aerodynamic decelators	Rocket engines	Aerodynamic decelerators & Rocket engines	Wings					None	**5**
Landing	LandO	Attribute of landing - Orientation	Horizontal	Vertical								**2**
	LandP	Attribute of landing - Place	Ground	Water								**2**
											Number of total combinations on module level	**21,600**	**O(5)**
											Number of total combinations for 3 modules	**120,932,352,000,000**	**O(15)**

A.7 Design and requirement variables used for design framework validation

Virgin Galactic's SpaceShipTwo [8, 44, 60, 78, 79]

Most of the numbers for the WhiteKnightTwo are extracted from a drawing found in a 2007 Virgin Galactic presentation [133] (see Figure 8-1).

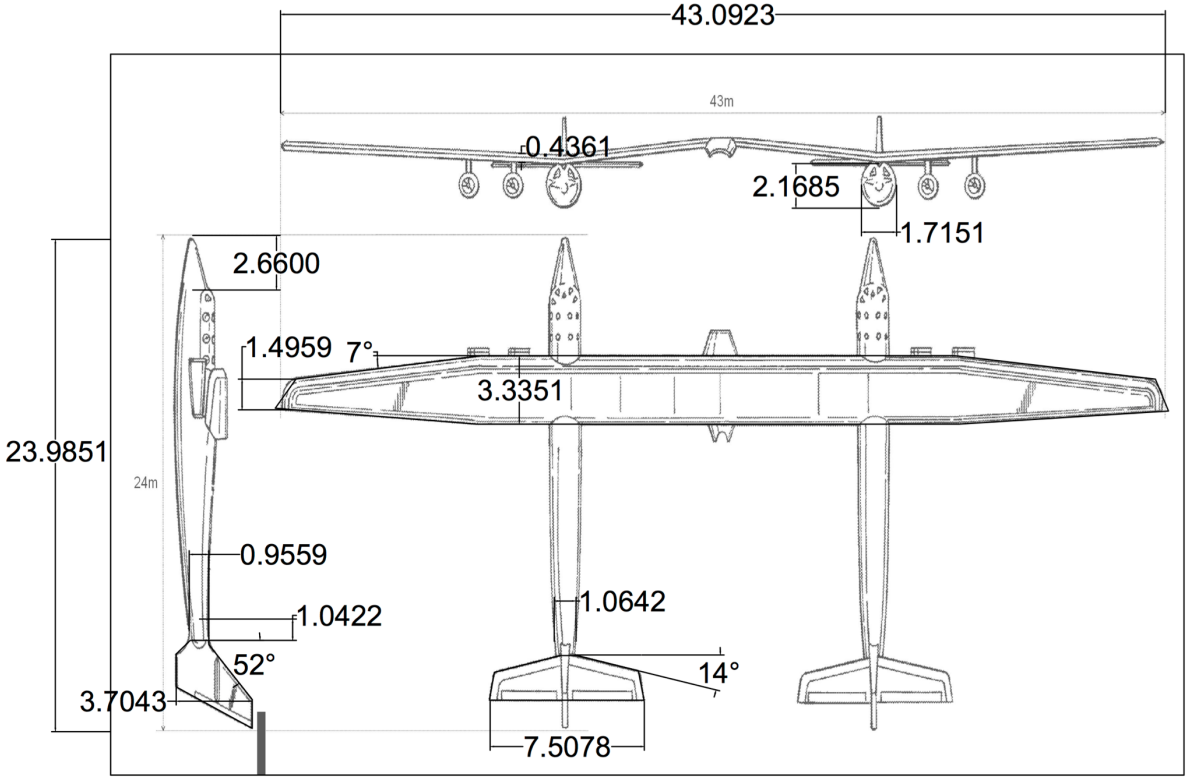

Figure 8-1: WhiteKnightTwo drawing with assigned dimensions and angles

Table 8-3: WhiteKnightTwo design variables

	Value	Unit		Value	Unit
nPAX	0	-	Propellant	0	-
nLaunch	12	launch/year/unit	epsilon	0	-
numbUnits	3	-	pc	0	MPa
nPilots	2	-	Tr	0	N
hTransition	0	m	dfus	2.75	m
vTransition	0	m/s	db	1.43	m
hSep	15,240	m	la	2.66	m

vSep	177	m/s	ln	1	m
nJet	4	-	Swing	124.2	m^2
Tj	30,690	N	tcWing	0.13	-
BPR	4.24	-	sweepWing	0.122	rad
afterburner	0	-	ARwing	14.89	-
TIT	1,200	K	TRwing	0.45	-
			sweepVTail	0.908	rad
			ARVTail	1.58	-
			sweepHTail	0.244	rad
			ARHTail	4.26	-

Table 8-4: SpaceShipTwo design variables

	Value	Unit		Value	Unit
nPAX	6	-	Propellant	7	-
nLaunch	12	launch/year/unit	epsilon	25	-
numbUnits	3	-	pc	3.3	MPa
nPilots	2	-	Tr	270,000	N
hTransition	0	m	dfus	2	m
vTransition	0	m/s	db	1	m
hSep	15,240	m	la	0.5	m
vSep	177	m/s	ln	0.5	m
nJet	0	-	Swing	35.82	m^2
Tj	0	N	tcWing	0.1	-
BPR	0	-	sweepWing	0.96	rad
afterburner	0	-	ARwing	1.88	-
TIT	0	K	TRwing	0.13	-
			sweepVTail	0.61	rad
			ARVTail	3	-
			sweepHTail	0.61	rad
			ARHTail	5	-

Table 8-5: Requirement variables SpaceShipTwo

	Value	Unit
hMax	100,000	m
nMax	4	g
seatPitch	1.5	m
programLength	10	years
runway	3500	m

Blue Origin's New Shepard [20, 41, 43, 75-77]

Table 8-6: New Shepard Module 1 design variables

	Value	Unit		Value	Unit
nPAX	0	-	Propellant	2	-
nLaunch	12	launch/year/unit	epsilon	50	-
numbUnits	3	-	pc	3	MPa
nPilots	0	-	Tr	489,304	N
hTransition	0	m	dfus	3.66	m
vTransition	0	m/s	db	1	m
hSep	45,000	m	la	2.22	m
vSep	0	m/s	ln	0.5	m
nJet	0	-	Swing	0	m^2
Tj	0	N	tcWing	0	-
BPR	0	-	sweepWing	0	rad
afterburner	0	-	ARwing	0	-
TIT	0	K	TRwing	0	-
			sweepVTail	0	rad
			ARVTail	0	-
			sweepHTail	0	rad
			ARHTail	0	-

Table 8-7: New Shepard Module 2 design variables

	Value	Unit		Value	Unit
nPAX	6	-	Propellant	0	-
nLaunch	12	launch/year/unit	epsilon	0	-
numbUnits	3	-	pc	0	MPa
nPilots	0	-	Tr	0	N
hTransition	0	m	dfus	3.66	m
vTransition	0	m/s	db	1	m
hSep	45,000	m	la	2.22	m
vSep	1,271	m/s	ln	0.5	m
nJet	0	-	Swing	0	m^2
Tj	0	N	tcWing	0	-
BPR	0	-	sweepWing	0	rad
afterburner	0	-	ARwing	0	-
TIT	0	K	TRwing	0	-
			sweepVTail	0	rad
			ARVTail	0	-
			sweepHTail	0	rad
			ARHTail	0	-

Table 8-8: Requirement variables New Shepard

	Value	Unit
hMax	132,000	m
nMax	5.4	g
seatPitch	0.74	m
programLength	10	years
runway	-	m

Rocketplane XP [20, 41, 59, 80, 81]

Table 8-9: Rocketplane XP design variables

	Value	Unit		Value	Unit
nPAX	5	-	Propellant	3	-
nLaunch	12	launch/year/unit	epsilon	20	-
numbUnits	3	-	pc	4	MPa
nPilots	1	-	Tr	160,000	N
hTransition	12,000	m	dfus	1.7	m
vTransition	200	m/s	db	1	m
hSep	0	m	la	0.5	m
vSep	0	m/s	ln	0.5	m
nJet	2	-	Swing	30	m^2
Tj	14,000	N	tcWing	0.1	-
BPR	0	-	sweepWing	0.78	rad
afterburner	1	-	ARwing	6	-
TIT	1,250	K	TRwing	0.13	-
			sweepVTail	0.35	rad
			ARVTail	3	-
			sweepHTail	0.35	rad
			ARHTail	3	-

Table 8-10: Requirement variables Rocketplane XP

	Value	Unit
hMax	104,000	m
nMax	4	g
seatPitch	0.91	m
programLength	10	years
runway	3500	m

A.8 Design optimization of each architecture

nPAX = 1

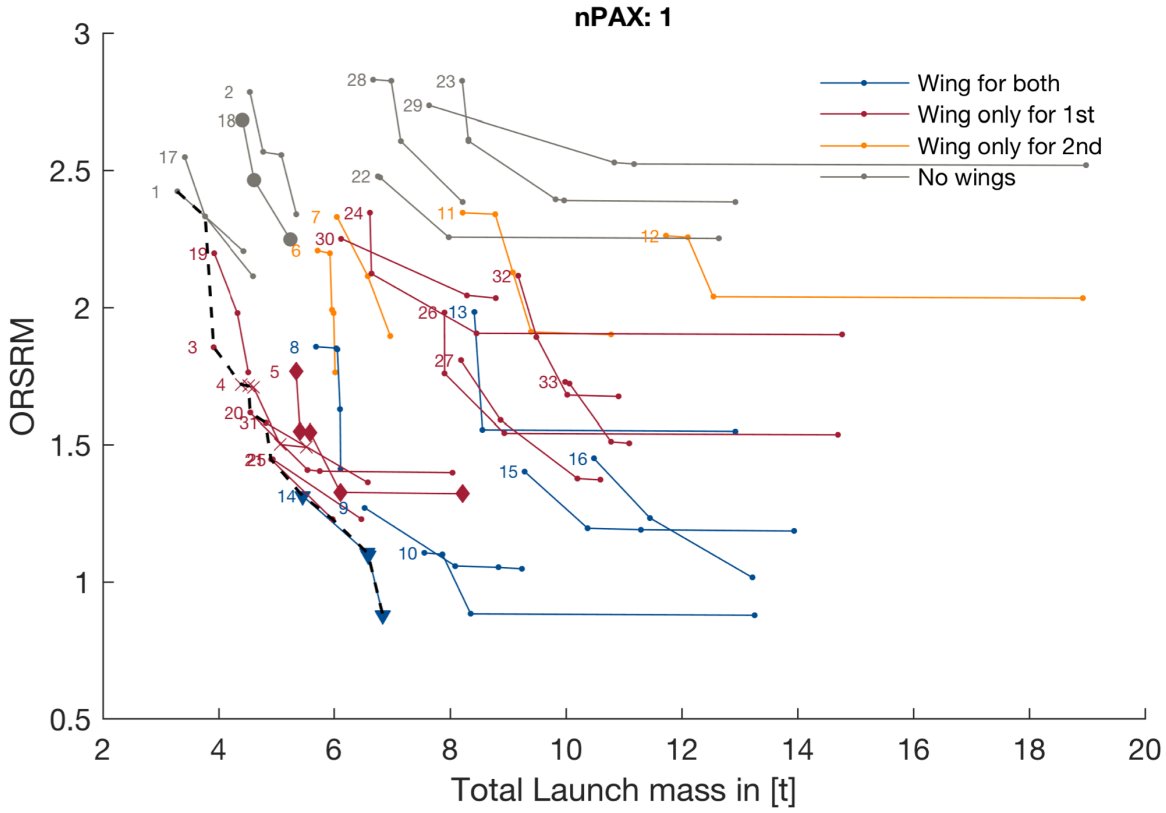

nPAX = 8

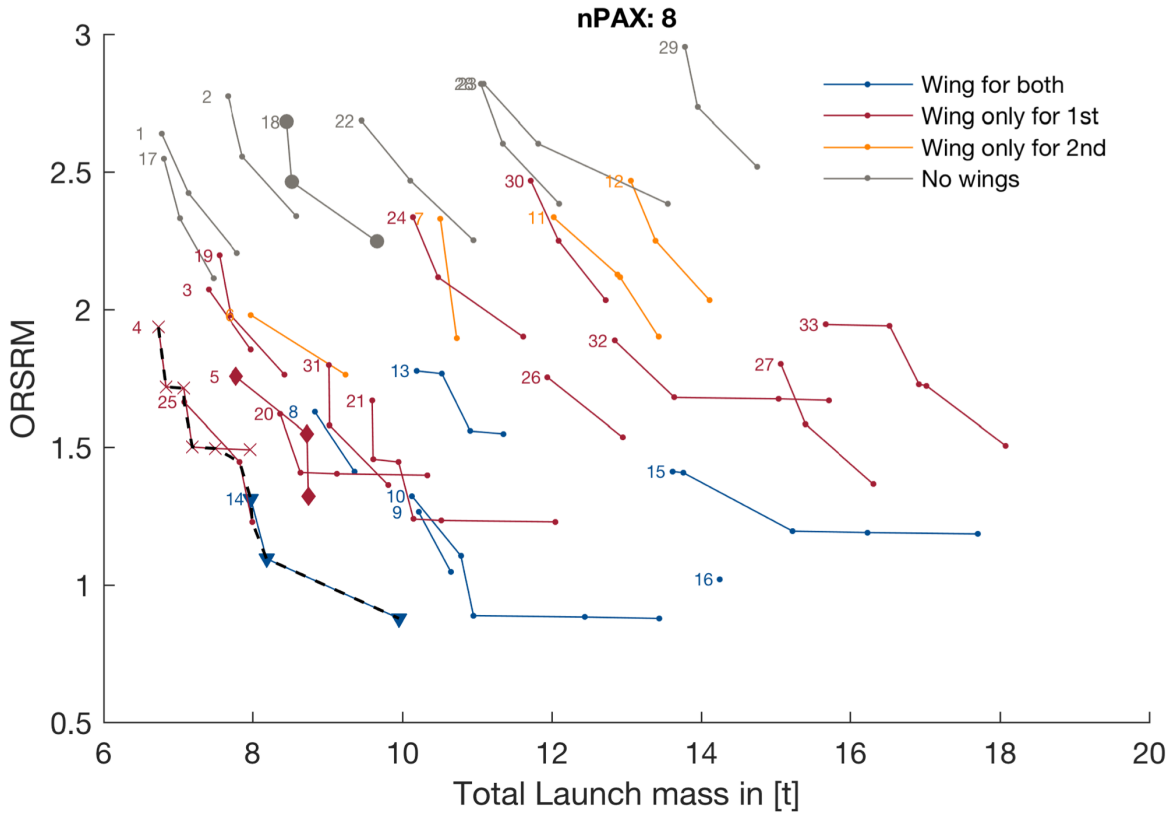

nPAX = 16

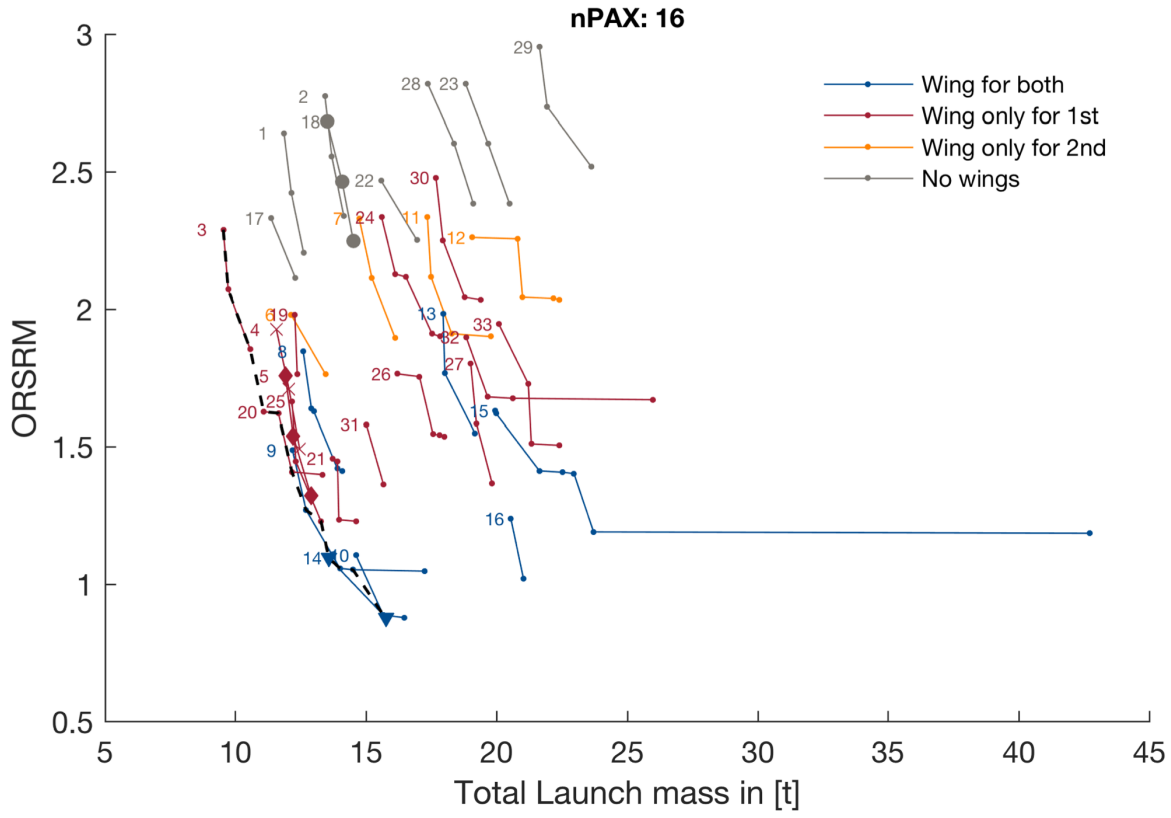

A.9 Financial optimization with fixed annual demand

nPAX = 1

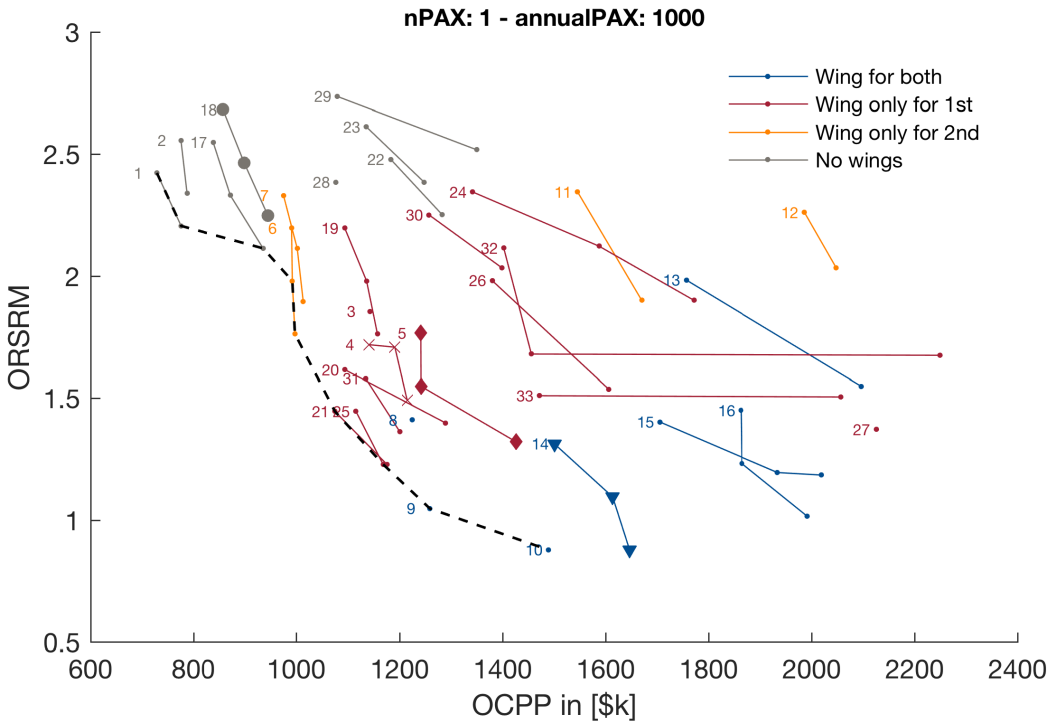

nPAX = 8

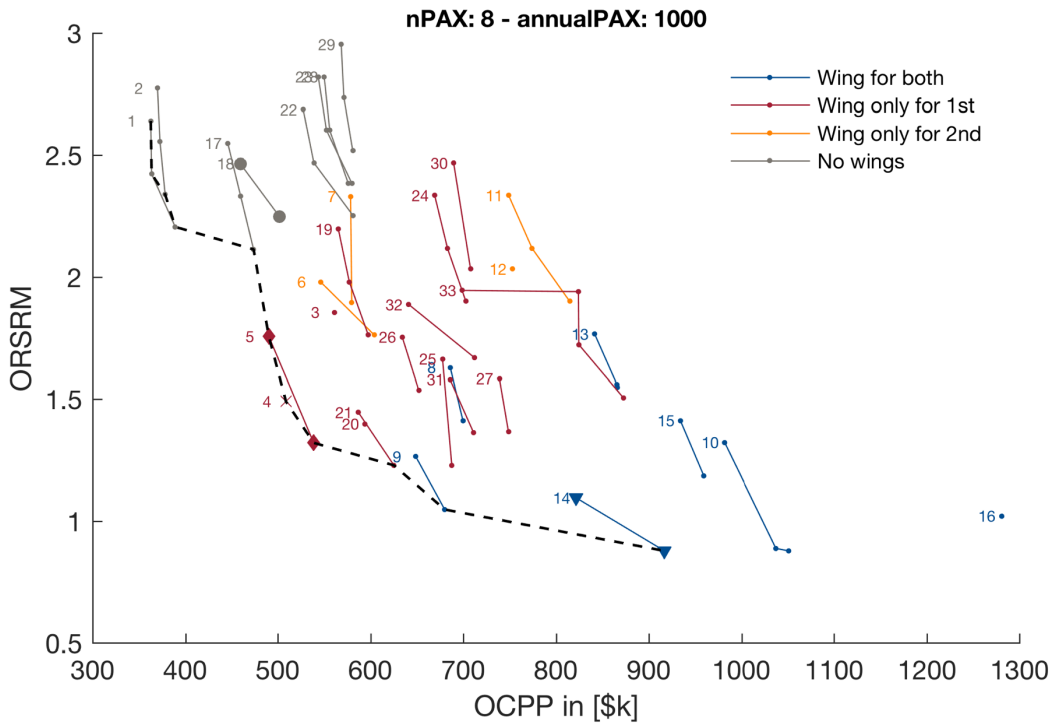

nPAX = 16

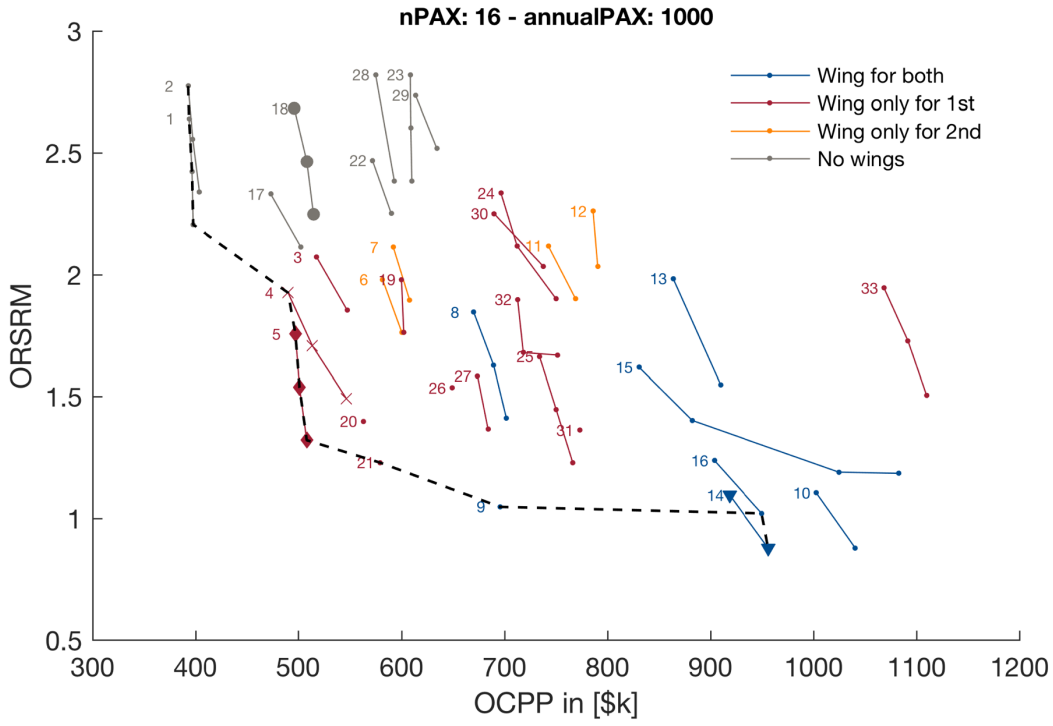

A.10 Comparison of the architecture #9 and #21 across all four sizes

Architecture #9

nPAX = 1

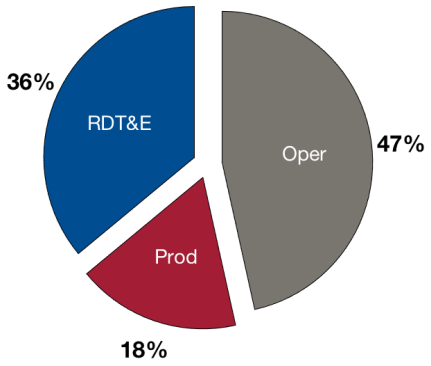

RDT&E	$6.1 billion
Production	$3.0 billion
Operation	$7.9 billion
Total	**$17.0 billion**

---

nPAX = 4

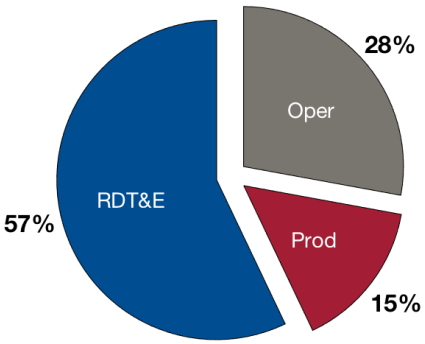

RDT&E	$6.2 billion
Production	$1.6 billion
Operation	$3.0 billion
Total	**$10.8 billion**

---

nPAX = 8

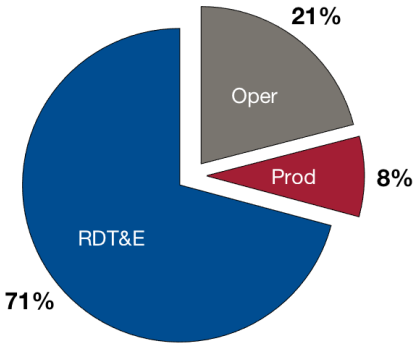

RDT&E	$6.4 billion
Production	$0.7 billion
Operation	$1.9 billion
Total	**$9.0 billion**

---

nPAX = 16

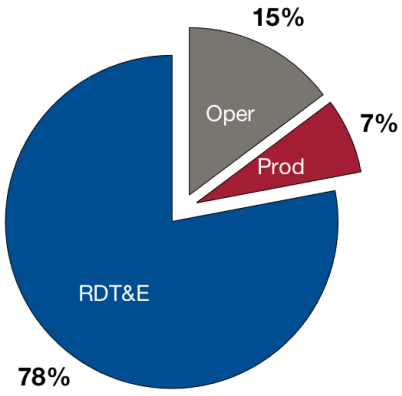

RDT&E	$7.5 billion
Production	$0.7 billion
Operation	$1.4 billion
Total	**$9.6 billion**

Architecture #21

nPAX = 1

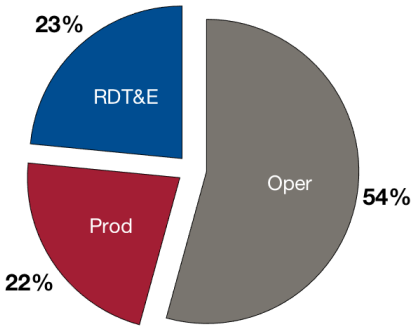

RDT&E	$3.4 billion
Production	$3.2 billion
Operation	$7.9 billion
Total	**$14.5 billion**

---

nPAX = 4

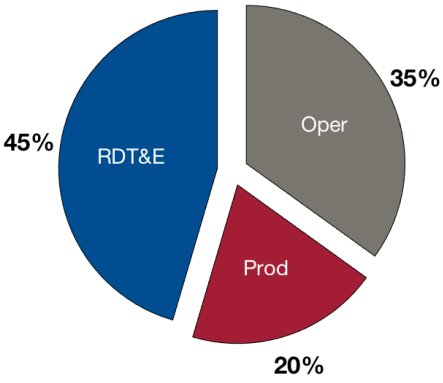

RDT&E	$3.9 billion
Production	$1.7 billion
Operation	$3.1 billion
Total	**$8.7 billion**

---

nPAX = 8

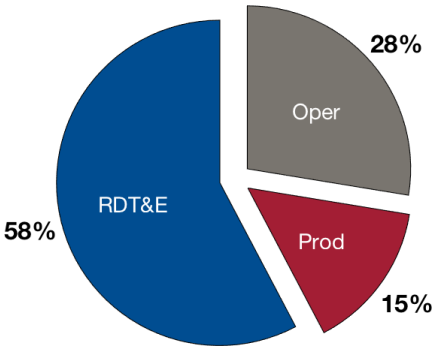

RDT&E	$4.6 billion
Production	$1.2 billion
Operation	$2.2 billion
Total	**$8.0 billion**

---

nPAX = 16

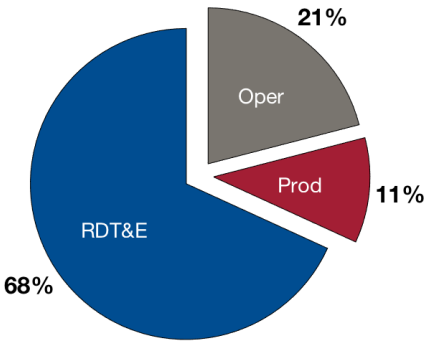

RDT&E	$5.3 billion
Production	$0.8 billion
Operation	$1.6 billion
Total	**$7.7 billion**

A.11 Sensitivity analysis

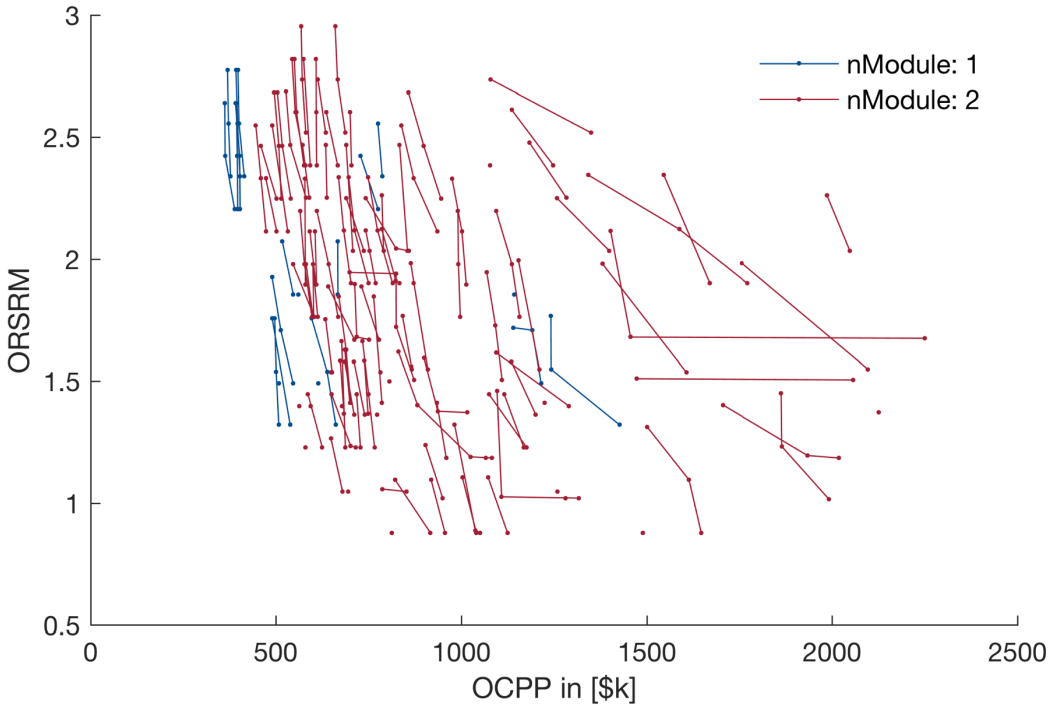

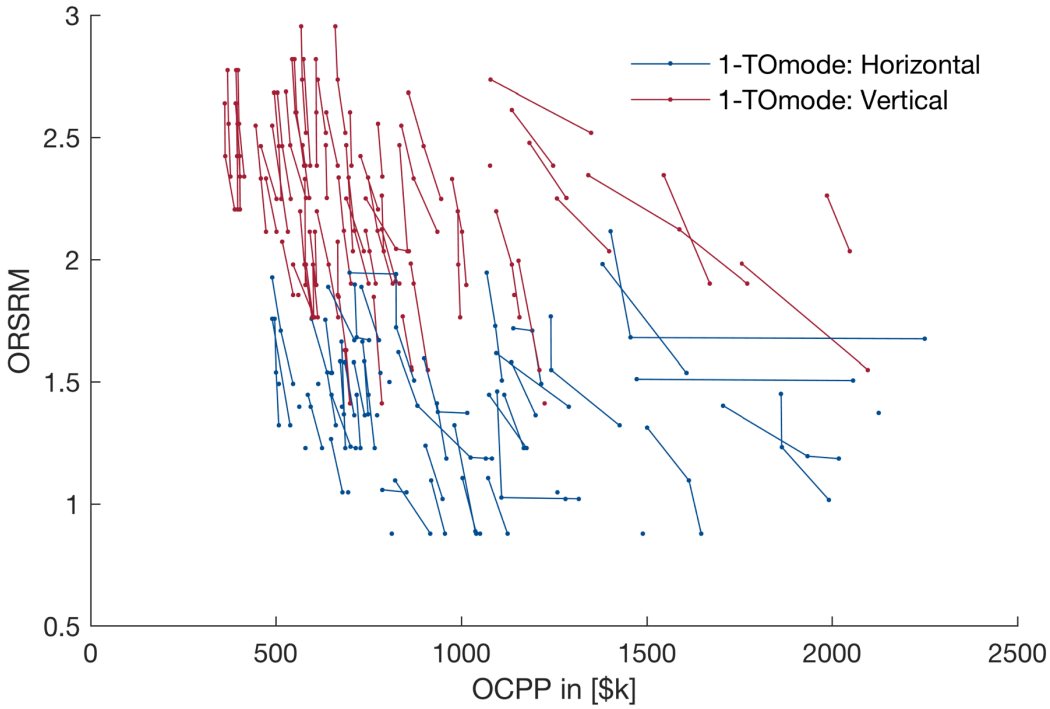

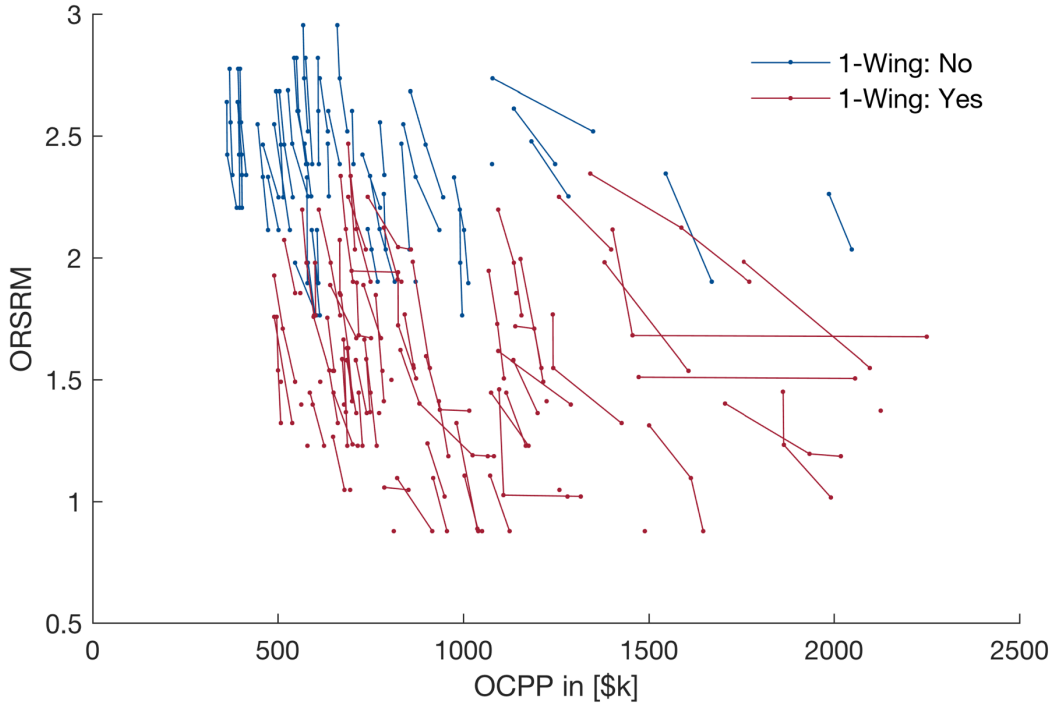
1-Wing: No
1-Wing: Yes
ORSRM
OCPP in [$k]
3
2.5
2
1.5
1
0.5
0
500
1000
1500
2000
2500

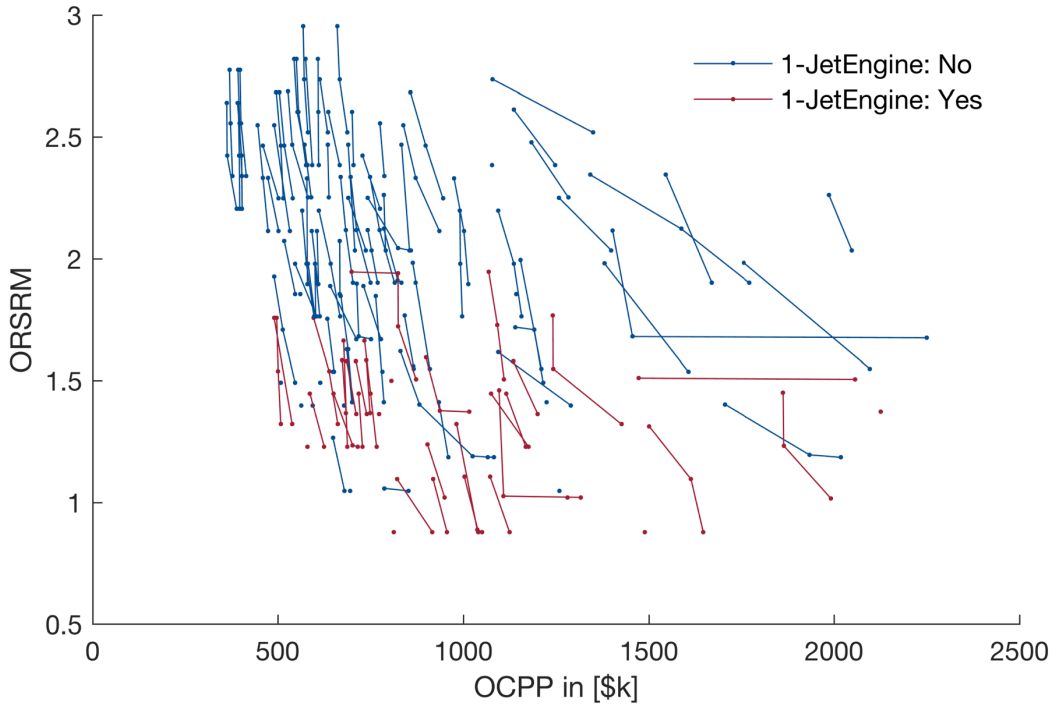
1-JetEngine: No
1-JetEngine: Yes
ORSRM
OCPP in [$k]
3
2.5
2
1.5
1
0.5
0
500
1000
1500
2000
2500

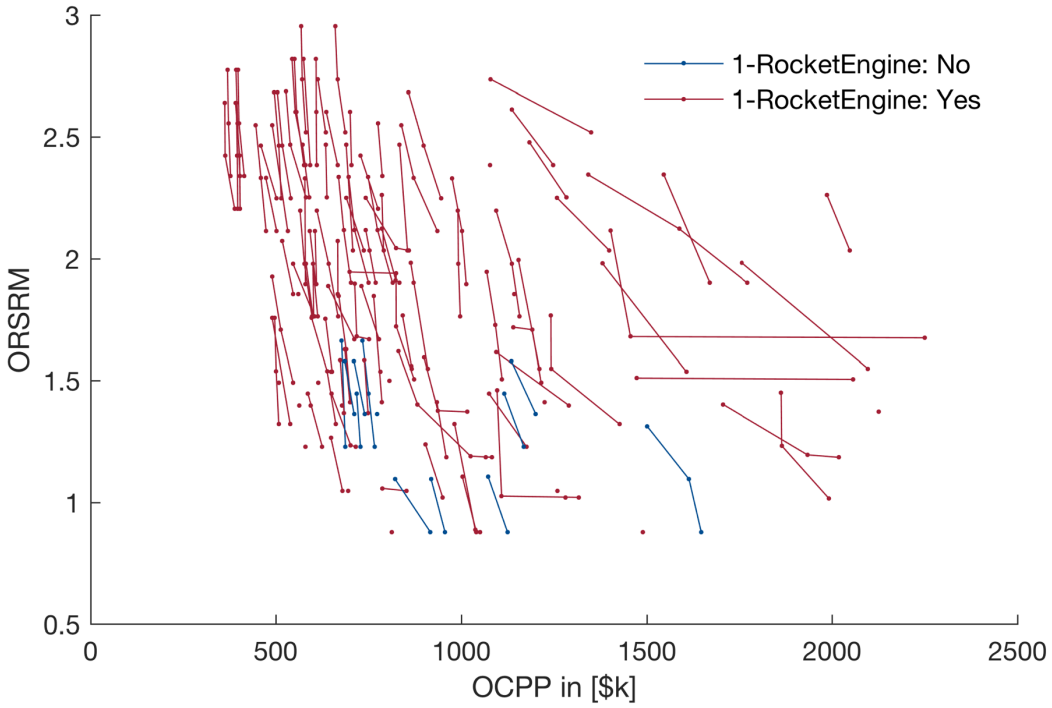
1-RocketEngine: No
1-RocketEngine: Yes
ORSRM
OCPP in [$k]
3
2.5
2
1.5
1
0.5
0
500
1000
1500
2000
2500

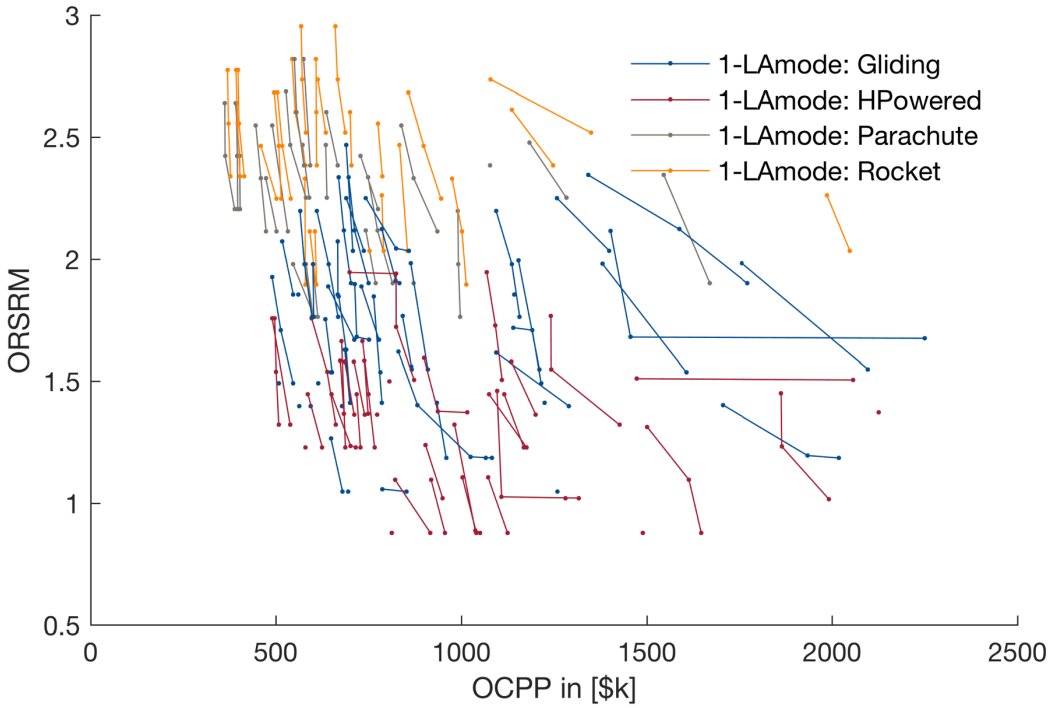
1-LAmode: Gliding
1-LAmode: HPowered
1-LAmode: Parachute
1-LAmode: Rocket
ORSRM
OCPP in [$k]
3
2.5
2
1.5
1
0.5
0
500
1000
1500
2000
2500

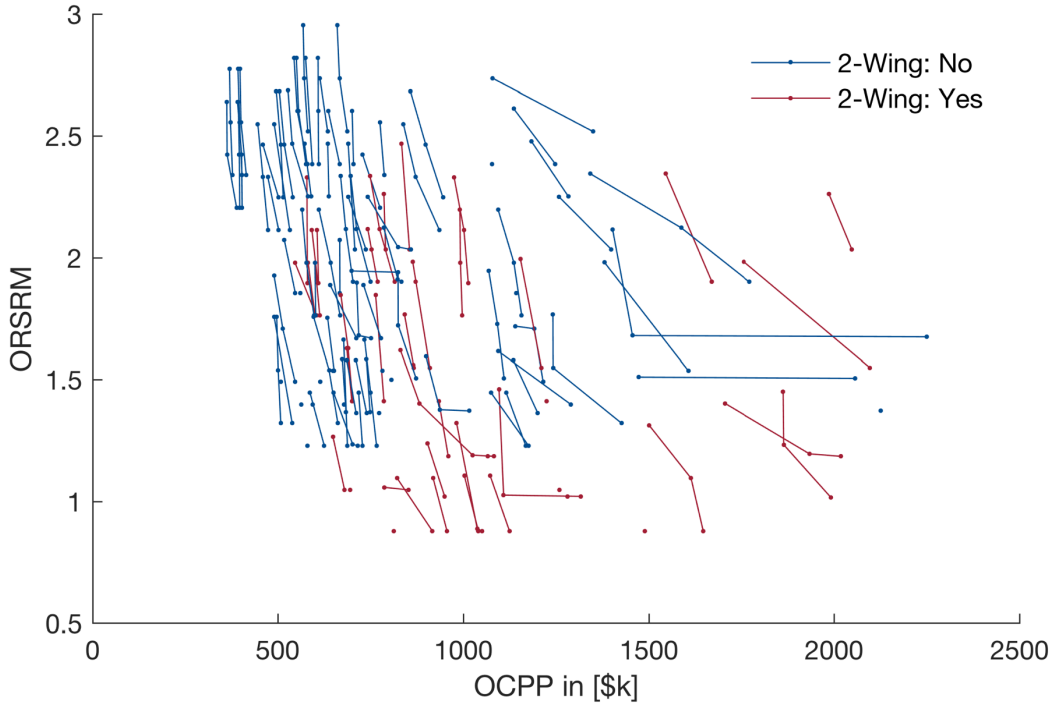
2-Wing: No
2-Wing: Yes
ORSRM
OCPP in [$k]
3
2.5
2
1.5
1
0.5
0
500
1000
1500
2000
2500

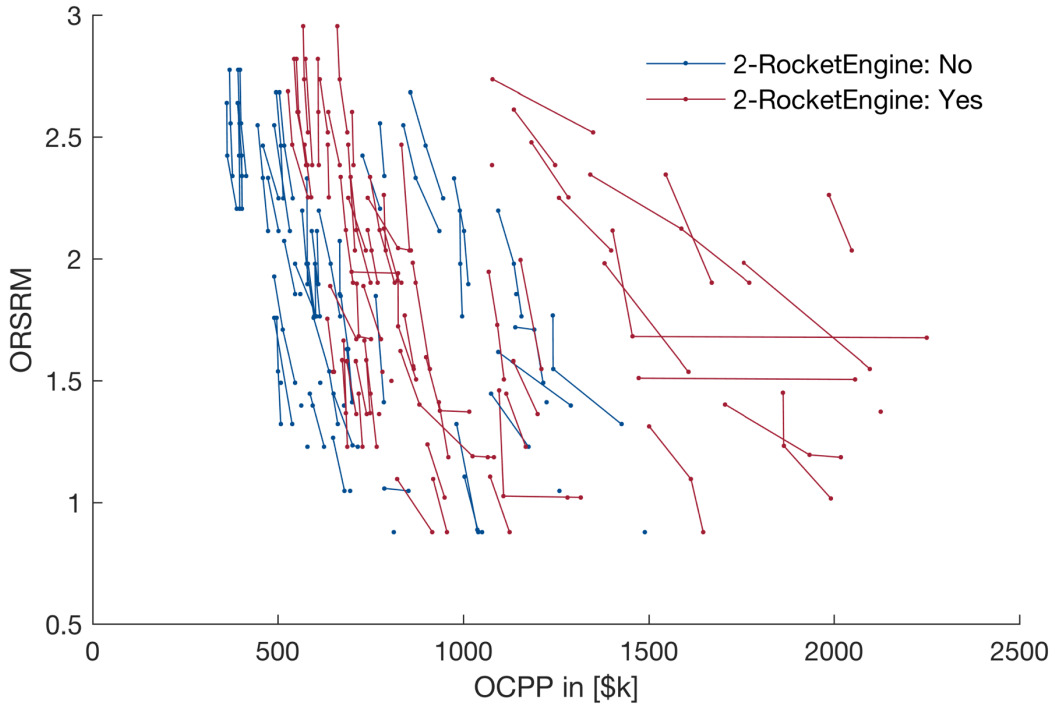
2-RocketEngine: No
2-RocketEngine: Yes
ORSRM
OCPP in [$k]
3
2.5
2
1.5
1
0.5
0
500
1000
1500
2000
2500

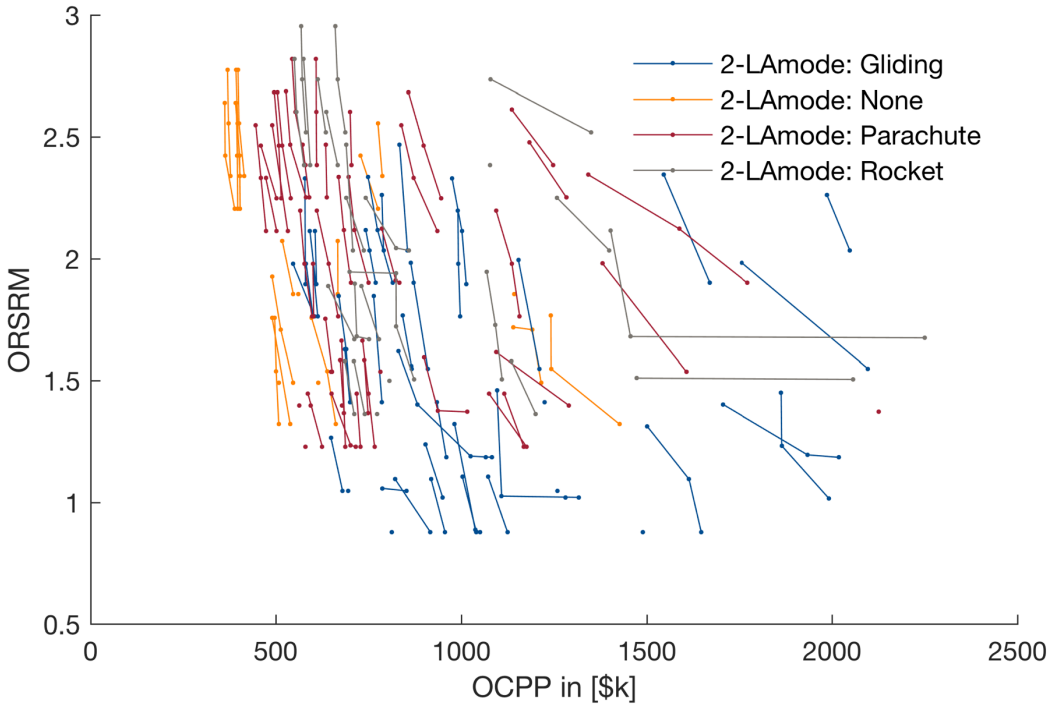

A.12 Degree of connectivity between the decisions

Decision		1	2	3	4	5	6	7	8	9
nModules	**1**	-				x		x	x	x
1-TOmode	**2**		-	x	x	x				
1-Wing	**3**		x	-			x			
1-JetEngine	**4**		x		-	x	x			
1-RocketEngine	**5**	x	x		x	-	x		x	
1-LAmode	**6**			x	x	x	-			
2-wing	**7**	x						-		x
2-RocketEngine	**8**	x				x			-	x
2-LAmode	**9**	x						x	x	-
Connectivity		**4**	**3**	**2**	**3**	**5**	**3**	**2**	**3**	**3**